Chapter 7
Bipolar Junction Transistors

The bipolar junction transistor was invented in 1947 by Shockley, Brattain, and Bardeen [1, 2]. Using insights gained from point-contact transistors [3], the group at Bell Telephone Laboratories found that a much more stable device could be created by using junctions [4]. The multifold advantages of replacing vacuum tubes with a solid-state device rapidly promulgated its use in applications. The availability of single-crystal silicon technology with greater purity levels together with the capability to form diffused junctions enabled the fabrication of transistors with high blocking voltage capability. Several decades of effort were undertaken to improve the photolithography techniques and epitaxial deposition capability culminating in the availability of 500 V Darlington power transistors in the late 1970s [5]. During this effort, it was recognized that one of the major shortcomings of the power bipolar transistor is its poor current gain. Consequently, these devices were soon eclipsed by the invention [6, 7] and rapid commercialization of the insulated gate bipolar transistor (IGBT). The high input impedance of the IGBT simplified the gate control circuit enabling its integration. The larger on-state current density and improved ruggedness of the IGBT when compared with the power bipolar transistor enabled major improvements in the size, cost, and performance of power electronic systems for numerous applications. The physics of operation of the IGBT and its applications are discussed in a subsequent chapter.

In this chapter, the basic structure and operation of the bipolar junction transistor are discussed. The bipolar transistor operates by the injection of minority carriers across one junction with these carriers collected across a second junction located in close proximity. The physics of current transport by the injection process in the bipolar transistor is reviewed in this chapter to provide a basic understanding of the factors that determine the current gain. From the perspective of power devices, the influence of high-level injection created by operation at elevated current density and the limitations produced by the need to support high voltages are analyzed in detail. Based upon analysis of the minority and majority carrier distributions within the structure, the output characteristics are then generated. The impact of emitter current crowding in the on-state and during turn-off is also included in this chapter.

© Springer International Publishing AG, part of Springer Nature 2019

B. J. Baliga, *Fundamentals of Power Semiconductor Devices*,
https://doi.org/10.1007/978-3-319-93988-9_7

The bipolar power transistor is primarily used as a switch. The switching time intervals when turning-on and turning-off the structure are therefore of interest from an applications viewpoint. The presence of minority carrier stored charge within the device is demonstrated to limit the operating frequency of these devices. In addition, the safe operating area of the bipolar transistor is shown to be constrained by the onset of second breakdown phenomena.

Although the power bipolar transistor has been supplanted by the IGBT in all power applications, a good understanding of the physics of current transport in the bipolar transistor is essential for power device specialists. In addition, the IGBT contains a bipolar transistor within its structure. Consequently, the analysis of the IGBT structure requires the application of the physics and concepts introduced in this chapter.

7.1 Power Bipolar Junction Transistor Structure

The basic structure for an N-P-N bipolar power transistor is illustrated in Fig. 7.1. In addition to the N^+ emitter and P-base region for the conventional bipolar transistor [8], the power transistor contains a lightly doped collector (N-drift) region to allow supporting high blocking voltages. When a positive bias is applied to the collector terminal of the device, the collector-base junction (J_1) becomes reverse biased and supports the voltage. The blocking voltage capability for the device is determined by the doping concentration and thickness of the N-drift region.

Current flow through the N-P-N bipolar transistor is induced by forward biasing the emitter-base junction (J_2) to initiate the injection of electrons. The injected electrons diffuse through the P-base region and arrive at the collector-base junction (J_1). When this junction is reverse biased, the electrons collected by the junction are

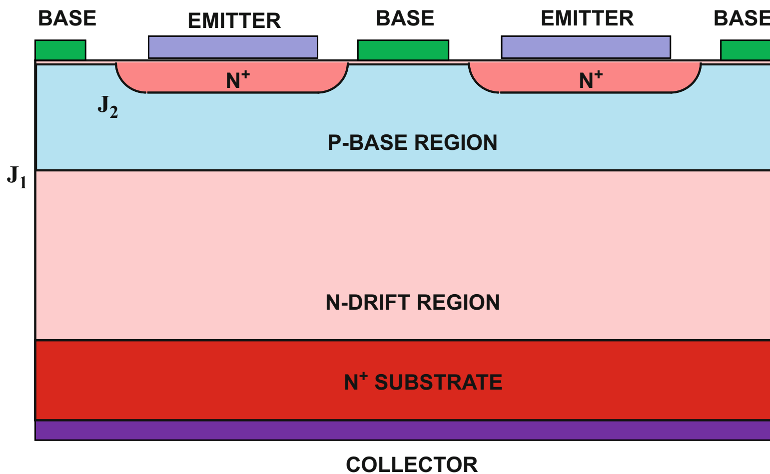

Fig. 7.1 The power bipolar N-P-N transistor structure

swept through its depletion region producing a collector current. It can be shown that a small base current can produce a large collector current resulting in a substantial current gain. In conjunction with the much larger collector voltage when compared with the base voltage, this produces a large power gain as well.

The bipolar transistor can be switching from its on-state to the blocking state by reversing the bias applied to the base region. The reverse bias not only stops the injection of minority carriers from the emitter-base junction but also removes some of the charge stored in the base region. In the case of the power bipolar transistor, a substantial amount of charge is stored within the thick N-drift region as well. This prolongs the time taken for the transistor to begin supporting voltage, limiting its maximum frequency of operation.

The vertical doping profile, extending through one of the N^+ emitter regions, for the power bipolar transistor is illustrated in Fig. 7.2. This profile is achieved by using starting material consisting of an N-type epitaxial layer grown on a heavily doped N-type substrate. The doping concentration and thickness of the epitaxial layer are chosen to obtain the desired voltage blocking capability for the power bipolar transistor. The P-type base region is then ion-implanted and diffused across the entire active area as shown in Fig. 7.1. However, the P-base region must be patterned at the edges of the device to form floating field rings to enhance the breakdown voltage. A mask is now used to define the locations of the N^+ emitter regions. The doping concentration and depth for the emitter must be carefully chosen to obtain a high current gain as discussed later in this chapter. The doping and thickness of the P-base region, determined by the combination of the P-type and N^+ ion-implants, are critical to both the blocking capability and the current gain for the power bipolar transistor. It is customary to interdigitate the emitter and base contacts as illustrated in Fig. 7.1 because the emitter current tends to concentrate at the periphery of the emitter regions due a current crowding phenomenon.

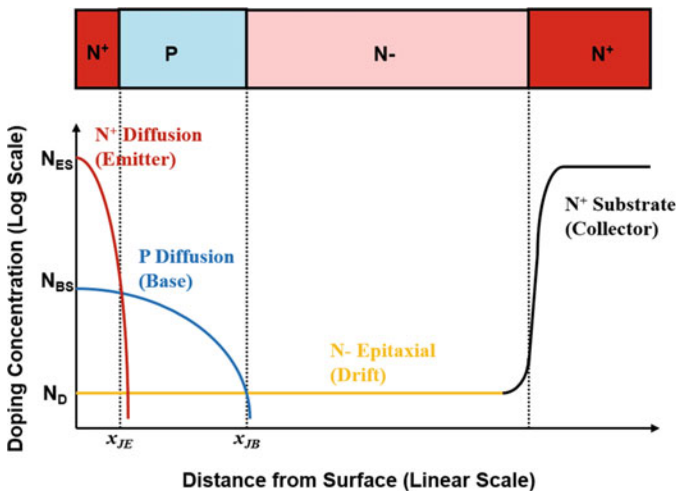

Fig. 7.2 Doping profile for the power bipolar N-P-N transistor structure

7.2 Basic Operating Principles

The power bipolar transistor is most often used in the common-emitter circuit configuration as illustrated in Fig. 7.3. In this case, the emitter terminal of the transistor is a common element between the input and output side of the circuit. The input side of the circuit is controlled by the drive circuit, which contains two power supplies that can be used to turn-on and turn-off the transistor. The voltage source V_{BS1} is used to drive the transistor when it is operating in the current conduction mode, while the voltage source V_{BS2} is used to turn-off the transistor and maintain it in its voltage blocking mode. The output side of the circuit contains a high-voltage source (V_{CS}) that delivers power to the load. The transfer of power from the voltage source to the load is controlled by the drive circuit using switches S_1 and S_2.

The bipolar transistor is operated in its current conduction mode by opening switch S_2 and closing switch S_1. This connects the input voltage source V_{BS1} across the base-emitter terminals of the bipolar power transistor through resistor R_{B1}. If the input source voltage exceeds the built-in potential ($V_{bi} \sim 0.7$ V) of the base-emitter junction, it becomes sufficiently forward biased to produce a base current given by:

$$i_B = \frac{V_{BS1} - V_{bi}}{R_{B1}} \tag{7.1}$$

The base current flow is accomplished by the injection of minority carriers (electrons for an N-P-N transistor) from the N^+ emitter region into the P-base region. These minority carriers diffuse from the emitter-base junction (J_2) through the P-base region and are collected by the reverse biased base-collector junction (J_1). The electrons captured by the base-collector junction are swept through its depletion region producing a collector current (i_C).

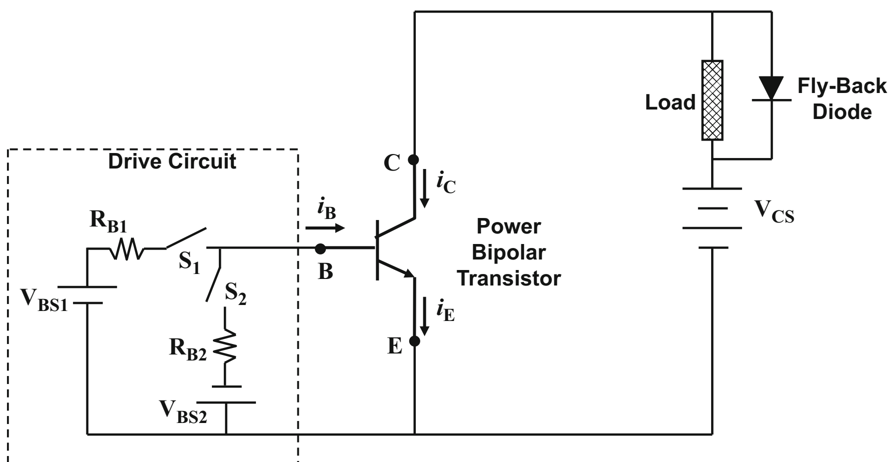

Fig. 7.3 Common-emitter configuration for an N-P-N bipolar transistor

When the bipolar transistor is operating in its forward active mode with a reverse biased base-collector junction, the collector and base currents are related by the *common-emitter current gain* called beta (β):

$$\beta = \frac{i_C}{i_B} \tag{7.2}$$

Based upon the application of Kirchhoff's current law for the bipolar transistor as a node:

$$i_E = i_B + i_C \tag{7.3}$$

Combining this relationship with that for the common-emitter current gain:

$$i_E = \left(1 + \frac{i_C}{i_B}\right) \ i_B = (1 + \beta) \ i_B \tag{7.4}$$

When the bipolar power transistor is operated as a switch, the power delivered to the load is proportional to ($i_C * V_{CS}$), while that utilized from the input control circuit is proportional to ($i_B * V_{BS1}$). The common-emitter power gain is then given by:

$$G_{P,CE} = \left(\frac{i_C V_{CS}}{i_B V_{BS1}}\right) = \beta \ \left(\frac{V_{CS}}{V_{BS1}}\right) \tag{7.5}$$

It is desirable to control a large collector current, which flows through the load, with a small base current in order to achieve a large power gain. This requires optimization of the bipolar transistor structure to obtain a large common-emitter current gain. The physical parameters within the bipolar transistor that determine the current gain are discussed in the next section.

The bipolar transistor is sometimes used in the common-base circuit configuration as illustrated in Fig. 7.4. In this case, the base terminal of the transistor is used as a common element between the input and output side of the circuit. The input side of the circuit is controlled by the drive circuit, which contains two power supplies that can be used to turn-on and turn-off the transistor. The voltage source V_{BS1} is used to drive the transistor when it is operating on the current conduction mode, while the voltage source V_{BS2} is used to turn-off the transistor and maintain it in its voltage blocking mode. The output side of the circuit contains a high-voltage source (V_{CS}) that delivers power to the load. The transfer of power from the voltage source to the load is controlled by the drive circuit using switches S_1 and S_2.

When the bipolar transistor is operating in its forward active mode with a reverse biased base-collector junction, the collector and emitter currents are related by the *common-base current gain* called alpha (α):

$$\alpha = \frac{i_C}{i_E} \tag{7.6}$$

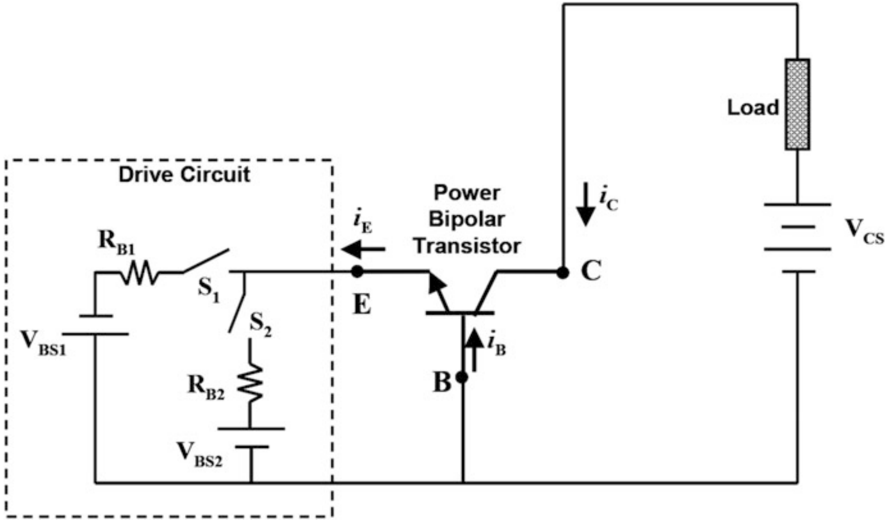

Fig. 7.4 Common-base configuration for an N-P-N bipolar transistor

Since only a fraction of the emitter current is delivered to the collector, the common-base current gain is always less than unity.

When the bipolar power transistor is operated as a switch in the common-base configuration, the power delivered to the load is proportional to (i_C*V_{CS}), while that utilized from the input control circuit is proportional to (i_E*V_{BS1}). The common-base power gain is then given by:

$$G_{P,CB} = \left(\frac{i_C V_{CS}}{i_E V_{BS1}}\right) = \alpha \left(\frac{V_{CS}}{V_{BS1}}\right) \tag{7.7}$$

Although the common-base current gain is less than unity, power gain can still be achieved because the collector source voltage is usually much larger than the base drive voltage.

The common-base current gain can be related to the common-emitter current gain by using Eq. (7.3):

$$\alpha = \frac{i_C}{(i_B + i_C)} = \frac{\beta.i_B}{(i_B + \beta.i_B)} = \frac{\beta}{(1+\beta)} \tag{7.8}$$

In a similar manner, the common-emitter current gain can be related to the common-base current gain:

$$\beta = \frac{i_C}{(i_E - i_C)} = \frac{\alpha.i_E}{(i_E - \alpha.i_E)} = \frac{\alpha}{(1-\alpha)} \tag{7.9}$$

7.3 Static Blocking Characteristics

In principle, the bipolar power transistor structure is capable of supporting voltage in the first and third quadrants of operation. In the first quadrant of operation with a positive bias applied to the collector electrode, the junction J_1 between the base and collector becomes reverse biased. Due to the incorporation of the N-drift region, this junction can be designed to support a high voltage. Devices with blocking voltages of over 1200 V in the first quadrant have been developed. In the third quadrant of operation with a negative bias applied to the collector electrode, the junction J_2 between the emitter and base becomes reverse biased. Since this junction is formed between two relatively highly doped regions, the breakdown voltage is usually less than 50 V. For this reason, the power bipolar transistor is usually used as a power switch in a DC circuit with a positive collector power source.

The voltage that can be supported by the power bipolar transistor depends on the bias applied to the base and emitter terminals. A typical set of blocking characteristics are illustrated in Fig. 7.5. It can be observed that the blocking voltage depends upon how the base terminal is connected. The open-base breakdown voltage is much smaller than the blocking voltage capability when the base terminal is shorted to the emitter terminal by the base drive circuit. However, even for the shorted base case, the blocking voltage collapses to that for the open-base case if the collector current increases. The lower blocking voltage capability is also observed when a finite base current is supplied by the drive circuit. Consequently, the actual blocking voltage rating for the power bipolar transistor is limited to the breakdown voltage of the open-base case.

7.3.1 Open-Emitter Breakdown Voltage

If the emitter terminal is open-circuited, the device operates like a diode between the base and collector terminals. In this case, the maximum blocking voltage is determined by the breakdown voltage of the base-collector junction (J_1). The open-

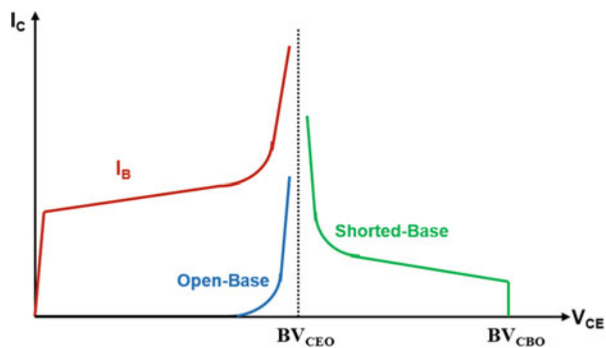

Fig. 7.5 Blocking characteristics for an N-P-N bipolar power transistor

emitter breakdown voltage (BV_{CBO}) is governed by the doping concentration and thickness of the lightly doped portion of the collector (N-drift region) and the edge termination for the base-collector junction (J_1). As shown in the next section, the actual maximum blocking voltage capability for the power bipolar transistor is a fraction of the open-base breakdown voltage. It is necessary to reduce the doping concentration and increase the thickness of the N-drift region to account for this difference. This has an adverse impact on the resistance of the N-drift region, which degrades the output characteristics as discussed later in the chapter. The increase in the thickness of the drift region also increases the turn-off time due to the larger stored charge.

7.3.2 Open-Base Breakdown Voltage

When the base terminal is open-circuited and a positive bias is applied to the collector electrode, the base-emitter junction becomes forward biased, and the base-collector junction becomes reverse biased. Most of the voltage is supported by the base-collector junction (J_1). However, the leakage current flowing through this junction must also flow through the base-emitter junction (J_2). Consequently, the leakage current is amplified by the gain of the transistor. This reduces the maximum blocking voltage capability.

In order to analyze the open-base breakdown voltage, consider the transistor structure shown in Fig. 7.6 with a positive bias applied to the collector electrode. A depletion region forms across the reverse biased base-collector junction (J_1) as

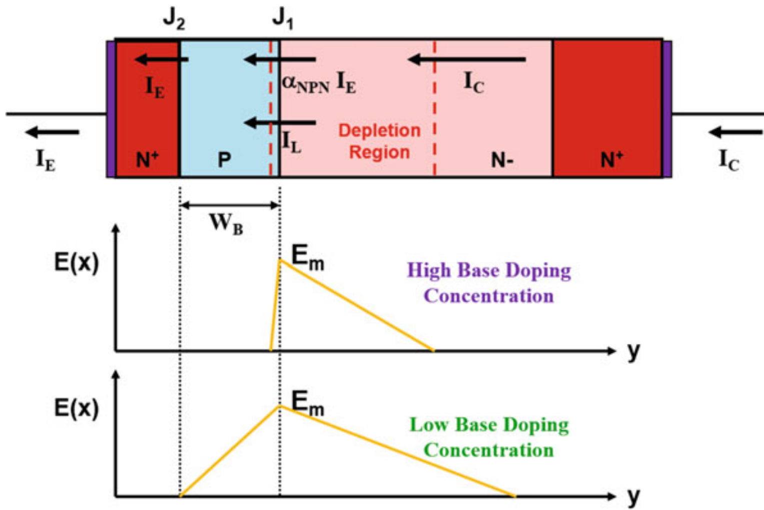

Fig. 7.6 Current transport and electric field profiles within an open-base N-P-N bipolar power transistor

indicated in the figure by the dashed lines. The minority carrier generation process produces a finite leakage current at this junction as discussed in Chaps. 2 and 3. Since the base terminal is open-circuited, the leakage current must flow through the base-emitter junction.

The injection of minority carriers across the forward biased base-emitter junction produces a current ($\alpha_{NPN}*I_E$) at the collector junction as indicated in the figure. The currents flowing through the open-base transistor structure are interrelated:

$$I_C = \alpha_{NPN} I_E + I_L = I_E \tag{7.10}$$

Consequently:

$$I_C = I_E = \frac{I_L}{(1 - \alpha_{NPN})} \tag{7.11}$$

From this expression, it can be concluded that the collector (and emitter) current will become very large as the alpha of the transistor approached unity. The criterion for breakdown for the open-base transistor can therefore be defined by:

$$\alpha_{NPN} = \gamma_E.\alpha_T.M = 1 \tag{7.12}$$

where γ_E is the emitter injection efficiency and α_T is the base transport factor. These terms will be discussed in more detail later in this chapter. It will be assumed here that they are not a strong function of the collector bias voltage. On the other hand, the multiplication coefficient (M) is a strong function of the collector bias voltage, as discussed in Chap. 3:

$$M = \frac{1}{1 - (V_C/BV_{CBO})^n} \tag{7.13}$$

At low collector bias voltages, the multiplication factor is equal to unity. In this case, a common-base current gain for low collector voltages is given by:

$$\alpha_{NPN}(0) = \gamma_E.\alpha_T \tag{7.14}$$

Using these relationships in Eq. (7.12):

$$\alpha_{NPN}(0) \frac{1}{1 - (BV_{CEO}/BV_{CBO})^n} = 1 \tag{7.15}$$

where BV_{CEO} is the open-base breakdown voltage. This expression can be rewritten as:

$$\frac{BV_{CEO}}{BV_{CBO}} = [1 - \alpha_{NPN}(0)]^{1/n} \tag{7.16}$$

In terms of the common-emitter current gain, the above expression can be written as:

$$\frac{BV_{CEO}}{BV_{CBO}} = \frac{1}{[1 + \beta_{NPN}(0)]^{1/n}} \tag{7.17}$$

As discussed in Chap. 3, the parameter n has a value of 6 for a P^+/N diode, which is appropriate for the base-collector junction. For a typical current gain (beta) of between 50 and 100 at low current levels in a power bipolar N-P-N transistor, the open-base breakdown voltage (BV_{CEO}) is reduced to half of the open-emitter breakdown voltage (BV_{CBO}). This reduction must be factored into the design of the N-drift region. The smaller doping concentration and larger width of the N-drift region required to obtain the larger open-emitter breakdown voltage produces a larger on-state voltage drop and slower switching speed for the bipolar power transistor.

The above discussion is pertinent when the doping concentration of the P-base region and its width (W_P) are relatively large. This suppresses the extension of the depletion region across the base-collector junction (J_1) into the P-base region as illustrated in Fig. 7.6. However, it will be shown later in this chapter that the current gain can be increased by reducing the doping concentration and width of the P-base region. As illustrated in the lower portion of Fig. 7.6, a reduction of the doping concentration of the P-base region promotes the extension of the depletion region across the base-collector junction (J_1) into the P-base region. If the base width is small, this can lead to the complete depletion of the P-base region before the initiation of impact ionization induced breakdown at the base-collector junction. In this case, the reach-through limited breakdown voltage will be much smaller than the open-base breakdown voltage given by Eq. (7.17). The reach-through breakdown voltage can be analyzed by using the procedure described in Chap. 3 after taking into account the sharing of the collector bias voltage with the lightly doped drift region.

7.3.3 Shorted Base-Emitter Operation

The power N-P-N bipolar transistor is illustrated in Fig. 7.7 with the base and emitter terminals short-circuited. When a positive bias is applied to the collector, the base-collector junction is reverse biased allowing the device to support a high voltage. The leakage current at the base-collector junction flows to the base contact as indicated by the dashed line. This current must flow via the resistance (R_B) of the P-base region before it reaches the base contact in this simplified lumped model. The current flow through the base resistance forward biases the base-emitter junction at location A. As long as the voltage drop produced across the base resistance is well below the built-in potential of the base-emitter junction, there is no injection initiated from this junction. The device then supports voltage as in the case of operation with an open emitter, and the blocking voltage is the same as the open-emitter breakdown voltage (BV_{CBO}). This is indicated by the vertical green line on the right-hand side of Fig. 7.5.

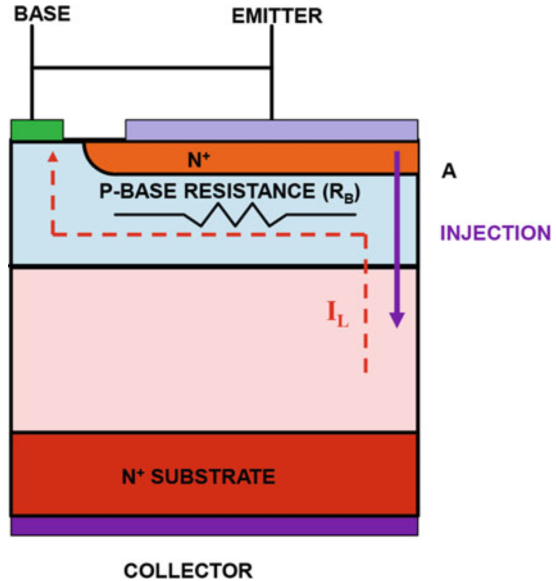

Fig. 7.7 Shorted base-emitter operation of the N-P-N bipolar power transistor

However, as the current flowing through the base-collector junction increases, the voltage drop across the base resistance becomes sufficient to promote the injection of minority carriers across the base-emitter junction at location A. This is indicated by the purple vertical arrow on the right-hand side in Fig. 7.7. Once the base-emitter junction begins to inject minority carriers, the device operates as a bipolar transistor with current gain that increases with increasing collector current. This positive feedback mechanism produces a collapse in the voltage supported by the transistor as shown in Fig. 7.5 by the green line until the collector voltage becomes equal to the open-base breakdown voltage (BV_{CEO}). Consequently, it is prudent to assume that the maximum blocking voltage capability for a power bipolar transistor operated with the base and emitter terminals shorted together (BV_{CES}) is equal to the open-base breakdown voltage (BV_{CEO}). In practical application circuits, it is customary to short circuit the base and emitter terminals with the control circuit during the blocking mode. The maximum collector voltage that is applied to the power bipolar transistor must then be less than the open-base breakdown voltage (BV_{CEO}) to avoid destructive failure.

Simulation Example

In order to gain further insight into the physics of operation for the bipolar power transistor under voltage blocking conditions, the results of two-dimensional numerical simulations for a typical structure are described here. The total width of the structure, as shown by the cross section in Fig. 7.7, was 200 μm (Area = 2×10^{-6} cm^{-2}) with an emitter finger half-width of 190 μm. The structure had a collector drift region doping concentration of 5×10^{13} cm^{-3}. The P-base region had a Gaussian doping profile with a surface concentration of 2×10^{17} cm^{-3} and a depth of 10 μm.

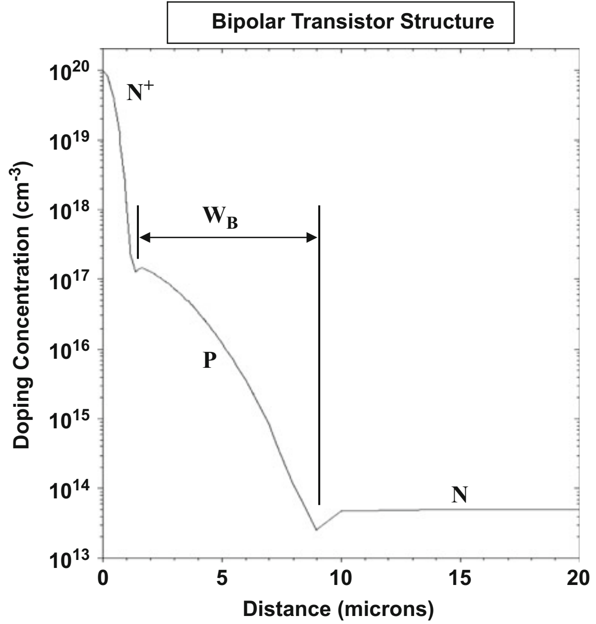

Fig. 7.8 Doping profile for the simulated N-P-N bipolar power transistor structure

The N^+ emitter region had a Gaussian doping profile with a surface concentration of 1×10^{20} cm^{-3} and a depth of 1 μm. The resulting doping profile is shown in Fig. 7.8.

The blocking characteristics for the bipolar transistor are shown in Fig. 7.9 for a variety of bias conditions at an ambient temperature of 400°K. The voltage blocking characteristics of the bipolar transistor operated under the open-emitter configuration is shown by the dashed line. The breakdown voltage (BV_{CBO}) is observed to be about 1700 V. The voltage blocking characteristics of the bipolar transistor operated under the open-base configuration is shown by the dotted line. The breakdown voltage (BV_{CEO}) is observed to be 900 V. When the bipolar transistor is operated with the base short-circuited to the emitter terminal, the characteristic shown with the solid line is observed with a snap-back behavior. At lower collector current levels, the transistor is able to support the open-emitter breakdown voltage, but when the collector current density exceeds 1 A/cm^2, the blocking voltage drops to the open-base breakdown voltage. The characteristic obtained with a base drive current of 4×10^{-7} A/μm (current density of 0.2 A/cm^2) is also shown in the figure. Using this characteristic, a common-emitter current gain (β) of 25 is obtained. Based upon Eq. (7.17), the open-base breakdown voltage is calculated to be 890 V using this gain and the observed open-emitter breakdown voltage providing validation for the simple analytical formulae that govern the breakdown voltage for the power bipolar transistor.

In Sect. 7.3.2, it was indicated that the breakdown voltage for the bipolar power transistor can be degraded by reach-though of the electric field within the P-base

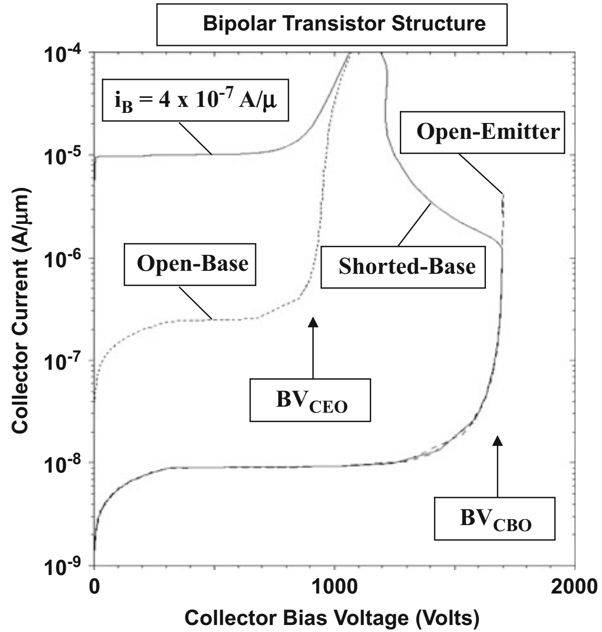

Fig. 7.9 Typical blocking characteristics for a N-P-N Bipolar power transistor structure

region. This problem becomes aggravated when the doping concentration of the P-base region is reduced in order to increase the current gain of the transistor. The extension of the electric field in the P-base region depends upon the doping concentration in the N-drift region and the doping profile for the P-base region. As an example, the electric field distributions in the vicinity of the base-collector junction are shown in Fig. 7.10 for four doping profiles for the P-base region. The doping profiles were altered by using four values for the surface concentration (N_{ABS}) for the acceptors used to form the P-base region. It can be observed that the electric field penetrates further into the P-base region toward the emitter-base junction when the surface concentration is reduced below 2×10^{17} cm^{-3}. This limits the ability to obtain a high current gain in bipolar power transistors.

7.4 Current Gain

Current transport through the bipolar transistor between its collector and emitter terminals can be induced by the application of a base drive current created with the input control circuit. One of the most important characteristics for a bipolar transistor is its current gain (alpha and beta) because this determines the power gain. The current gain for a bipolar transistor can be related to its structural parameters. The treatment of the basic bipolar transistor structure is available in many previously published textbooks [8, 9]. This section begins with a review of this treatment

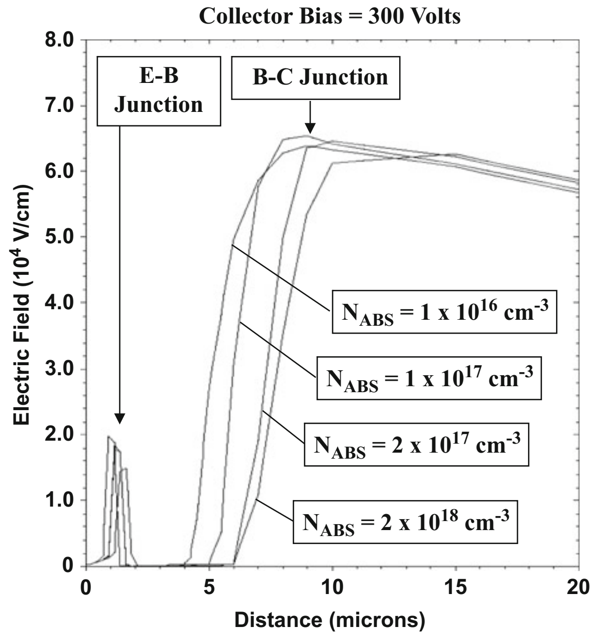

Fig. 7.10 Electric field profiles within N-P-N bipolar power transistors

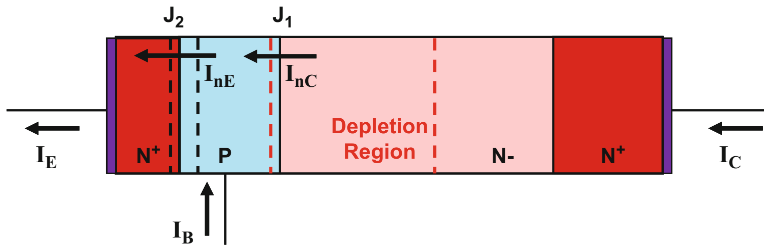

Fig. 7.11 Current flow within the N-P-N bipolar power transistor

followed by a discussion of the physics that uniquely impacts the power bipolar transistor structure.

The current flow within the power bipolar transistor is illustrated in Fig. 7.11. The base-emitter junction is assumed to be under forward bias producing a base current (I_B), while the base-collector junction is assumed to be reverse biased by the collector bias supply voltage (see Fig. 7.4). The forward bias across the base-emitter junction (J_2) results in the simultaneous injection of electrons into the base region and the injection of holes into the emitter region. The current I_{nE} is associated with the injection of electrons into the P-base region. The electrons injected into the P-base region diffused through it and reach the base-collector junction (J_1). This produces a current at the base-collector junction indicated as I_{nC} in the figure. If the voltage across the reverse biased base-collector junction is large, the electric field at

the junction can be sufficiently high to induce impact ionization. Thus, the collector current I_C is not the same as that at the junction (I_{nC}).

The common-base current gain (alpha) for the power bipolar transistor can be written in terms of the current transport components:

$$\alpha_{NPN} = \frac{\delta I_C}{\delta I_E} = \left(\frac{\delta I_{nE}}{\delta I_E}\right)\left(\frac{\delta I_{nC}}{\delta I_{nE}}\right)\left(\frac{\delta I_C}{\delta I_{nC}}\right) \quad (7.18)$$

It can be concluded that the current gain is determined by three factors indicated with the brackets in this equation. The first term is referred to as the *emitter injection efficiency*:

$$\gamma_E = \left(\frac{\delta I_{nE}}{\delta I_E}\right) \quad (7.19)$$

It is the portion of the emitter current due to the injection of electrons into the P-base region. This fraction of the emitter current is responsible for producing the collector current. The component of the emitter current due to the injection of holes into the emitter region is wasted from the point of view of deriving collector current flow in the bipolar transistor. The emitter injection efficiency term is always less than unity. In addition, the emitter injection efficiency is reduced by recombination within the depletion region of the base-emitter junction.

The second term in brackets in Eq. (7.18) is referred to as the *base transport factor*:

$$\alpha_T = \left(\frac{\delta I_{nC}}{\delta I_{nE}}\right) \quad (7.20)$$

It is a measure of the ability of the electrons injected at the base-emitter junction to reach the base-collector junction. All of the electrons injected into the P-base region are unable to reach the base-collector junction due to recombination within the base region. The base transport factor is always less than unity for a bipolar transistor.

The third term in brackets in Eq. (7.18) is referred to as the *collector efficiency*:

$$\gamma_C = \left(\frac{\delta I_C}{\delta I_{nC}}\right) \quad (7.21)$$

This parameter is a measure of electron transport through the collector region. When the base-collector junction is reverse biased as shown in the figure, a high electric field can be developed within its depletion region. The electrons that enter the depletion region from the base region can undergo multiplication due to the impact ionization process if the electric field is sufficiently large. Consequently, the collector efficiency is equal to the multiplication coefficient (M) that was discussed in Chap. 3. At low collector bias voltages, the collector efficiency term can be assumed to be equal to unity. At large collector bias voltages, this term can become greater than unity.

The above parameters that determine the common-base current gain can be related to the physical properties of the bipolar transistor. In the case of the power bipolar transistor, it becomes necessary to account for high-level injection effects in the P-base region because of operation at relatively large current densities. At very high collector current densities, a base-widening effect occurs that also degrades the current gain. The analysis of the emitter injection efficiency and base transport factor for a power bipolar transistor is provided below.

7.4.1 Emitter Injection Efficiency

As discussed above, the emitter injection efficiency is a measure of the emitter current due to the injection of electrons into the P-base region. When the base-emitter junction is forward biased, current flow across the junction occurs by the injection of electrons into the base region as well as the injection of holes into the emitter region. The carrier distribution profiles in the base and emitter regions are illustrated in Fig. 7.12 using a linear scale for the concentrations.

The injected carrier concentrations on both sides of the base-emitter junction are related to the corresponding minority carrier concentrations in equilibrium by the "Law of the Junction" [8]:

$$n_B(0) = n_{0B}.e^{qV_{BE}/kT} \tag{7.22}$$

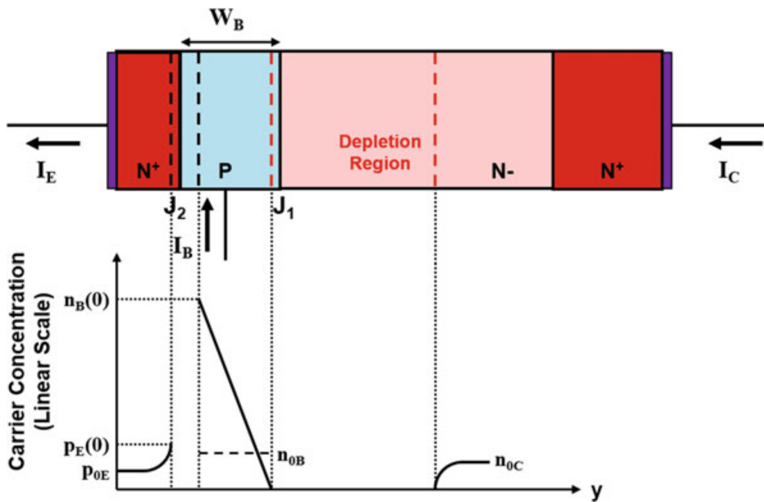

Fig. 7.12 Minority carrier distribution within the N-P-N bipolar power transistor

$$p_E(0) = p_{0E}.e^{qV_{BE}/kT} \tag{7.23}$$

where $V_{\rm BE}$ is the forward bias across the base-emitter junction. In these equations, $n_{\rm 0B}$ and $p_{\rm 0E}$ are the minority carrier concentrations in equilibrium within the P-base and N$^+$ emitter regions, respectively. Note that the minority carrier concentration in equilibrium is larger within the P-base region than within the N$^+$ emitter region due to the larger doping concentration in the emitter for a bipolar transistor.

The minority carriers (holes) injected into the N$^+$ emitter region diffuse away from the junction producing a hole current component for the total emitter current. The holes within the emitter region obey the continuity equation:

$$\frac{d^2p}{dy^2} - \frac{p}{L_{\rm pE}^2} = 0 \tag{7.24}$$

where $L_{\rm pE}$ is the diffusion length for holes in the emitter. The diffusion length for holes is small (sub-micron) due to the high doping concentration in the emitter (see high doping effects discussed in Chap. 2). If the emitter thickness is much greater than the diffusion length for holes in the emitter, the minority carrier profile exhibits an exponential decay away from the junction as illustrated in the figure (see Chap. 5 for a more detailed discussion of the injected minority carrier concentration for a P-N junction diode). This profile is given by:

$$p(y) = p_{\rm E}(0)\, e^{-\left(y/L_{\rm pE}\right)} \tag{7.25}$$

where y is the distance measured moving to the left away from the junction.

The hole current density flowing at the base-emitter junction is given by:

$$J_{\rm p}(0) = -qD_{\rm pE}\left(\frac{dp}{dy}\right)_{y=0} \tag{7.26}$$

where $D_{\rm pE}$ is the diffusion coefficient for holes in the emitter. Note that the diffusion coefficient for holes in the emitter must be computed after taking into account the reduction of the mobility ($\mu_{\rm pE}$) due to heavy doping effects. In Chap. 2, a reduction of the majority carrier mobility with increasing doping concentration was attributed to enhanced Coulombic scattering. Empirical studies [10, 11] on the minority carrier mobility within heavily doped regions indicate a similar reduction of the minority carrier mobility. In this case, the mobility for holes in the emitter region should be computed by using the relationship:

$$\mu_{\rm pE}(N_{\rm DE}) = \frac{2.9 \times 10^{15} + 47.7N_{\rm DE}^{0.76}}{5.86 \times 10^{12} + N_{\rm DE}^{0.76}} \tag{7.27}$$

where $N_{\rm DE}$ is the donor concentration in the emitter. Using Eq. (7.25) in Eq. (7.26) provides the hole current component of the total emitter current:

$$J_{\mathrm{p}}(0) = \frac{qD_{\mathrm{pE}}}{L_{\mathrm{pE}}} p_{\mathrm{E}}(0) = \frac{qD_{\mathrm{pE}}}{L_{\mathrm{pE}}} p_{0\mathrm{E}}.e^{qV_{\mathrm{BE}}/kT} \tag{7.28}$$

after incorporating Eq. (7.23).

To determine the electron component of the total emitter current, consider the continuity equation for electrons in the P-base region:

$$\frac{d^2n}{dy^2} - \frac{n}{L_{\mathrm{nB}}^2} = 0 \tag{7.29}$$

where L_{nB} is the diffusion length for electrons in the base and y is the distance measured moving to the right away from the base-emitter junction. In this section, it will be assumed that the width of the P-base region (W_{B} in the figure) is much smaller than the diffusion length for electrons in the base region. In this case, recombination in the base region is negligible allowing analysis of the impact of the emitter injection efficiency on the gain of the bipolar transistor. The continuity equation for electrons in the P-base region then becomes:

$$\frac{d^2n}{dy^2} = 0 \tag{7.30}$$

indicating that the slope (dn/dy) of the minority carrier concentration is constant in the P-base region. This linear electron concentration profile is illustrated in the figure. Due to the reverse bias at the base-collector junction, the minority carrier concentration at this junction is forced to zero as shown in the figure. Consequently, the electron concentration decreases linearly from an injected concentration [$n_{\mathrm{B}}(0)$] at the base-emitter junction to zero at the base-collector junction:

$$n(y) = n_{\mathrm{B}}(0)\left(1 - \frac{y}{W_{\mathrm{B}}}\right) \tag{7.31}$$

In writing this expression, it has been assumed that the widths of the depletion regions within the P-base region can be neglected. This holds true at small collector bias voltages. The impact of large collector bias voltages on the base width (the Kirk effect) is taken into account later in the chapter.

The electron current component of the total emitter current can be derived from the above electron carrier distribution:

$$J_{\mathrm{n}}(0) = -qD_{\mathrm{nB}}\left(\frac{dn}{dy}\right)_{y=0} \tag{7.32}$$

where D_{nB} is the diffusion coefficient for electrons in the base region. Note that the diffusion coefficient for electrons in the base region must be computed after taking into account the reduction of the mobility (μ_{nB}) due to heavy doping effects in the base region even though its doping is not as high as in the emitter. In this case, the

mobility for electrons in the base region should be computed by using the relationship:

$$\mu_{nB}(N_{AB}) = \frac{5.1 \times 10^{18} + 92N_{AB}^{0.91}}{3.75 \times 10^{15} + N_{AB}^{0.91}} \tag{7.33}$$

where N_{AB} is the acceptor concentration in the base region. Using Eq. (7.31) in Eq. (7.32) provides the electron current component of the total emitter current:

$$J_n(0) = \frac{qD_{nB}}{W_B} n_B(0) = \frac{qD_{nB}}{W_B} n_{0B}\, e^{qV_{BE}/kT} \tag{7.34}$$

after incorporating Eq. (7.22). Since the recombination in the base region has been assumed to be negligible, the electron current component at the base-emitter junction is also equal to the collector current density if carrier multiplication is ignored.

The emitter injection efficiency can be obtained by using the electron and hole current components:

$$\gamma_E = \frac{J_n(0)}{J_n(0) + J_p(0)} \tag{7.35}$$

Substituting Eqs. (7.28 and 7.34) for the current densities:

$$\gamma_E = \frac{D_{nB}L_{pE}n_{0B}}{D_{nB}L_{pE}n_{0B} + D_{pE}W_B p_{0E}} \tag{7.36}$$

Using this relationship, the emitter injection efficiency can be computed from the physical parameters for the power bipolar transistor. In order to facilitate this computation, it is beneficial to relate the minority carrier concentrations in equilibrium to the doping concentrations in the regions:

$$n_{0B} = \frac{n_{iB}^2}{N_{AB}} \tag{7.37}$$

$$p_{0E} = \frac{n_{iE}^2}{N_{DE}} \tag{7.38}$$

Note that the intrinsic carrier concentrations in the base and emitter regions are not equal due to the difference in doping concentrations, which impacts the bandgap narrowing for the regions. Using these relationships in Eq. (7.36):

$$\gamma_E = \frac{D_{nB}L_{pE}n_{iB}^2 N_{DE}}{D_{nB}L_{pE}n_{iB}^2 N_{DE} + D_{pE}W_B n_{iE}^2 N_{AB}} = \alpha_E \tag{7.39}$$

The common-base current gain (α_E), *as determined purely by the emitter injection efficiency*, can be computed by using the above expression.

The common-emitter current gain (β_E), *as determined purely by the emitter injection efficiency*, can also be obtained by using the electron and hole current components of the total emitter current:

$$\beta_E = \frac{J_n(0)}{J_p(0)} \tag{7.40}$$

Substituting Eqs. (7.28 and 7.34) for the current densities:

$$\beta_E = \frac{D_{nB} L_{pE} n_{0B}}{D_{pE} W_B p_{0E}} \tag{7.41}$$

Using Eqs. (7.37 and 7.38) for the minority carrier concentrations in equilibrium:

$$\beta_E = \frac{D_{nB} L_{pE} n_{iB}^2 N_{DE}}{D_{pE} W_B n_{iE}^2 N_{AB}} \tag{7.42}$$

For a power bipolar transistor, it is desirable to obtain a high current gain in order to control a large load (collector) current with a small input drive (base) current. Based upon the expressions for the emitter injection efficiency, a high gain can be obtained by using a large doping concentration for the emitter region and a low doping concentration for the base region. In practice, it is not possible to use an arbitrarily high doping concentration for the N^+ emitter region due to heavy doping effects, which produce (a) a reduction of the diffusion length for holes in the emitter and (b) a large increase in the intrinsic carrier concentration in the emitter due to bandgap narrowing. An optimum doping concentration for the emitter has been reported to be about 1×10^{19} cm^{-3}. In this case, typical values for the common-base and common-emitter current gains are 0.96 and 25, respectively, if a base doping concentration of 1×10^{17} cm^{-3} is assumed. In addition, from the above equations for the current gain as determined by the emitter injection efficiency, it is desirable to have a lightly doped base region with a narrow base width. However, this can compromise the blocking voltage capability of the power bipolar transistor due to the reach-through phenomenon as discussed previously in the chapter. A low P-base doping concentration also results in high-level injection effects occurring in the base region at lower current densities. This reduces the emitter injection efficiency as discussed in Sect. 7.4.3.

7.4.2 Emitter Injection Efficiency with Recombination in the Depletion Region

In the previous analysis, the current transport across the base-emitter junction was assumed to occur purely by the diffusion process. However, at low current densities, it is necessary to account for the recombination current at the base-emitter junction. The recombination current for a P-N junction was discussed in Sect. 5.1.1.

The current at the junction produced by recombination within the depletion region is given by:

$$J_r = \frac{qn_i W_D}{\tau_{SC}} e^{qV_{BE}/2kT} \tag{7.43}$$

where W_D is the depletion layer width and τ_{SC} is the space-charge generation lifetime. The emitter injection efficiency at low current levels can be obtained by including this current component:

$$\gamma_E = \frac{J_n(0)}{J_n(0) + J_p(0) + J_r} \tag{7.44}$$

Using the previously derived equations (Eqs. 7.28 and 7.34) for the diffusion currents with the above equation for the recombination current:

$$\gamma_E = \frac{D_{nB} L_{pE} n_{0B}}{D_{nB} L_{pE} n_{0B} + D_{pE} W_B p_{0E} + \left[(n_i W_D W_B L_{pE})/(\tau_{SC} e^{qV_{BE}/2kT})\right]} \tag{7.45}$$

At low forward bias voltages across the base-emitter junction, the last term in square brackets in the denominator of this equation becomes dominant producing a reduction of the emitter injection efficiency and the current gain. As the forward bias across the base-emitter junction is increased, the diffusion currents become much larger than the recombination current, and the emitter injection efficiency becomes equal to that discussed in the previous section.

As an example, consider a power bipolar transistor with an N^+ emitter doping concentration of 2×10^{19} cm^{-3} with a diffusion length of 1 μm for the holes and a P-base doping concentration of 1×10^{17} cm^{-3} with a width of 5 μm. The current gains (β_E) computed for this case with a depletion region width of 0.01 μm and various values for the space-charge generation lifetime are shown in Fig. 7.13. For the case of a space-charge generation lifetime of 1×10^{-7} s, the recombination current begins to dominate leading to a falloff in the current gain when the current density becomes less than 0.1 A/cm^2. When the current density becomes more than 1 A/cm^2, the current gain approaches 25 as limited by the injection of holes into the emitter region. As the space-charge generation lifetime is increased, a high gain is retained to lower collector current levels. The rate of falloff in the current gain with decreasing collector current density is therefore a strong function of the space-charge generation lifetime.

7.4.3 Emitter Injection Efficiency with High-Level Injection in the Base

From the analysis in the previous section, it may be inferred (see Eq. (7.42)) that the doping concentration in the base region for the power bipolar transistor should be

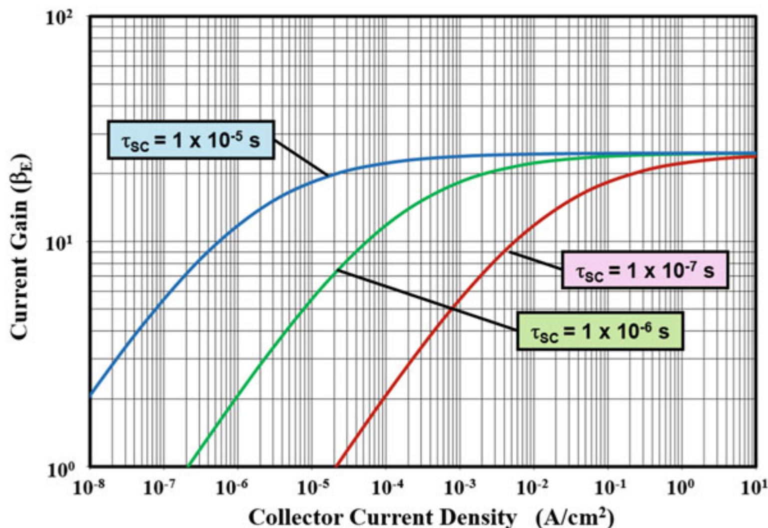

Fig. 7.13 Reduction of current gain at low collector current levels for the N-P-N bipolar power transistor

reduced to achieve a high current gain. However, at low base doping levels, the injected minority (electron) carrier concentration in the P-base region can exceed its doping concentration when the bipolar power transistor is operated at high current densities. This is referred to as the onset of *high-level injection in the base region*. In order to satisfy charge neutrality, the majority (hole) carrier concentration in the base region increases under high-level injection conditions. This enhances the injection of holes from the P-base region into the N^+ emitter region, which results in a reduction of the injection efficiency and current gain of the power bipolar transistor. The reduction of the current gain of a bipolar transistor with increasing current density due to high-level injection in the base region is referred to as the *Webster effect* [12].

The minority carrier distribution profiles in the base and emitter regions are shown in Fig. 7.14 under high-level injection conditions in the base region. The majority carrier profiles are also shown in the figure. The majority carrier concentration in the emitter remains equal to the emitter doping concentration because of low injection levels in the emitter region. However, the majority carrier concentration in the base is enhanced because the minority carrier density exceeds the doping concentration of the base region in the vicinity of the base-emitter junction. Charge neutrality in the base region requires:

$$p_B(0) - p_{0B} = n_B(0) - n_{0B} \tag{7.46}$$

where $p_B(0)$ and $n_B(0)$ are the majority and minority carrier densities in the P-base region at the base-emitter junction as indicated in the figure. Since the concentration of the minority carriers (n_{0B}) in equilibrium for the base region is much smaller than the other concentrations in the above equation:

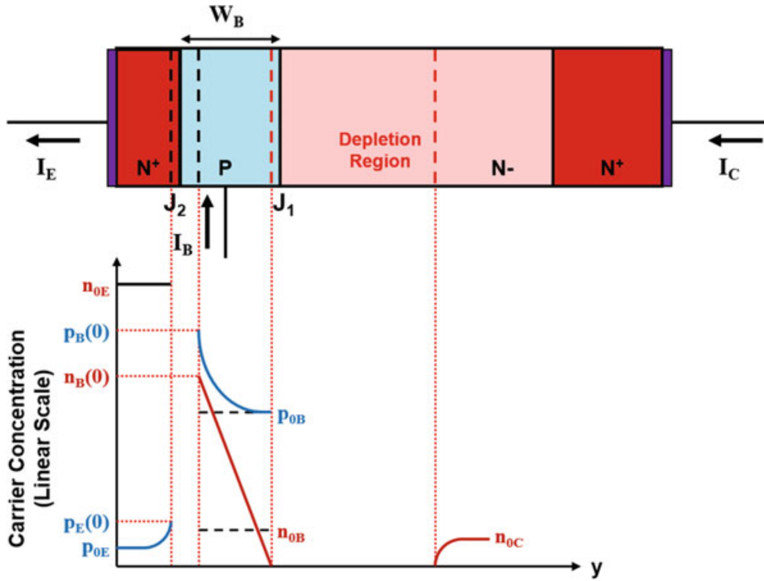

Fig. 7.14 Minority and majority carrier profiles within the N-P-N bipolar power transistor under high-level injection conditions in the base

$$p_B(0) = p_{0B} + n_B(0) \tag{7.47}$$

The Boltzmann quasi-equilibrium boundary condition for a P-N junction requires:

$$\frac{p_E(0)}{p_B(0)} = \frac{n_B(0)}{n_E(0)}\left(\frac{n_{iE}}{n_{iB}}\right)^2 \tag{7.48}$$

Since the doping concentration in the emitter (N_{DE}) is very high:

$$n_E(0) = n_{0E} = N_{DE} \tag{7.49}$$

Combining the above relationships:

$$p_E(0) = \frac{p_B(0).n_B(0)}{n_E(0)}\left(\frac{n_{iE}}{n_{iB}}\right)^2 = \frac{n_B(0)}{N_{DE}}\left(\frac{n_{iE}}{n_{iB}}\right)^2 [p_{0B} + n_B(0)] \tag{7.50}$$

According to the "Law of the Junction":

$$n_B(0) = n_{0B}\, e^{qV_{BE}/kT} \tag{7.51}$$

where V_{BE} is the forward bias voltage across the base-emitter junction. Substituting this in Eq. (7.50):

$$p_E(0) = \frac{p_{0B} n_{0B}}{N_{DE}} \left(\frac{n_{iE}}{n_{iB}} \right)^2 \left[1 + \frac{n_B(0)}{p_{0B}} \right] e^{qV_{BE}/kT} \tag{7.52}$$

The majority and minority carriers in equilibrium are interrelated through the intrinsic carrier concentrations in the emitter and base regions:

$$p_{0B} . n_{0B} = n_{iB}^2 \tag{7.53}$$

$$p_{0E} . n_{0E} = p_{0E} . N_{DE} = n_{iE}^2 \tag{7.54}$$

Combining these with Eq. (7.52) yields:

$$p_E(0) = p_{0E} \left[1 + \frac{n_B(0)}{p_{0B}} \right] e^{qV_{BE}/kT} \tag{7.55}$$

The term within the square brackets in this equation is the increase in the injected hole (minority carrier) concentration in the emitter due to high-level injection in the base region. When the concentration of minority carriers (electrons) injected into the P-base region [$n_B(0)$] is small compared with the majority carrier concentration [p_{0B}] in the base region, this term becomes equal to unity as expected for low-level injection conditions.

The emitter injection efficiency under high-level injection conditions in the base region can be derived by taking into account the enhanced injection of holes into the emitter. Based upon an exponential decrease in the minority carrier (hole) concentration within the emitter:

$$p(y) = p_E(0) \, e^{-\left(y/L_{pE} \right)} \tag{7.56}$$

where y is the distance measured moving to the left away from the junction with $p_E(0)$ given by Eq. (7.55). The hole current density flowing at the base-emitter junction is then given by:

$$J_p(0) = -qD_{pE} \left(\frac{dp}{dy} \right)_{y=0} = \frac{qD_{pE}}{L_{pE}} p_E(0) \tag{7.57}$$

This is also the base current density (J_B) because it has been assumed in this section that all the base current is used to supply the injection into the emitter. If the diffusion length for electrons in the base region is much larger than the base width (i.e., when recombination in the base is neglected), the minority carrier concentration in the base region has a linear distribution as shown in the figure. The collector current is then equal to the electron current at the base-emitter junction:

$$J_C = J_n(0) = \frac{qD_{nB}}{W_B} n_B(0) = \frac{qD_{nB}}{W_B} n_{0B} \, e^{qV_{BE}/kT} \tag{7.58}$$

From this equation:

$$n_{\mathrm{B}}(0) = \frac{J_{\mathrm{C}} W_{\mathrm{B}}}{q D_{\mathrm{nB}}} \tag{7.59}$$

Using this expression in Eq. (7.55):

$$p_{\mathrm{E}}(0) = p_{0\mathrm{E}} \left[1 + \frac{J_{\mathrm{C}} W_{\mathrm{B}}}{q D_{\mathrm{nB}} p_{0\mathrm{B}}} \right] e^{q V_{\mathrm{BE}}/kT} \tag{7.60}$$

Substituting this expression in Eq. (7.57):

$$J_{\mathrm{B}} = J_{\mathrm{p}}(0) = \left(\frac{q D_{\mathrm{pE}} p_{0\mathrm{E}}}{L_{\mathrm{pE}}} \right) \left[1 + \frac{J_{\mathrm{C}} W_{\mathrm{B}}}{q D_{\mathrm{nB}} p_{0\mathrm{B}}} \right] e^{q V_{\mathrm{BE}}/kT} \tag{7.61}$$

The common-emitter current gain (β_{E}) *as determined by emitter injection efficiency* under high-level injection conditions in the base region is then obtained by using Eqs. (7.58 and 7.61):

$$\beta_{\mathrm{E}} = \frac{J_{\mathrm{C}}}{J_{\mathrm{B}}} = \frac{D_{\mathrm{nB}} L_{\mathrm{pE}} n_{0\mathrm{B}}}{D_{\mathrm{pE}} W_{\mathrm{B}} p_{0\mathrm{E}}} \frac{1}{[1 + (J_{\mathrm{C}} W_{\mathrm{B}} / q D_{\mathrm{nB}} p_{0\mathrm{B}})]} \tag{7.62}$$

Substituting for the minority carrier densities using Eqs. (7.53 and 7.54):

$$\beta_{\mathrm{E}} = \frac{D_{\mathrm{nB}} L_{\mathrm{pE}} N_{\mathrm{DE}}}{D_{\mathrm{pE}} W_{\mathrm{B}} N_{\mathrm{AB}}} \left(\frac{n_{\mathrm{iB}}}{n_{\mathrm{iE}}} \right)^2 \frac{1}{[1 + (J_{\mathrm{C}} W_{\mathrm{B}} / q D_{\mathrm{nB}} N_{\mathrm{AB}})]} \tag{7.63}$$

In writing this expression, the majority carrier concentration in the base region ($p_{0\mathrm{B}}$) has been replaced with the doping concentration (N_{AB}).

At high collector current densities, the second term in the square brackets becomes dominant, and the current gain decreases inversely with increasing current density. The falloff in the current gain occurs when the collector current density approaches and exceeds a Webster current density:

$$J_{\mathrm{W}} = \frac{q D_{\mathrm{nB}} N_{\mathrm{AB}}}{W_{\mathrm{B}}} \tag{7.64}$$

At current densities well below the Webster current density, the current gain remains constant at a value β_{LL} as given by Eq. (7.42) derived earlier under low-level injection conditions for the base region. Thus, the current gain can be expressed as:

$$\beta_{\mathrm{E}} = \frac{\beta_{\mathrm{LL}}}{[1 + (J_{\mathrm{C}} / J_{\mathrm{W}})]} \tag{7.65}$$

As an example, consider the case of a power N-P-N bipolar transistor with an emitter doping concentration of 2×10^{19} cm^{-3} and base doping concentration of 1×10^{17} cm^{-3}. The common-emitter current gain at low injection levels for this transistor is 25. The Webster current density using these doping concentrations for

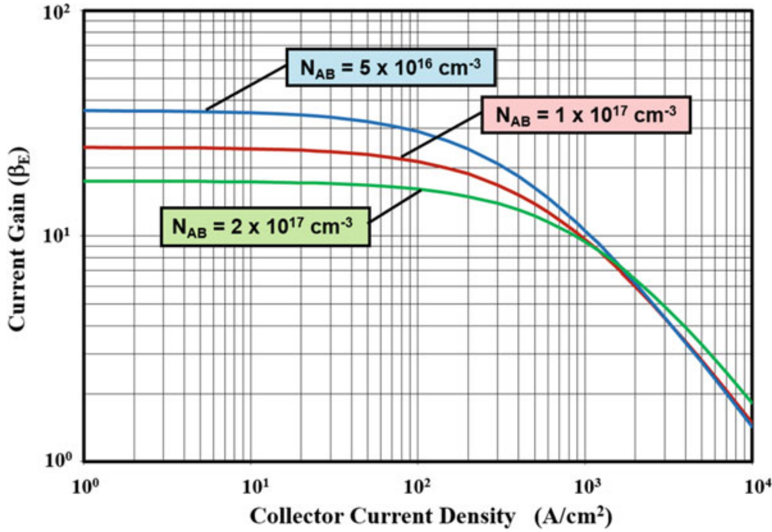

Fig. 7.15 Falloff in the current gain for a N-P-N bipolar power transistor due to high-level injection conditions in the base

the base and emitter regions is 640 A/cm^2. Consequently, the current gain falls off when the collector current density approaches and exceeds this value as shown in Fig. 7.15. When the doping concentration of the P-base region is reduced by a factor of 2x, the common-emitter current gain at low injection levels increases to 36. However, the Webster current density using these doping concentrations for the base and emitter regions is also reduced to 410 A/cm^2. Consequently, the common-emitter current gain falls off at lower current densities resulting in approximately the same gain at high current densities (1000 A/cm^2). Similarly, when the doping concentration of the P-base region is increased by a factor of 2x, the common-emitter current gain at low injection levels decreases to 17.5, and the Webster current density is increased to 1160 A/cm^2. Consequently, the current gain falls off at higher current densities resulting in approximately the same gain (about 10) at high current densities. Such high emitter current densities are encountered in power bipolar transistors due to the emitter current crowding phenomenon discussed later in the chapter.

According to Eq. (7.65), the current gain becomes inversely proportional to the collector current density when it becomes much larger than the Webster current density:

$$\beta_{\mathrm{EH}} = \frac{\beta_{\mathrm{LL}} J_{\mathrm{W}}}{J_{\mathrm{C}}} \tag{7.66}$$

Consequently, the base drive current density required to sustain the collector current is given by:

$$J_{\mathrm{B}} = \frac{J_{\mathrm{C}}}{\beta_{\mathrm{EH}}} = \frac{J_{\mathrm{C}}^2}{\beta_{\mathrm{LL}} J_{\mathrm{W}}} \tag{7.67}$$

Thus, the base drive current increases as the square of the collector current for a power bipolar transistor upon the onset of high-level injection in the base region. This degrades the power gain of the device making the gate control circuit bulky and expensive.

7.4.4 Base Transport Factor

The base transport factor is a measure of the ability for the minority carriers injected from the base-emitter junction to reach the base-collector junction. For an N-P-N transistor, it is expressed in terms of the ratio of the electron current at the base-emitter junction to the electron current at the base-collector junction (see Eq. (7.20)). In the previous section, it was assumed that the diffusion length for electrons (L_{nB}) in the P-base region is much larger than its width (W_{B}). In this case, the base transport factor is equal to unity. However, in a power bipolar transistor, the base width can be relatively large to prevent reach-through breakdown at high collector bias voltages.

The base-emitter junction of the bipolar transistor is forward biased in order to induce current flow. This produces the injection of electrons into the P-base region. These electrons diffuse through the P-base region and arrive at the base-collector junction producing the collector current. The diffusion equation for electrons in the P-base region under steady-state conditions is:

$$\frac{d^2 n}{dy^2} - \frac{n}{L_{\mathrm{nB}}^2} = 0 \tag{7.68}$$

where L_{nB} is the diffusion length for electrons in the base and y is the distance measured moving to the right away from the base-emitter junction. The solution for this equation has the form:

$$n(y) = A\,e^{-y/L_{\mathrm{nB}}} + B\,e^{+y/L_{\mathrm{nB}}} \tag{7.69}$$

where A and B are constants determined by the following boundary conditions. At the base-emitter junction ($y = 0$), the electron concentration is given by:

$$n(0) = n_{\mathrm{B}}(0) = n_{0\mathrm{B}}\,e^{qV_{\mathrm{BE}}/kT} \tag{7.70}$$

due to the forward bias (V_{BE}) across the base-emitter junction. At the base-collector junction, the electron concentration is zero due to the reverse bias:

$$n(W_{\mathrm{B}}) = 0 \tag{7.71}$$

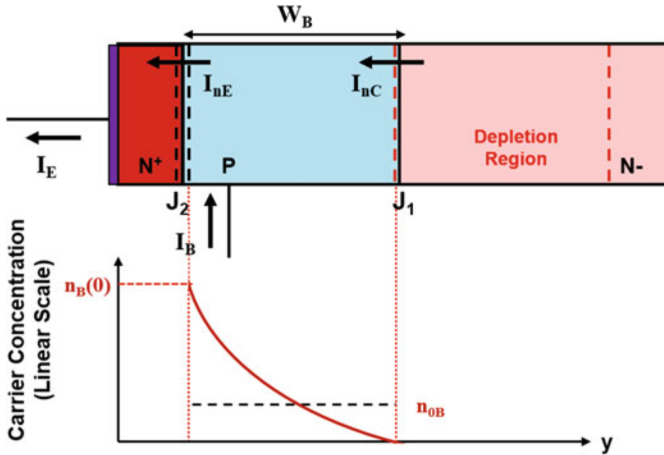

Fig. 7.16 Minority carrier distribution within the N-P-N bipolar power transistor including recombination in the base

Using these boundary conditions to solve for the constants A and B provides the electron concentration profile:

$$n(y) = n_{0B} \left\{ \frac{\sinh[(W_B - y)/L_{nB}]}{\sinh(W_B/L_{nB})} \right\} e^{qV_{BE}/kT} \tag{7.72}$$

This profile for the injected electrons in the P-base region is illustrated in Fig. 7.16 together with the minority carrier concentration in equilibrium.

The electron current at the base-emitter junction (J_{nE}) and the base-collector junction (J_{nC}) can be derived from this electron carrier distribution profile:

$$J_{nE} = -qD_{nB}\left(\frac{dn}{dy}\right)_{y=0} = \frac{qD_{nB}}{L_{nB}}\left(\frac{\cosh(W_B/L_{nB})}{\sinh(W_B/L_{nB})}\right) e^{qV_{BE}/kT} \tag{7.73}$$

$$J_{nC} = -qD_{nB}\left(\frac{dn}{dy}\right)_{y=W_B} = \frac{qD_{nB}}{L_{nB}}\left(\frac{1}{\sinh(W_B/L_{nB})}\right) e^{qV_{BE}/kT} \tag{7.74}$$

Using these equations, the base transport factor is obtained:

$$\alpha_T = \frac{J_{nC}}{J_{nE}} = \frac{1}{\cosh(W_B/L_{nB})} \tag{7.75}$$

The base transport factor is determined by the width of the P-base region relative to the diffusion length for electrons in the base region. If the diffusion length is much larger than the base width, the base transport factor becomes equal to unity. When the base width is increased in order to suppress reach-through breakdown, the base transport factor becomes less than unity.

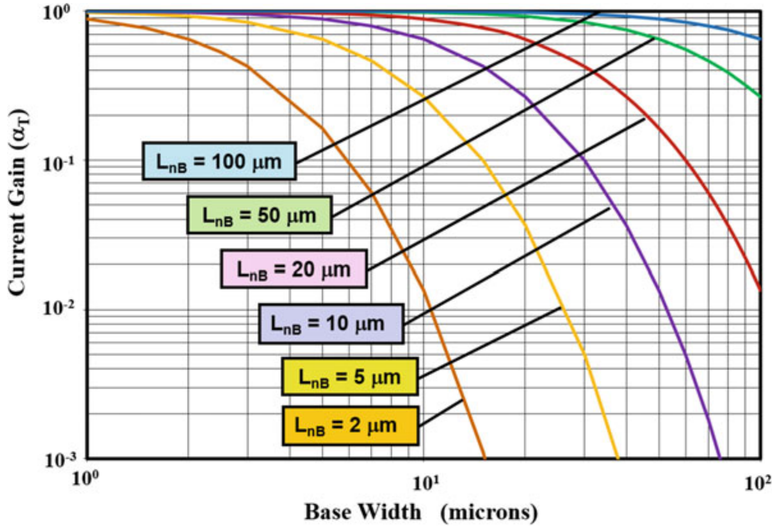

Fig. 7.17 Base transport factor limited common-base current gain for the N-P-N bipolar power transistor

The variation of the common-base current gain (α_T) is shown in Fig. 7.17 as a function of the base width for various values for the electron diffusion length in the base region. From this graph, it can be concluded that a diffusion length of at least 50 μm is required in order to achieve a common-base current gain close to unity for a base width of 10 μm. For a typical base doping concentration of 1×10^{17} cm^{-3}, the electron mobility (μ_{nB}) is 750 cm^2/V-s leading to a diffusion coefficient (D_{nB}) of 19.4 cm^2/s. Based upon this value, the minority carrier lifetime in the P-base region must exceed 1.3 μs to achieve a high current gain.

The common-emitter current gain, *as determined exclusively by the base transport factor*, is given by:

$$\beta_T = \frac{\alpha_T}{(1 - \alpha_T)} = \frac{1}{[\cosh(W_B/L_{nB}) - 1]} \tag{7.76}$$

The variation of the common-emitter current gain (β_T) is shown in Fig. 7.18 as a function of the base width for various values for the electron diffusion length in the base region. From this graph, it can be concluded that a diffusion length of 50 μm will produce a common-emitter current gain of 50 for a base width of 10 μm. The current gain drops to only 8 if the diffusion length for electrons in the base is reduced to 20 μm. Consequently, the degradation of the current gain due to finite recombination in the base region must be accounted for during the analysis of power bipolar transistors.

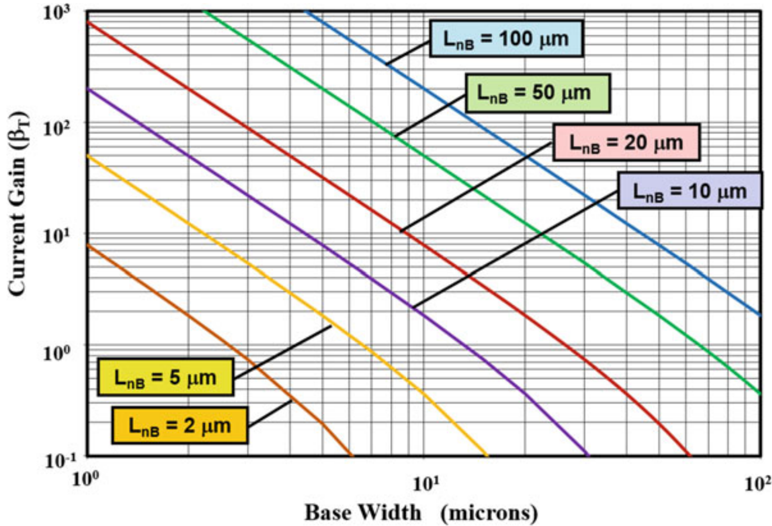

Fig. 7.18 Common-emitter current gain for the N-P-N bipolar power transistor as limited by the base transport factor

7.4.5 *Base Widening at High Collector Current Density*

When the collector current density is large, another phenomenon that reduces the current gain is an increase in the *effective base width*, which is referred to as the *Kirk effect* [13]. This phenomenon occurs when the bipolar transistor is biased in its forward active regime of operation with a large collector bias voltage. The collector bias is supported across the base-collector junction with a triangular profile at low collector current densities as shown in Fig. 7.19 by the line labeled *a*. This profile is governed by the solution for Poisson's equation with the doping concentration of the N-drift region determining the charge in the depletion region, as previously discussed in Chap. 3:

$$\frac{dE}{dy} = -\frac{qN_D}{\varepsilon_S} \tag{7.77}$$

With a reverse biased base-collector junction, the current in the bipolar transistor is transported through the collector drift region by electrons drifting under the influence of the electric field in the depletion region. At large collector bias voltages, the electric field in the depletion region is sufficient to accelerate the electrons to their saturated drift velocity ($v_{sat,n}$), as discussed in Chap. 2. The concentration of the electrons in the depletion region is then related to the collector current density (J_C) by:

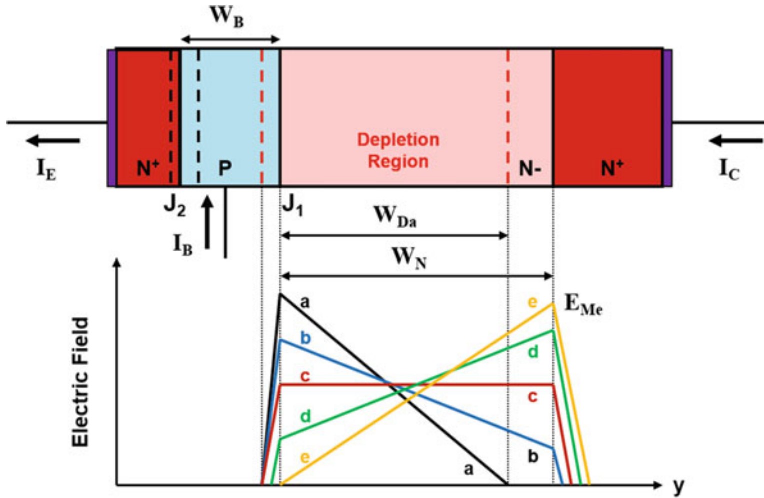

Fig. 7.19 Electric field profiles in the N-P-N bipolar power transistor at various collector current levels

$$n = \frac{J_C}{q v_{sat,n}} \tag{7.78}$$

This equation indicates that the concentration of electrons in the depletion region increases in proportion to the collector current density. As the collector current density increases, the electron concentration in the drift region becomes comparable in magnitude to the charge for the donor atoms in the drift region. The compensation of the positive charge due to the donors by the negative charge due to the electrons must be accounted for in determining the electric field profile.

Poisson's equation that governs the electric field distribution at high collector current densities is given by:

$$\frac{dE}{dy} = -\frac{q}{\varepsilon_S}[N_D - n] \tag{7.79}$$

The electric field profile is then given by:

$$E(y) = E(0) - \frac{q}{\varepsilon_S}[N_D - n]y \tag{7.80}$$

Using Eq. (7.78) for the electron concentration:

$$E(y) = E(0) - \frac{q}{\varepsilon_S}\left[N_D - \left(\frac{J_C}{q v_{sat,n}}\right)\right]y \tag{7.81}$$

where $E(0)$ is the electric field at the base-collector junction. This expression for the electric field indicates that the profile is linear in shape and that its slope becomes

smaller as the collector current density is increased. Thus, for the same applied collector bias, the electric field profile changes to the one labeled *b* with a large collector current density J_{Cb}. Note that the reduction of the slope for the electric field in the drift region promotes its punch-through to the N^+ substrate as illustrated in the figure with the electric field truncated in the N^+ substrate due to its relatively high doping.

As the collector current density is increased, the electric field profile eventually becomes completely flat as shown in the figure by the profile labeled *c*. A flat electric field profile occurs when the charge in the depletion region is equal to zero. In this case, the number of electrons per unit volume transported through the depletion region is exactly equal to the doping concentration for the drift region. This corresponds to the second term in Eq. (7.81) becoming equal to zero, which occurs at a collector current density:

$$J_{Cc} = qv_{sat,n}N_D \tag{7.82}$$

When the collector current density is increased even further, the electron concentration in the drift region exceeds the doping concentration of the donors in the drift region. In this case, the net charge in the depletion region becomes negative. The reversal of the net charge governing Poisson's equation for the depletion region produces a reversal of the slope for the electric field profile as shown by the case labeled *d* in the figure. This electric field profile is then described by:

$$E(y) = E(0) + \frac{q}{\varepsilon_S}\left[\left(\frac{J_C}{qv_{sat,n}}\right) - N_D\right]y \tag{7.83}$$

where the term in square brackets is positive. Under the same applied collector bias voltage, the peak in the electric field profile shifts from the base-collector junction to the interface between the N-drift region and the N^+ substrate as shown in the figure.

Eventually, at an even larger collector current density, the electric field becomes equal to zero at the base-collector junction as shown by the profile labeled *e* in the figure. The electric field profile in this case is given by:

$$E(y) = \frac{q}{\varepsilon_S}\left[\left(\frac{J_C}{qv_{sat,n}}\right) - N_D\right]y \tag{7.84}$$

The maximum electric field occurs at the interface between the N-drift region and the N^+ substrate at a distance $y = W_N$:

$$E_{Me} = \frac{q}{\varepsilon_S}\left[\left(\frac{J_{Ce}}{qv_{sat,n}}\right) - N_D\right]W_N \tag{7.85}$$

The collector voltage supported by the electric field profile is given by:

$$V_C = \frac{1}{2}E_{Me}W_N = \frac{q}{2\varepsilon_S}\left[\left(\frac{J_{Ce}}{qv_{sat,n}}\right) - N_D\right]W_N^2 \tag{7.86}$$

The collector current density can be expressed in terms of the device physical parameters and the applied collector bias voltage from this equation:

$$J_{\mathrm{Ce}} = qv_{\mathrm{sat},n}\left(\frac{2\varepsilon_{\mathrm{S}}V_{\mathrm{C}}}{qW_{\mathrm{N}}^{2}} + N_{\mathrm{D}}\right) = J_{\mathrm{K}} \tag{7.87}$$

The collector current density at which the electric field becomes equal to zero at the base-collector junction is referred to as the *Kirk current density (J_K)* as indicated in the above equation.

The Kirk current density is of significance for a power bipolar transistor because a *current-induced base region* develops within the collector drift region when the collector current density exceeds its magnitude. The electric field profile *f* for this case is illustrated in Fig. 7.20. Note that a neutral region develops in the drift region adjacent to the base-collector junction. The electrons injected into the P-base region must now diffuse not only through the physical base width (W_B) but through an extra distance called the *current-induced base width* (W_{CIB}). The effective base width for the bipolar transistor then becomes:

$$W_{\mathrm{B,EFF}} = W_{\mathrm{B}} + W_{\mathrm{CIB}} \tag{7.88}$$

This enlargement of the base width reduces the base transport factor and the current gain for the bipolar transistor.

When the electric field profile has taken the form shown in Fig. 7.20, the electron concentration in the drift region has become much larger than the doping concentration of the drift region. This electric field profile can therefore be expressed as:

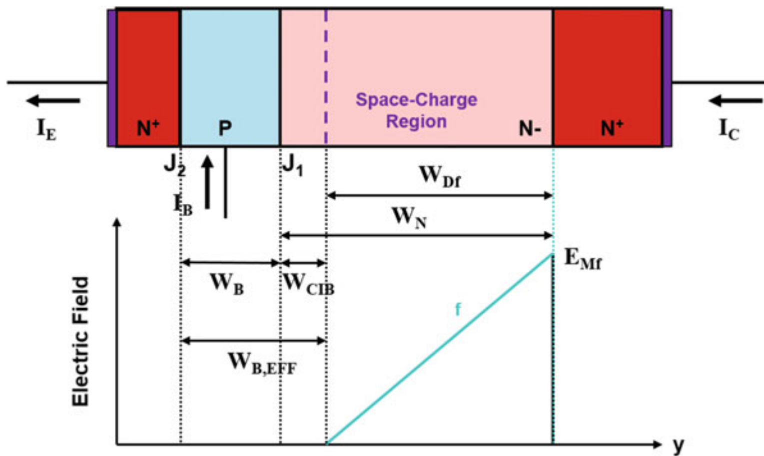

Fig. 7.20 Electric field profile in the N-P-N bipolar power transistor with a current-induced base region

$$E(y) = \left(\frac{J_{\mathrm{Cf}}}{\varepsilon_{\mathrm{S}} v_{\mathrm{sat},n}} - \frac{qN_{\mathrm{D}}}{\varepsilon_{\mathrm{S}}} \right) y \tag{7.89}$$

In this expression, J_{Cf} is the collector current density corresponding to the electric field profile shown in Fig. 7.20. If the electric field supported in the N^+ substrate is neglected due to its high doping concentration, the width of the depletion region is given by:

$$W_{\mathrm{Df}} = \sqrt{\frac{2\varepsilon_{\mathrm{S}} V_{\mathrm{C}}}{[(J_{\mathrm{Cf}}/v_{\mathrm{sat},n}) - qN_{\mathrm{D}}]}} \tag{7.90}$$

The width of the current-induced base region is then given by:

$$W_{\mathrm{CIB}} = W_{\mathrm{N}} - W_{\mathrm{Df}} = W_{\mathrm{N}} - \sqrt{\frac{2\varepsilon_{\mathrm{S}} V_{\mathrm{C}}}{[(J_{\mathrm{Cf}}/v_{\mathrm{sat},n}) - qN_{\mathrm{D}}]}} \tag{7.91}$$

and the effective base width for the bipolar transistor becomes:

$$W_{\mathrm{B,EFF}} = W_{\mathrm{B}} + W_{\mathrm{CIB}} = W_{\mathrm{B}} + W_{\mathrm{N}} - \sqrt{\frac{2\varepsilon_{\mathrm{S}} V_{\mathrm{C}}}{[(J_{\mathrm{Cf}}/v_{\mathrm{sat},n}) - qN_{\mathrm{D}}]}} \tag{7.92}$$

The common-base and common-emitter current gains, as limited by recombination in the base region, are then given by Eqs. (7.75 and 7.76) with the effective base width ($W_{\mathrm{B,EFF}}$) substituted in place of the physical base width (W_{B}). As an example, consider the case of a power N-P-N bipolar transistor with a physical base width of 5 μm (W_{B}) and an N-drift region thickness (W_{N}) of 30 μm with a doping concentration of 1×10^{14} cm^{-3}. The Kirk current density for the onset of the current-induced base in this case is 736 A/cm^2 at a collector bias (V_{C}) of 250 V. The width of the current-induced base region is shown in Fig. 7.21 for this case as a function of the collector current density. Note that the current-induced base width becomes equal in magnitude to the physical base width at a collector current density of 1000 A/cm^2 in this example leading to an effective base width of twice the physical base width.

The physical basis for the increase in the width of the current-induced base with increasing collector current density is related to the change in the electric field profile as illustrated in Fig. 7.22. At a lower collector current density (J_{C1}), the slope for the electric field profile is more gradual due to the smaller electron density in the drift region. When the collector current density is increased (J_{C2}), the slope for the electric field profile becomes steeper due to the larger electron density in the drift region. The same collector bias voltage is then supported across a smaller depletion width, with a larger maximum electric field, producing an enlargement of the current-induced base width.

The impact of the current-induced base width on the common-base and common-emitter current gains is shown in Figs. 7.23 and 7.24 for the power bipolar transistor with the parameters given above as an example. It can be observed that the current

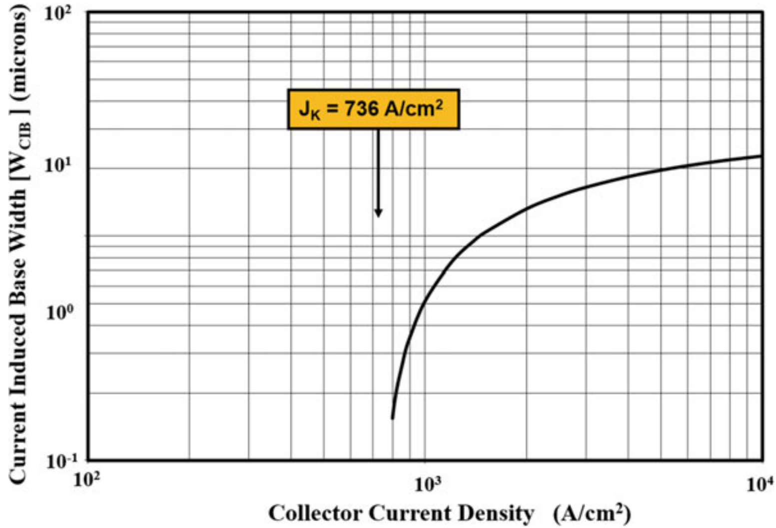

Fig. 7.21 Current-induced base width for the N-P-N bipolar power transistor

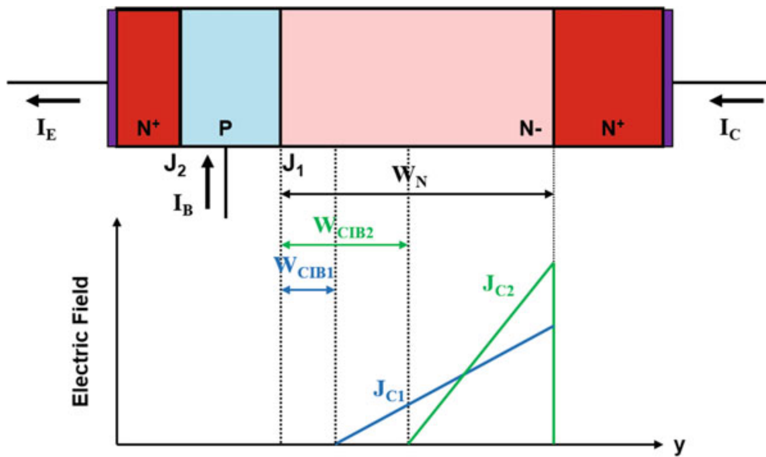

Fig. 7.22 Impact of the collector current density on the electric field profile for the N-P-N bipolar power transistor

gain begins to decrease when the width of the current-induced base region becomes comparable to the physical base width at a collector current density of about 1000 A/cm^2. This has a strong impact on the current gain when the diffusion length for the electrons is small. It is therefore necessary to account for this phenomenon when designing power bipolar transistors because high collector current densities are created by emitter current crowding under on-state operating conditions.

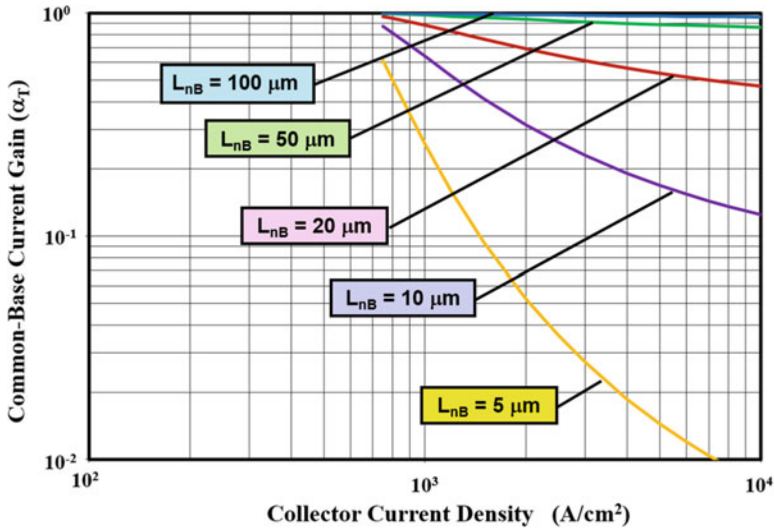

Fig. 7.23 Impact of base widening on the common-base current gain for the N-P-N bipolar power transistor

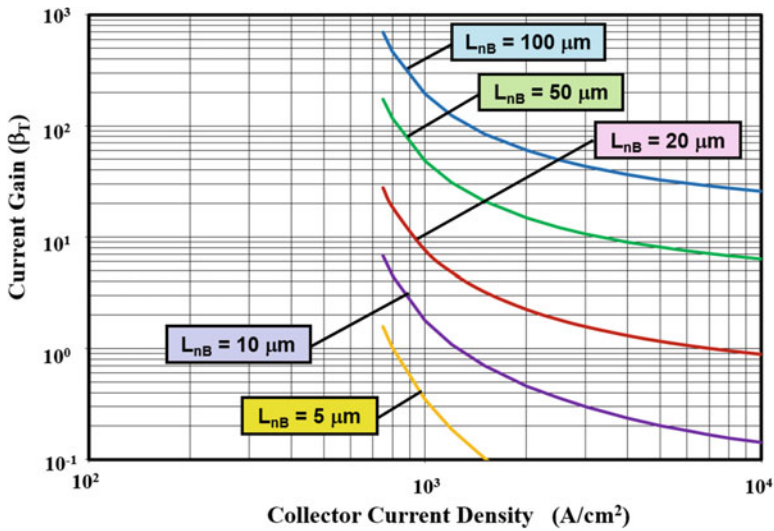

Fig. 7.24 Impact of base widening on the common-emitter current gain for the N-P-N bipolar power transistor

The Kirk current density and the width of the current-induced base region are dependent on the collector bias voltage as indicated by Eqs. (7.87 and 7.91). This is illustrated in Fig. 7.25 for the case of the power bipolar transistor with the parameters

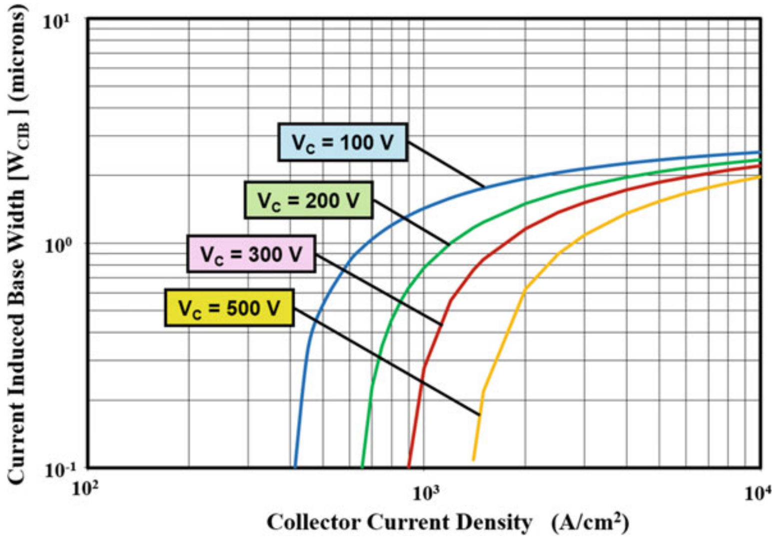

Fig. 7.25 Impact of the collector bias voltage on the current-induced base width for the N-P-N bipolar power transistor

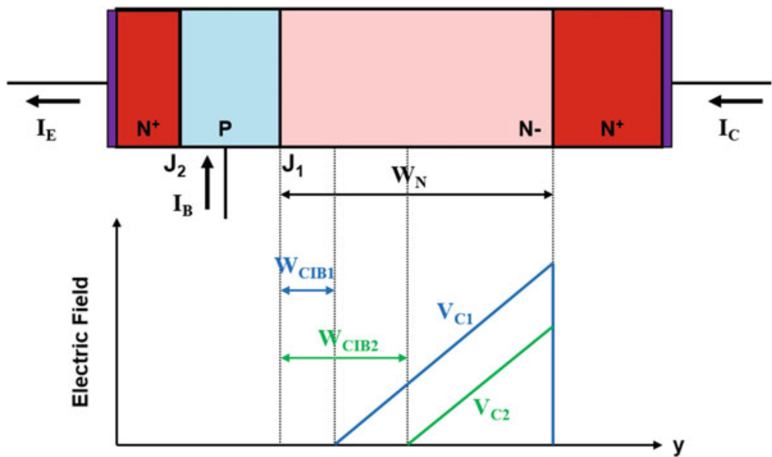

Fig. 7.26 Impact of the collector bias voltage on the electric field profile for the N-P-N bipolar power transistor

previously used as the example. The Kirk current density becomes smaller when the collector bias voltage is reduced and the width of the current-induced base becomes larger. The physical basis for this change is related to the change in the electric field profile as illustrated in Fig. 7.26. It can be observed that a smaller collector bias voltage (V_{C2}) is supported over a smaller space-charge region width producing an enlargement of the current-induced base width.

Simulation Example
In order to provide further insight into the physics of operation of the power bipolar transistor, the results of two-dimensional numerical simulations are provided in this section for a variety of device structures. The doping profile for all the structures is similar to that shown in Fig. 7.8. The emitter and base doping concentrations were varied to elucidate the impact on the current gain. In addition, the impact of bandgap narrowing and Auger recombination in the emitter is provided here.

The baseline N-P-N bipolar power transistor structure (bjt8) had a Gaussian emitter diffusion with a surface concentration of 1×10^{20} cm^{-3} and a Gaussian P-base diffusion with a surface concentration of 2×10^{17} cm^{-3}. The junction depth for the P-base region was 10 μm and that for the emitter region 1 μm leading to a base width of 9 μm. A lifetime (τ_{n0}, τ_{p0}) of 1 μs was used for all the structures. The output characteristics for the device were derived by using a base drive current density ranging from 1 to 7 A/cm^2. The resulting output characteristics are shown in Fig. 7.27. The current gain is observed to be relatively independent of the collector bias voltage once it exceeds 200 V due to the high output resistance.

The current gain extracted from the simulations for the baseline bipolar power transistor structure (bjt8) is shown in Fig. 7.28 as a function of the collector current density. Note that the average collector current density (total collector current divided by the cell area) has been used for this plot. It can be observed that the current gain (beta) is relatively constant with a value of about 15 for collector current densities below 10 A/cm^2. As the collector current density is increased beyond this point, the current gain falls off. The rate of falloff in the current gain is much steeper

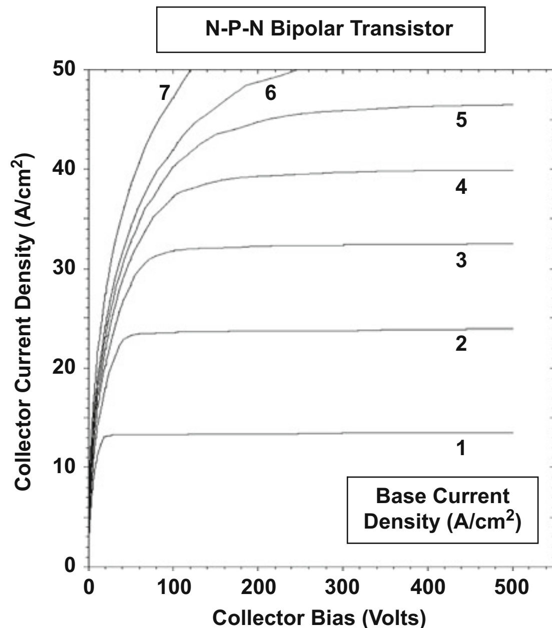

Fig. 7.27 Output characteristics for a N-P-N bipolar power transistor

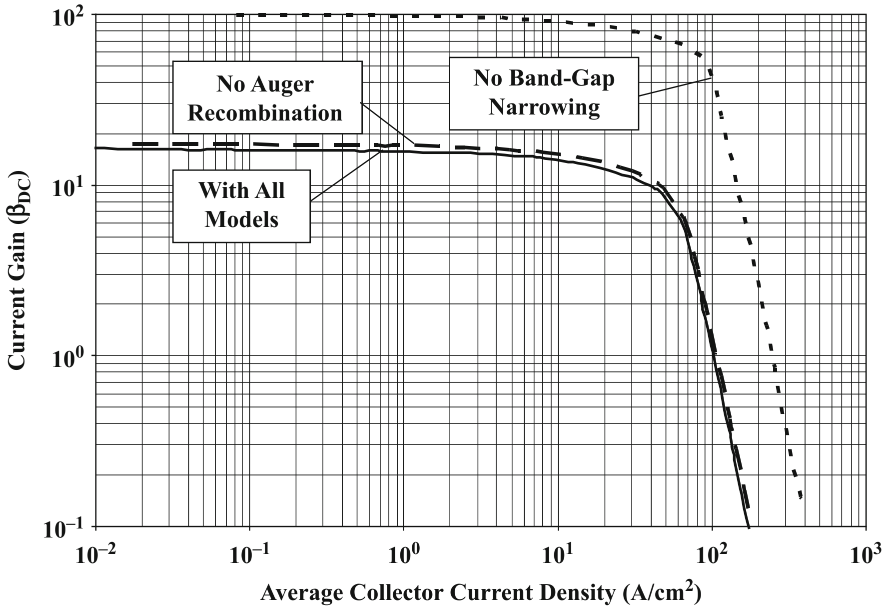

Fig. 7.28 Current gain (β) for a N-P-N bipolar power transistor

than predicted by either the Webster effect or the Kirk effect. This is due to strong impact of emitter current crowding as the base drive current is increased.

The current crowding at the emitter edge located in proximity to the base contact is shown in Fig. 7.29 for the baseline bipolar power transistor structure. It can be observed that the collector current density is uniform at the lowest base drive current of 0.05 A/cm^2. When the base drive current density is raised to 0.5 A/cm^2, the collector current density becomes nonuniform with a much larger value near the base contact. The physics responsible for the current crowding phenomenon is discussed in a later section of this chapter. As the base drive current density is increased, the nonuniformity of the collector current density becomes worse resulting in extremely high current densities at the edge of the emitter. This enhancement of the collector current density exacerbates the Webster and Kirk effects producing a faster falloff in the current gain with average collector current density than described by the models which are based upon a uniform (or local) current density.

The impact of the semiconductor models on the current gain for the baseline bipolar power transistor can be extracted from the numerical simulations by turning them on and off during the analysis. When the Auger recombination phenomenon is turned off, the current gain increases only slightly as shown in Fig. 7.28 by the dashed line. In contrast, a much stronger effect is observed when the bandgap narrowing effect is turned off as shown by the dotted line in this figure. The current gain increases from about 14 to 75, which is consistent with the increase in the gain obtained using Eq. (7.42) with equal values for the intrinsic carrier concentration in the emitter and base regions.

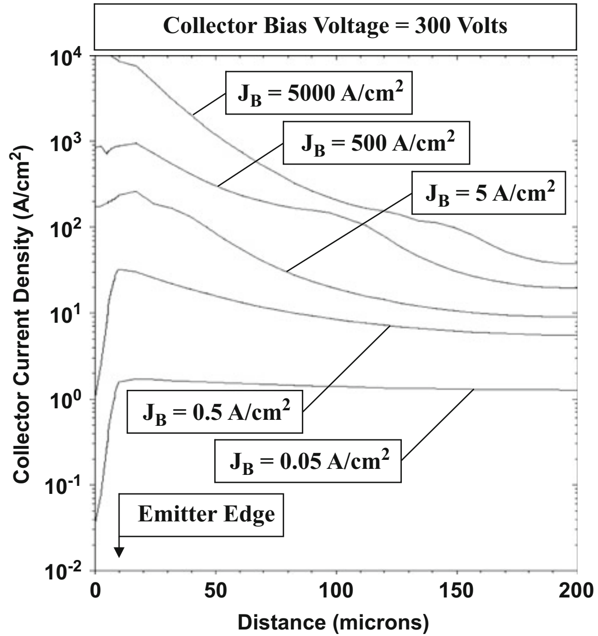

Fig. 7.29 Emitter current crowding in a N-P-N bipolar power transistor

The impact of the doping concentration of the emitter region on the gain of the bipolar power transistor is illustrated in Fig. 7.30. Here, the surface concentration of the N^+ emitter diffusion was changed from 1×10^{20} cm^{-3} for the baseline bipolar power transistor structure to 1×10^{19} cm^{-3}. It can be observed that the current gain at collector current densities below 10 A/cm^2 decreases from about 15 to 10 due to the smaller emitter doping concentration. In these structures, the P-base doping profile was created using a surface concentration of 2×10^{17} cm^{-3}. From the doping profile shown in Fig. 7.8 for the baseline structure, it is obvious that the doping concentration in the emitter and base regions varies over many orders of magnitude. In order to relate the simulation results to the analytical model, it is therefore necessary to define an effective doping concentration for these regions representative of uniformly doped regions with the same thickness. From the doping profile provided in Fig. 7.8, an effective doping concentration of 7×10^{16} cm^{-3} can be estimated for the P-base region. At this doping concentration, the diffusion coefficient for electrons in the base is found to be 23.3 cm^2/s, and the intrinsic carrier concentration is found to be 1.57×10^{10} cm^{-3} based upon the models and information provided in Chap. 2. The corresponding parameters for the N^+ emitter region for the two cases are provided in Fig. 7.31 together with the value for beta obtained using these values in the analytical model (Eq. 7.42). The analytical model predicts the appropriate value for the gain with judicious choice of the effective doping concentrations for the emitter and base regions.

The impact of changing the P-base doping profile can be observed in Fig. 7.32 where the current gain is plotted for various values for the surface concentration used

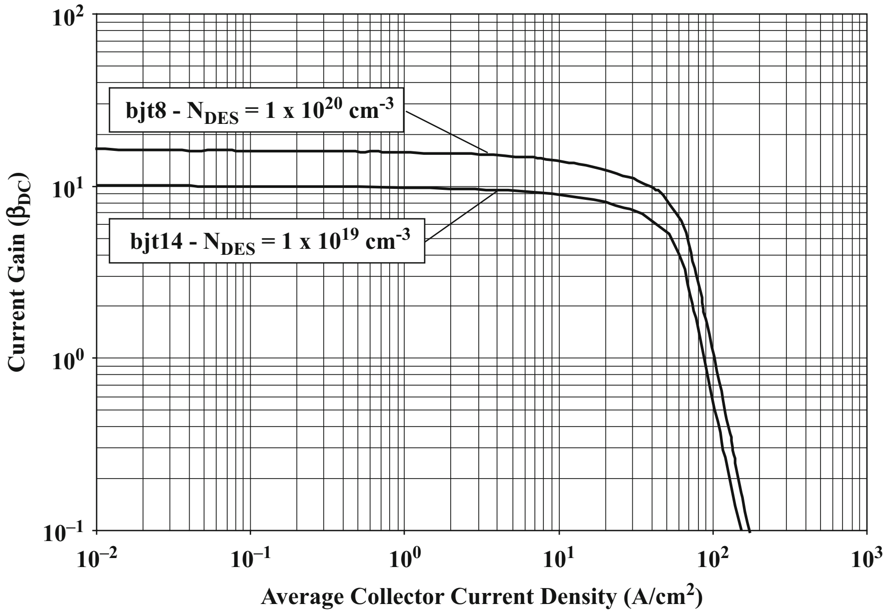

Fig. 7.30 Current gain (β) for N-P-N bipolar power transistors

Structure	Effective N_{DE} (cm^{-3})	D_{pE} (cm^2/s)	n_{iE} (cm^{-3})	Beta
bjt8	2×10^{19}	1.30	9.7×10^{10}	15.0
bjt14	5×10^{18}	3.52	3.69×10^{10}	9.5

Fig. 7.31 Analytically calculated parameters for N-P-N bipolar power transistors: impact of emitter doping concentration

to produce the P-base region. In these structures, the N^+ emitter doping profile was created using a surface concentration of 1×10^{20} cm^{-3}. As the doping concentration in the P-base region increases, the current gain decreases as expected. The P-base surface concentration must be reduced to 1×10^{17} cm^{-3} to obtain a gain of 20. This makes the structure prone to reach-through limited breakdown. In order to relate the current gain for these structures with the analytical model, it is necessary to extract an effective doping concentration for the P-base region. This is provided in Fig. 7.33 together with values for the diffusion coefficient for electrons and the intrinsic carrier concentration in the base region. The diffusion coefficient for holes and the intrinsic carrier concentration of the emitter region are given in Fig. 7.31 (structure bjt8) for this case. The current gain computed by using the analytical model (Eq. 7.42) is

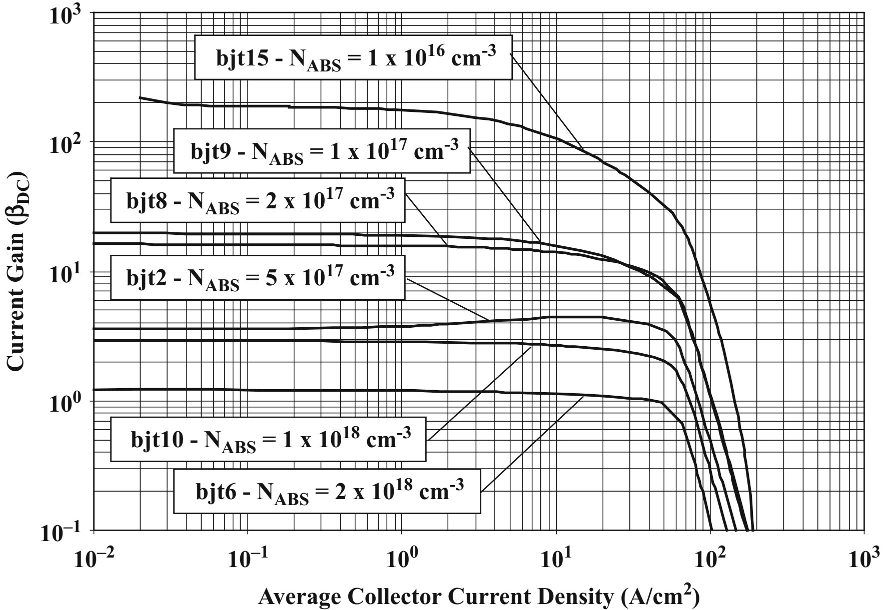

Fig. 7.32 Current gain (β) for N-P-N bipolar power transistors: impact of P-base doping concentration

Structure	Effective N_{AB} (cm^{-3})	D_{nB} (cm^2/s)	n_{iB} (cm^{-3})	Beta
bjt6	6×10^{17}	8.94	1.95×10^{10}	1.03
bjt10	3×10^{17}	12.85	1.77×10^{10}	2.45
bjt2	2×10^{17}	15.6	1.70×10^{10}	4.12
bjt8	7×10^{16}	23.3	1.57×10^{10}	15.0
bjt9	5×10^{16}	25.5	1.54×10^{10}	22.1
bjt15	6×10^{15}	33.3	1.50×10^{10}	228

Fig. 7.33 Analytically calculated parameters for N-P-N bipolar power transistors: impact of P-base doping concentration

provided in Fig. 7.33. Comparing these values with those in Fig. 7.32 obtained with the simulations at collector current densities below 1 A/cm^2, it can be concluded that the analytical model predicts the appropriate value for the gain with judicious choice of the effective doping concentrations for the emitter and base regions.

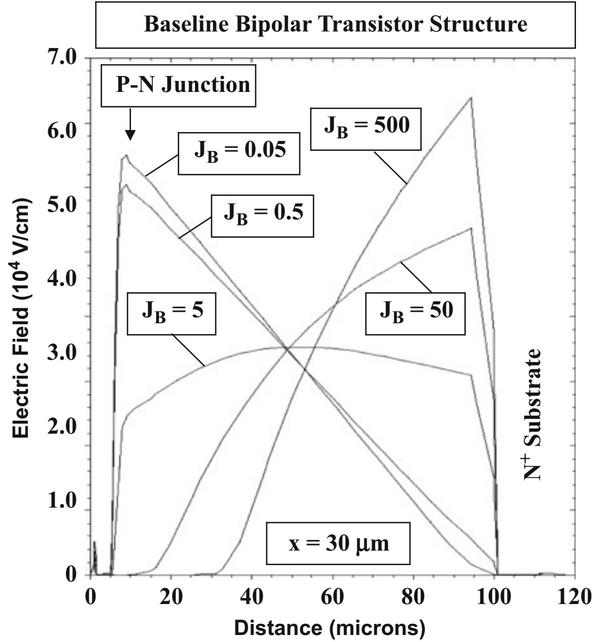

Fig. 7.34 Electric field profiles for a N-P-N bipolar power transistor when operating at high collector current densities: base current dependence

As described earlier in the section, the reduction of the current gain at very high current levels (the Kirk effect) is associated with a widening of the effective base width due to the formation of a current-induced neutral region within the N-drift region adjacent to the base region. The formation of the current-induced base region can be observed by examination of the electric field profile in the bipolar power transistor. As an example, the electric field profiles are shown in Fig. 7.34 for the baseline bipolar power transistor structure (bjt8) under increasing base drive current conditions at an x location of 30 μm from the left-hand side in the cross section shown in Fig. 7.7. At the lowest base drive current density of 0.05 A/cm^2, the peak of the electric field occurs at the junction between the P-base region and the N-drift region similar to the case of normal reverse blocking conditions for a P-N junction. When the base drive current density is increased to 0.5 A/cm^2, the slope of the electric field profile becomes slightly smaller due to the additional (negative) charge associated with the electrons transported through the drift region. When the base drive current density is increased to 5 A/cm^2, the slope of the electric field profile becomes flat indicating that the additional (negative) charge associated with the electrons transported through the drift region is now equal to the background charge (positive) due to donors in the drift region (5×10^{13} cm^{-3}). At an even larger base drive current density of 50 A/cm^2, the slope of the electric field profile reverses with its peak now located at the interface between the N-drift region and the N$^+$ substrate. Under these conditions, a current-induced base region is observed below the P-base region. When the base drive current density is increased to 500 A/cm^2, there is an increase in the width of the current-induced base region. These electric field profiles

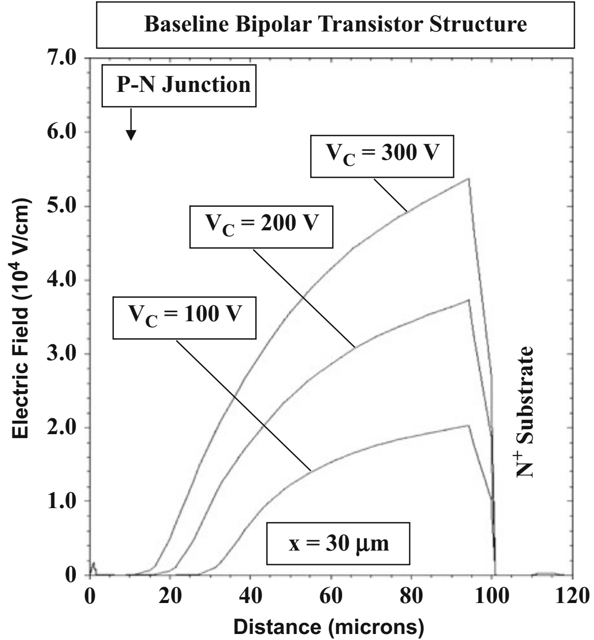

Fig. 7.35 Electric field profiles for a N-P-N bipolar power transistor when operating at high collector current densities: collector voltage dependence

are similar to those shown in Figs. 7.19 and 7.22 for the analysis of the Kirk effect confirming the validity of the underlying physical mechanism responsible for the reduction of the gain at very high collector current levels.

The impact of changes to the collector bias voltage on the width of the current-induced base region can be observed in Fig. 7.35. These profiles were obtained using a base drive current density of 50 A/cm^2. The width of the current-induced base region becomes larger when the collector bias is reduced leading to a reduction of the current gain. These results are consistent with plots in Fig. 7.26 providing further validation for the model.

7.5 Emitter Current Crowding

The analytical treatment for the current transport within the bipolar power transistor was performed in the previous sections under one-dimensional conditions. This analysis is pertinent for a local region under the emitter within the transistor. The current distribution within the emitter in a bipolar power transistor is however not uniform. The drive current applied at the base terminal of the bipolar power transistor must flow through the base region to reach the center of the emitter finger as illustrated in Fig. 7.36. A voltage drop is produced by this current flow in the P-base region due to its finite resistance (R_B). The largest forward bias across the

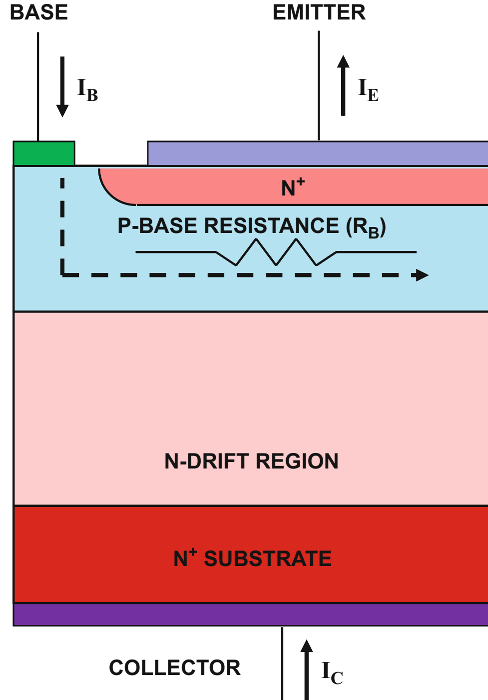

Fig. 7.36 Base drive current flow within the N-P-N bipolar power transistor

emitter-base junction then occurs in the vicinity of the base contact with smaller base-emitter voltage available at the center of the emitter finger to induce injection of electrons into the base region. Consequently, the emitter (and collector) current density are nonuniform with their highest values under the emitter region located in proximity with the base contact. Analytical treatment of the emitter current crowding phenomenon can be performed under low-level and high-level injection conditions in the P-base region.

7.5.1 Low-Level Injection in the Base

Analytical treatment for the emitter current crowding under low-level injection conditions can be performed under certain simplifying assumptions [14, 15]. A cross section of the bipolar power transistor is illustrated in Fig. 7.25 with half of the emitter finger with a width of W_E. A linear geometry is assumed for the transistor with an emitter finger length L_E orthogonal to the cross section in the figure. Consider a segment of the emitter finger of width dx located at a distance of x from the edge of the emitter located closest to the base contact. The emitter current flowing through the segment is given by:

$$dI_E(x) = J_E(x)\,L_E.dx \tag{7.93}$$

where $J_E(x)$ is the local emitter current density at a distance x from the edge of the emitter located closest to the base contact. The base current required to support this emitter current is given by:

$$dI_B(x) = (1-\alpha)\,dI_E(x) = (1-\alpha).J_E(x)\,L_E.dx \tag{7.94}$$

In writing this equation, it has been assumed that the current gain is independent of the emitter current density to simplify the analysis.

The voltage drop produced in the base region across the segment due to the base current flow is given by:

$$dV_{BE}(x) = dI_B(x)\,dR_B = dI_B(x)\left(\frac{\rho_{B0}dx}{W_B L_E}\right) \tag{7.95}$$

where ρ_{B0} is the resistivity of the P-base region:

$$\rho_{B0} = \frac{1}{q\mu_p N_{AB}} \tag{7.96}$$

where N_{AB} is the acceptor doping concentration for the P-base region. In writing this equation, any depletion of the P-base region due to the applied collector bias has been neglected. Transposing dx and then taking the derivative of Eq. (7.95):

$$\frac{d^2V_{BE}(x)}{dx^2} = \frac{\rho_{B0}}{W_B L_E}\frac{dI_B(x)}{dx} \tag{7.97}$$

Using Eq. (7.94):

$$\frac{d^2V_{BE}(x)}{dx^2} = \frac{\rho_{B0}}{W_B}(1-\alpha)J_E(x) \tag{7.98}$$

The emitter current density at location x is determined by the local forward voltage drop across the base-emitter junction:

$$J_E(x) = J_{S,LL}e^{qV_{BE}/kT} \tag{7.99}$$

where $J_{S,LL}$ is the diode saturation current density under low-level injection conditions (see Eq. (5.14) derived for a diode operating under low-level injection conditions). Using this expression in Eq. (7.98) yields:

$$\frac{d^2V_{BE}(x)}{dx^2} = \frac{\rho_{B0}}{W_B}(1-\alpha)J_{S,LL}e^{qV_{BE}(x)/kT} \tag{7.100}$$

A general solution for this equation is of the form:

$$V_{BE}(x) = A \ln (Bx + C) \tag{7.101}$$

where A, B, and C are constants. Substitution into Eq. (7.100) allows extraction of these constants:

$$A = -\frac{2kT}{q} \tag{7.102}$$

$$B = -\sqrt{\frac{q\rho_{B0}}{2kTW_B}(1-\alpha)J_{S,LL}} \tag{7.103}$$

$$C = e^{-qV_{BE}(0)/2kT} \tag{7.104}$$

where $V_{BE}(0)$ is the base-emitter bias at the edge of the emitter closest to the base contact. Using this voltage distribution in Eq. (7.99) yields:

$$J_E(x) = \frac{J_E(0)}{(1 + x/x_{0LL})^2} \tag{7.105}$$

where x_{0LL} is a *current crowding parameter under low-level injection conditions in the P-base region* given by:

$$x_{0LL} = \sqrt{\frac{2kTW_B}{q(1-\alpha)\rho_{B0}J_E(0)}} \tag{7.106}$$

The emitter current density $J_E(0)$ at the edge of the emitter closest to the base contact can be obtained by using Eq. (7.99) with the applied base-emitter bias $V_{BE}(0)$ at the base contact.

The distribution of the emitter current within the bipolar power transistor is shown in the lower part of Fig. 7.37 for various cases of the ratio (x_{0LL}/W_E). It can be observed from the plots that the emitter current density is larger at the edge of the emitter closest to the base contact. This is referred to as *emitter current crowding*. The emitter current crowding is observed to worsen as the ratio (x_{0LL}/W_E) becomes smaller. Using a typical base width of 10 μm, a current gain (alpha) of 0.95, and a P-base doping concentration of 1×10^{17} cm^{-3}, yields a value for x_{0LL} of 62 μm at an emitter current density of 100 A/cm^2 at the edge of the emitter closest to the base contact. This corresponds to a ratio (x_{0LL}/W_E) of 0.31 for an emitter width of 200 μm, which would result in significant current crowding as shown in Fig. 7.37. According to Eq. (7.106), the value for x_{0LL} becomes larger when the current gain increases. This is due to the smaller base current required to sustain current flow within the transistor, which produces a smaller voltage drop along the base resistance. The value for x_{0LL} becomes larger when the base resistivity is reduced by increasing its doping level. However, the resulting improvement in current distribution is obtained with a lower current gain, partially canceling the benefit derived from the lower base resistivity.

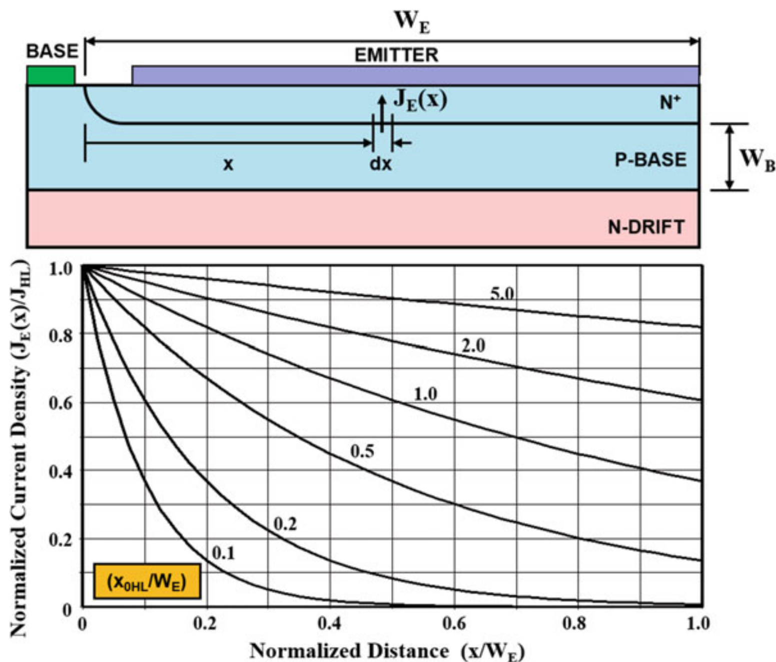

Fig. 7.37 Emitter current distribution within the bipolar power transistor with low level injection in the base

The current crowding parameter is a function of the doping concentration of the P-base region because this determines not only the resistivity of the P-base region but also the current gain (alpha) of the transistor. As the doping concentration of the P-base region is increased, the resistivity decreases, while the current gain becomes smaller due a reduction of the emitter injection efficiency. The net result is a relatively weak dependence of the current crowding parameter on the doping concentration in the P-base region with a minimum value at a doping concentration of about 5×10^{17} cm^{-3} as illustrated in Fig. 7.38.

However, the current crowding parameter decreases significantly with increasing emitter current density at the edge of the emitter closest to the base contact. This can also be observed in Fig. 7.38 where the emitter current density at the edge of the emitter has been used as a parametric variable. This implies that the current crowding will become worse as the transistor is driven harder to try to obtain a larger collector current. The enhanced current crowding aggravates the current gain reduction mechanisms producing a more rapid drop-off in the current gain (see simulation results in the previous section). Note that the impact of high emitter current density on the current gain has been ignored when making the plots in Fig. 7.38 in order to simplify the analysis. Inclusion of the impact of the reduction of the current gain due to high-level injection in the P-base region will make the current crowding parameter smaller enhancing the current crowding of the emitter current density.

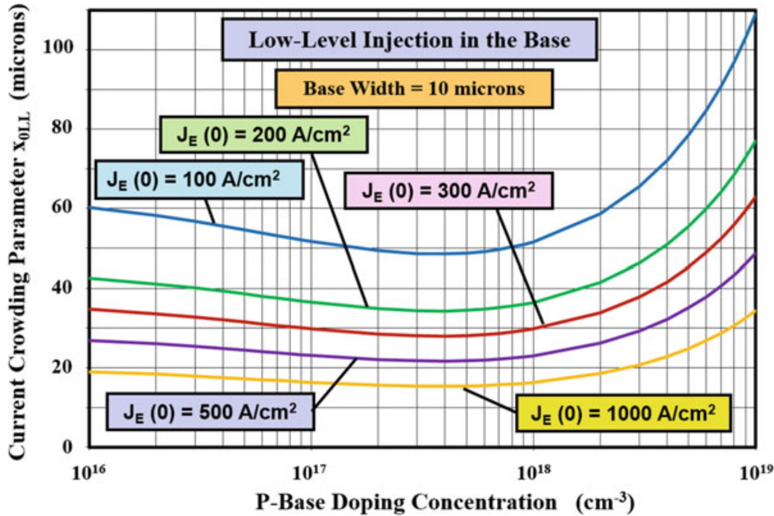

Fig. 7.38 Current crowding parameter for the N-P-N bipolar power transistor for low-level injection conditions in the P-base region

7.5.2 High-Level Injection in the Base

Analytical treatment for the emitter current crowding under high-level injection conditions in the P-base region can be performed under certain simplifying assumptions [16, 17]. A cross section of the bipolar power transistor is illustrated in Fig. 7.39 with half of the emitter finger with a width of W_E. A linear geometry is assumed for the transistor with an emitter finger length L_E orthogonal to the cross section in the figure. Consider a segment of the emitter finger of width dx located at a distance of x from the edge of the emitter located closest to the base contact. The emitter current flowing through the segment is given by:

$$dI_E(x) = J_E(x)\,L_E\,dx \tag{7.107}$$

where $J_E(x)$ is the local emitter current density at a distance x from the edge of the emitter located closest to the base contact. The base current required to support this emitter current is given by:

$$dI_B(x) = (1-\alpha)\,dI_E(x) = (1-\alpha)\,J_E(x)\,L_E.dx \tag{7.108}$$

In writing this equation, it has been assumed that the current gain is independent of the emitter current density to simplify the analysis.

The voltage drop produced in the base region across the segment due to the base current flow is given by:

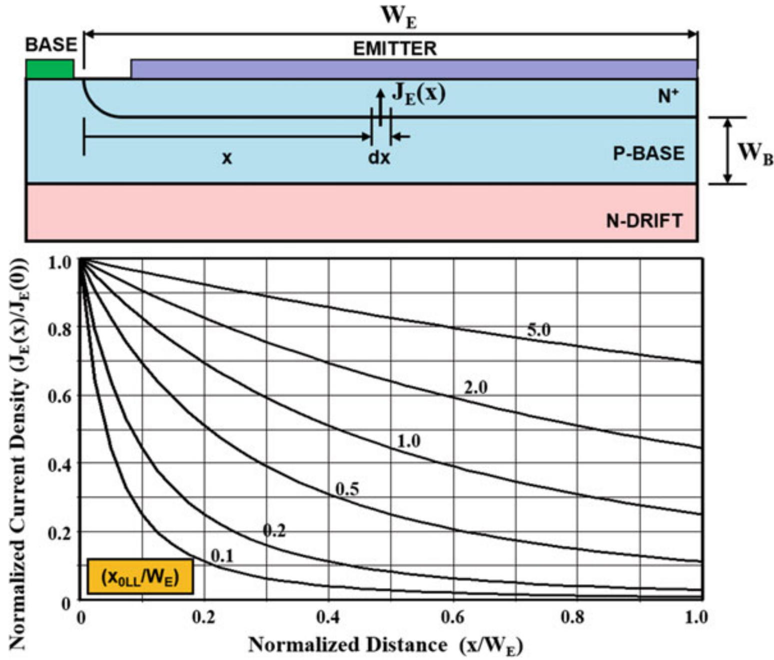

Fig. 7.39 Emitter current distribution within the bipolar power transistor with high level injection in the base region

$$dV_{\mathrm{BE}}(x) = dI_{\mathrm{B}}(x)\,dR_{\mathrm{B}} = dI_{\mathrm{B}}(x)\left(\frac{\rho_{\mathrm{B}}dx}{W_{\mathrm{B}}L_{\mathrm{E}}}\right) \tag{7.109}$$

where ρ_{B} is the resistivity of the P-base region. Unlike the case for low-level injection where the resistivity is determined by the doping concentration of the P-base region, the resistivity for the P-base region under high-level injection conditions is given by:

$$\rho_{\mathrm{B}} = \rho_{\mathrm{B0}}\frac{J_{\mathrm{HL}}}{J_{\mathrm{E}}(x)} \tag{7.110}$$

where J_{HL} is the emitter current density for the onset of high-level injection in the P-base region. The emitter current density at location x is determined by the local forward voltage drop across the base-emitter junction:

$$J_{\mathrm{E}}(x) = J_{\mathrm{S,HL}}e^{qV_{\mathrm{BE}}/2kT} \tag{7.111}$$

where $J_{\mathrm{S,HL}}$ is the diode saturation current density under high-level injection conditions (see Eq. (5.57) derived for a diode operating under high-level injection conditions). Taking the first derivative with respect to x yields:

$$\frac{dJ_E(x)}{dx} = \frac{qJ_E(x)}{2kT}\frac{dV_{BE}(x)}{dx} \tag{7.112}$$

Using Eq. (7.109) in the above expression:

$$\frac{dJ_E(x)}{dx} = \frac{qJ_E(x)}{2kT}\frac{\rho_B\, dI_B(x)}{W_B L_E} \tag{7.113}$$

Using Eq. (7.110) for the conductivity-modulated resistivity gives:

$$\frac{dJ_E(x)}{dx} = \frac{qJ_{HL}}{2kT}\frac{\rho_{B0}\, dI_B(x)}{W_B L_E} \tag{7.114}$$

Taking the derivative of this equation yields:

$$\frac{d^2 J_E(x)}{dx^2} = \frac{qJ_{HL}}{2kT}\frac{\rho_{B0}}{W_B L_E}\frac{dI_B(x)}{dx} \tag{7.115}$$

Utilizing Eq. (7.108), a second-order differential equation for the emitter current distribution is obtained:

$$\frac{d^2 J_E(x)}{dx^2} - \frac{qJ_{HL}}{2kT}\frac{\rho_{B0}}{W_B}(1-\alpha)J_E(x) = 0 \tag{7.116}$$

The solution for this differential equation is:

$$J_E(x) = J_E(0)\, e^{-x/x_{0HL}} \tag{7.117}$$

where x_{0HL} is a *current crowding parameter under high-level injection conditions in the P-base region* given by:

$$x_{0HL} = \sqrt{\frac{2kTW_B}{q(1-\alpha)\rho_{B0}J_{HL}}} \tag{7.118}$$

The distribution of the emitter current within the bipolar power transistor is shown in the lower part of Fig. 7.39 for various cases of the ratio (x_{0HL}/W_E). It can be observed from the plots that the emitter current density is larger at the edge of the emitter closest to the base contact. The emitter current crowding is observed to worsen as the ratio (x_{0HL}/W_E) becomes smaller. Using a typical base width of 10 μm, a current gain (alpha) of 0.95 and a P-base doping concentration of 1×10^{17} cm^{-3} yield a value for x_{0HL} of 62 μm at an emitter high-level injection current density of 100 A/cm^2. This corresponds to a ratio (x_{0HL}/W_E) of 0.31 for an emitter width of 200 μm, which would result in significant current crowding as shown in Fig. 7.39. According to Eq. (7.118), the value for x_{0HL} becomes larger when the current gain increases. This is due to the smaller base current required to sustain current flow within the transistor, which produces a smaller voltage drop along the base

resistance. The value for x_{0HL} becomes larger when the base resistivity is reduced by increasing its doping level. However, the resulting improvement in current distribution is obtained with a lower current gain, partially canceling the benefit derived from the lower base resistivity.

The current crowding parameter under high-level injection conditions is a function of the doping concentration of the P-base region because this determines not only the resistivity of the P-base region but also the current gain (alpha) of the transistor. As the doping concentration of the P-base region is increased, the resistivity decreases, while the current gain becomes smaller due a reduction of the emitter injection efficiency. The net result is a relatively weak dependence of the current crowding parameter on the doping concentration in the P-base region with a minimum value at a doping concentration of about 5×10^{17} cm^{-3} as illustrated in Fig. 7.38 by the uppermost curve. However, the current crowding parameter under high-level injection conditions is not dependent on the emitter current density because of a proportionate decrease in the resistivity of the P-base region.

Simulation Example

In order to validate the models for the emitter current crowding, the results of two-dimensional numerical simulations for the power bipolar transistor are described here. In all cases, the emitter current distribution was obtained at a collector bias of 300 V and a base drive current density of 5 A/cm^2. The collector current density is shown in Fig. 7.40 for three device structures designed with P-base surface concentrations of 2×10^{17} cm^{-3}, 5×10^{17} cm^{-3}, and 1×10^{18} cm^{-3}, respectively. The width of the P-base region for all the structures is close to 9 μm as

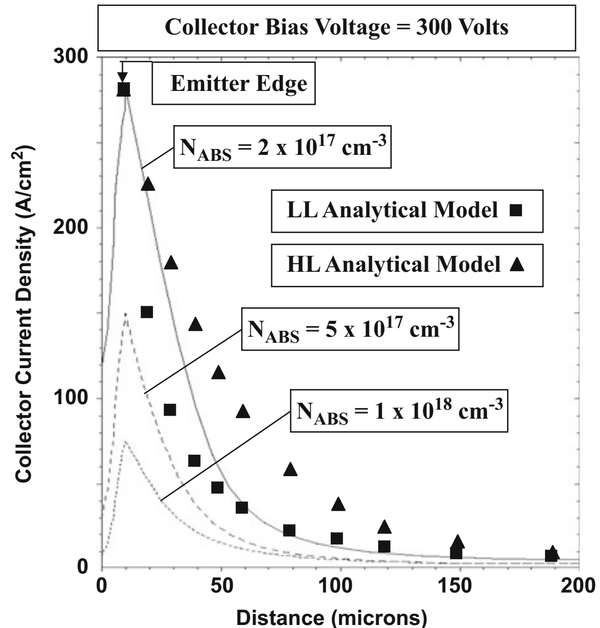

Fig. 7.40 Emitter current crowding in bipolar power transistors

indicated by the doping profile in Fig. 7.8. In all the cases, a much greater collector current density is observed at the edge of the emitter closest to the base contact. When the doping concentration of the P-base region is increased, the current gain becomes smaller due to the reduced injection efficiency. This leads to a reduction of the collector current density for these structures as observed in Fig. 7.40.

In order to relate the results of the numerical simulations to the two models described in this section, the collector current density computed using these models is shown by the square and triangular symbols in Fig. 7.40 for the device (baseline structure bjt8) with a P-base surface concentration of 2×10^{17} cm^{-3}. For the models, an effective P-base doping concentration of 7×10^{16} cm^{-3} was used for consistency with the results discussed in the previous section on current gain. It can be observed on the one hand that the values computed using the model based upon low-level injection conditions in the P-base region are in agreement with the simulation results when the collector current density falls below 50 A/cm^2. On the other hand, the values computed using the model based upon high-level injection conditions in the P-base region are in agreement with the simulation results when the collector current density is greater than 150 A/cm^2. Using Eq. (7.59), the electron concentration $n_B(0)$ is 2.4×10^{16} cm^{-3} at a collector current density of 100 A/cm^2. Consequently, a significant portion of the P-base region operates under high-level injection conditions when the collector current density approaches and exceeds this value. The observed emitter current distribution is therefore determined by a portion of the emitter near the base contact operating under high-level injection conditions, while the rest of the emitter operates under low-level injection conditions. Consequently, both models for the emitter current crowding within the bipolar power transistor are required to describe the current distribution within the emitter finger.

7.5.3 Emitter Geometry

From the previous sections, it is apparent that most of the collector current flows at the edge of the emitter finger located closest to the base contact electrode. Consequently, a large amount of surface area can be wasted in the bipolar power transistor if the emitter finger is made wider than about twice the parameter x_0 described in the previous sections. Based upon the information provided in Fig. 7.38, this corresponds to a typical emitter width of about 100 μm. In addition, it is necessary to surround the emitter finger with the base contact fingers to ensure maximum utility of the emitter fingers. A typical device layout that accomplishes these objectives is illustrated in Fig. 7.41. This layout is referred to as the *interdigitated finger geometry*. Note the presence of base contact fingers on the outside edges of the emitter fingers. The base contact fingers can be made narrower than the emitter contact fingers because of the smaller currents flowing through them. The edge termination surrounds the P-base region in order to protect the base-collector junction.

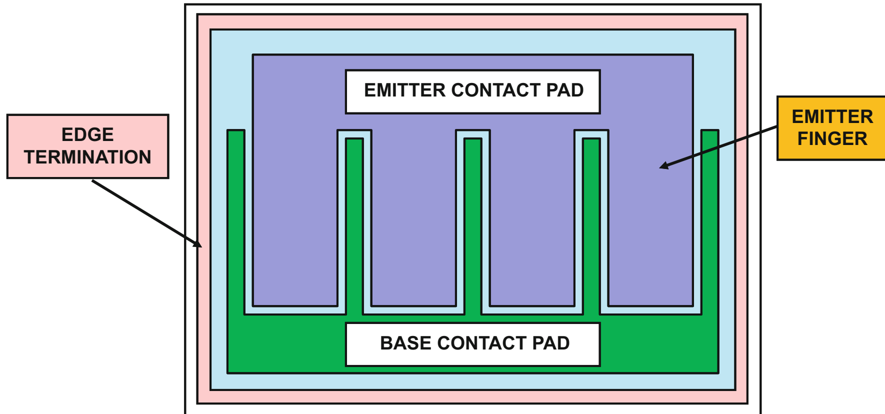

Fig. 7.41 Die layout for a typical bipolar power transistor

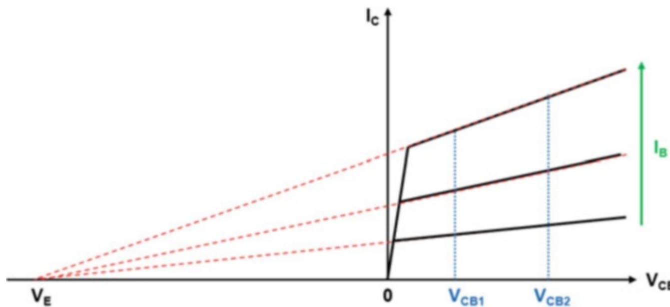

Fig. 7.42 Typical output characteristics for the bipolar power transistor

7.6 Output Characteristics

The typical output characteristics for the power bipolar transistor structure are shown in Fig. 7.42. The slope of the output characteristics has been exaggerated in order to discuss the output resistance of the device. The finite output resistance for the bipolar transistor is related to a change in the current gain with increasing collector bias voltage. As the collector bias is increased, the depletion region across the base-collector junction expands within the P-base region even though most of the voltage is supported across the collector drift region. The electrons injected from the base-emitter junction have to diffuse only through the un-depleted portion of the P-base region. Consequently, the current gain increases due to an increase in the injection efficiency and base transport factor because the base width that determines the current gain becomes smaller than the physical base width. For a constant base drive current, the collector current increases with increasing collector bias voltage because of the increase in the current gain.

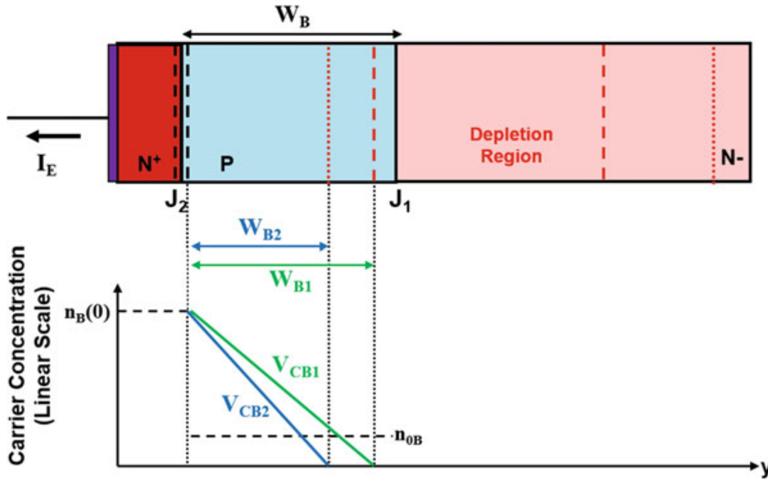

Fig. 7.43 Effect of collector bias on the minority carrier profile in the base region for the bipolar power transistor

The impact of the depletion of the P-base region by the applied collector bias voltage on the minority carrier profile is illustrated in Fig. 7.43. The depletion layer boundaries are shown by the dashed line at a bias V_{CB1}, while those for a larger bias V_{CB2} are indicated by the dotted lines. If the forward bias across the base-emitter junction (and the base current) is held constant, the injected electron concentration at the base-emitter junction $n_{\mathrm{B}}(0)$ is equal for the two cases as shown in the lower portion of the figure. The minority carrier density is forced to zero at the edge of the depletion region of the reverse biased base-collector junction. Consequently, the slope of the minority carrier profile in the P-base region becomes greater for the case of a larger collector bias voltage. Since the collector current density is proportional to the slope of the minority carrier profile at the base-collector junction, this implies an increase in the collector current with increasing collector bias voltage as illustrated in Fig. 7.42.

The P-base region of bipolar power transistors is formed by the diffusion of boron which results in a graded doping profile as illustrated in Fig. 7.2 with low concentrations at the base-collector junction. A significant depletion of the P-base region occurs due to the low doping levels in the base near the junction. The shape of the output characteristics can be analyzed by taking into account the width of the depletion region within the P-base region. For the case of uniform doping concentration in the base and collector regions, the depletion layer width in the P-base region is given by [8]:

$$W_{\mathrm{BD}} = \sqrt{\frac{2\varepsilon_{\mathrm{S}} V_{\mathrm{CB}}}{q N_{\mathrm{AB}}} \left(\frac{N_{\mathrm{D}}}{N_{\mathrm{AB}} + N_{\mathrm{D}}} \right)} \tag{7.119}$$

where V_{CB} is the base-collector reverse bias voltage, N_{AB} is the doping concentration in the P-base region, and N_D is the doping concentration in the N-drift region. This expression accounts for a finite doping concentration on both sides of the P-N junction. The width of the un-depleted portion of the P-base region is then given by:

$$W_{B,UD} = W_B - W_{BD} = W_B - \sqrt{\frac{2\varepsilon_S V_{CB}}{qN_{AB}}\left(\frac{N_D}{N_{AB}+N_D}\right)} \tag{7.120}$$

corresponding to a base-collector bias V_{CB}. (The collector-emitter voltage is approximately equal to the base-collector voltage here.) The collector current density for this case is given by:

$$J_C = qD_{nB}\frac{dn}{dx} = qD_{nB}\frac{n_B(0)}{W_{B,UD}} \tag{7.121}$$

Using Eq. (7.120):

$$J_C = qD_{nB}\frac{n_B(0)}{W_B}\frac{1}{\left\{1-\sqrt{2\varepsilon_S V_{CB}N_D/\left[qN_{AB}W_B^2(N_{AB}+N_D)\right]}\right\}} \tag{7.122}$$

The collector current density at small collector bias voltages is given by:

$$J_{C0} = qD_{nB}\frac{n_B(0)}{W_B} \tag{7.123}$$

because the depletion of the P-base region can be neglected. Consequently:

$$J_C = J_{C0}\frac{1}{\left\{1-\sqrt{2\varepsilon_S V_{CB}N_D/\left[qN_{AB}W_B^2(N_{AB}+N_D)\right]}\right\}} \tag{7.124}$$

When the base doping concentration (N_{AB}) is much greater than the drift region doping concentration (N_D), the term within the square root in the denominator becomes much smaller than unity. In this case, the application of Maclaurin series gives:

$$J_C \approx J_{C0}\left[1+\frac{\varepsilon_S N_D V_{CB}}{qN_{AB}W_B^2(N_{AB}+N_D)}\right] \tag{7.125}$$

This expression implies a linear output characteristic as illustrated in Fig. 7.42. Extrapolation of the collector current density to zero, as indicated by the dashed lines in the figure, provides a voltage intercept on the negative x-axis which is referred [18] to as the *Early voltage* (V_E). From Eq. (7.125), the Early voltage is given by:

$$V_{\mathrm{E}} = \frac{qW_{\mathrm{B}}^2}{\varepsilon_{\mathrm{S}}}\left(\frac{N_{\mathrm{AB}}}{N_{\mathrm{D}}}\right)(N_{\mathrm{AB}} + N_{\mathrm{D}}) \tag{7.126}$$

According to this equation, the Early voltage is independent of the collector current density resulting in all the extrapolated output characteristics intersecting the x-axis at the same voltage [8].

The output characteristics computed by using the model in Eq. (7.124) are shown in Fig. 7.44 for three values for the doping concentration of the P-base region by the solid lines. In all the cases, a doping concentration of $5 \times 10^{13}\ \mathrm{cm}^{-3}$ was used for the N-drift region together with a P-base width of 10 μm. As expected, the slope of the output characteristics decreases when the doping concentration of the P-base region is increased. It is worth pointing out that the output characteristics are not perfectly straight lines.

The increase in the collector current is found to be much smaller than that predicted by Eq. (7.124) when the linear output characteristic model described by Eq. (7.125) is used. A match to the nonlinear model can be obtained by including a constant (K_{E}) in Eq. (7.125):

$$J_{\mathrm{C}} \approx J_{\mathrm{C0}}\left[1 + \frac{K_{\mathrm{E}}\varepsilon_{\mathrm{S}}N_{\mathrm{D}}V_{\mathrm{CB}}}{qN_{\mathrm{AB}}W_{\mathrm{B}}^2(N_{\mathrm{AB}} + N_{\mathrm{D}})}\right] \tag{7.127}$$

The results obtained for the three values for the P-base doping concentration are shown in Fig. 7.44 by the dashed lines for $K_{\mathrm{E}} = 8$. It is worth pointing out that the negative intercept of these lines with the x-axis increases with larger P-base doping

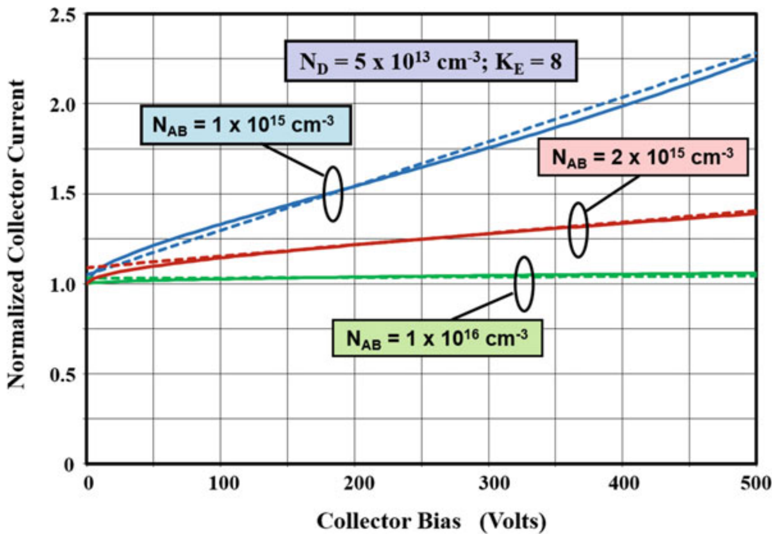

Fig. 7.44 Normalized output characteristics for the bipolar power transistor

concentration, i.e., the Early voltage increases with increasing P-base doping concentration.

The specific output impedance for the bipolar power transistor can be derived from the output characteristics described by Eq. (7.124):

$$\frac{dJ_{\mathrm{C}}}{dV_{\mathrm{CB}}} = \frac{1}{R_{\mathrm{O,sp}}} \tag{7.128}$$

Taking the derivative of Eq. (7.124) yields:

$$R_{\mathrm{O,sp}} = \sqrt{\frac{2qN_{\mathrm{AB}}W_{\mathrm{B}}^{2}(N_{\mathrm{AB}} + N_{\mathrm{D}})V_{\mathrm{CB}}}{\varepsilon_{\mathrm{S}}N_{\mathrm{D}}J_{\mathrm{C0}}}}\left(1 - \sqrt{\frac{2\varepsilon_{\mathrm{S}}N_{\mathrm{D}}V_{\mathrm{CB}}}{qN_{\mathrm{AB}}W_{\mathrm{B}}^{2}(N_{\mathrm{AB}} + N_{\mathrm{D}})}}\right) \tag{7.129}$$

According to this relationship, the output impedance is a function of the collector bias voltage and the collector current density. A large output resistance is desirable for power transistors. This can be achieved for the bipolar power transistor by using a larger doping concentration for the P-base region. However, this will reduce the current gain making the control circuit more expensive and bulky.

Simulation Example

In order to validate the model for the output characteristics of the bipolar power transistor, the results of two-dimensional numerical simulations are described for several devices with different P-base doping concentrations. In all cases, a doping concentration of 5×10^{13} cm^{-3} was used for the N-drift region. The physical base width (W_{B}) for all the devices was 9 μm. The output characteristics for the baseline structure (bjt8) were previously shown in Fig. 7.27. Due to the relatively large surface doping concentration (2×10^{17} cm^{-3}) for the base region for this structure, the output characteristics are flat with a high output resistance.

The output characteristics for the bipolar power transistor structure (bjt15) with a P-base surface concentration reduced to 1×10^{16} cm^{-3} are shown in Fig. 7.45. Due to the much larger current gain for this structure, the base drive current has been reduced by an order of magnitude. This structure (bjt15) exhibits output characteristics with a distinct slope indicating a low output resistance. The dashed lines in the figure have been drawn (slightly above the simulation data for clarity) to provide a linear fit to the output characteristics. The Early voltage extracted by using these lines is also given in the figure. The values are approximately equal indicating that all the lines intersect the *x*-axis at the same voltage.

The impact of reducing the surface concentration of the P-base diffusion on the output characteristics of the bipolar power transistor can be observed in Fig. 7.46. In this figure, the characteristics for the structure with P-base surface concentration of 1×10^{16} cm^{-3} and 2×10^{17} cm^{-3} are displayed at the same base drive current density. The dashed lines in the figure have been drawn (slightly above the simulation data for clarity) to provide a linear fit to the output characteristics. The specific output resistance extracted using these lines is 43 Ω-cm^{2} for the structure with P-base

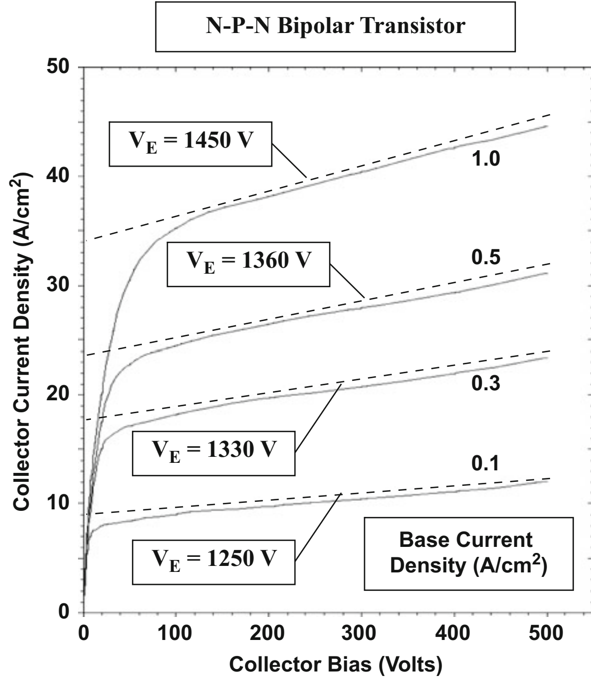

Fig. 7.45 Output characteristics for a bipolar power transistor

surface concentration of 1×10^{16} cm^{-3} and 5000 Ω-cm^2 for the structure with P-base surface concentration of 2×10^{17} cm^{-3}. From these results, it is apparent that the P-base doping concentration must be typically above 1×10^{17} cm^{-3} to obtain a high output resistance for the bipolar power transistor.

7.7 On-State Characteristics

The output characteristics for a bipolar power transistor are shown in Fig. 7.47 at low collector bias voltages for the common-emitter configuration. In addition to the *forward active region* where the collector current is determined by the base drive current via the current gain of the transistor, two new regions of operation are evident. At very low collector bias voltages, the transistor operates in its *saturation region*. In addition, there is a gradual transition between the saturation region and the active region called the *quasi-saturation region*.

In the saturation region of operation, the collector bias voltage becomes sufficiently low so that the base-collector junction becomes forward biased because the collector bias voltage falls below the base drive voltage. This produces an injection of minority carriers into the very lightly doped N-drift region. The injected carrier concentration in the N-drift region exceeds its doping level at typical operating

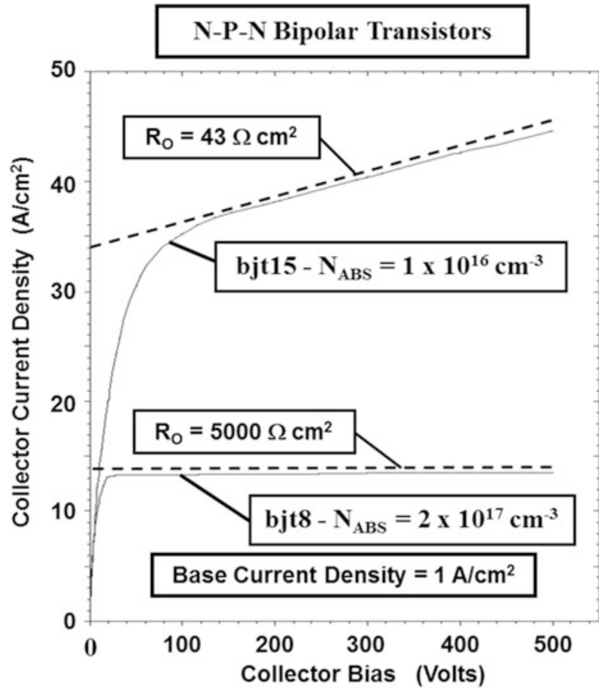

Fig. 7.46 Comparison of the output characteristics of bipolar power transistors with different P-base doping concentrations

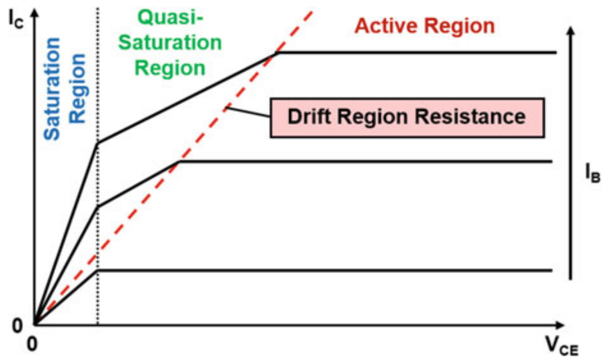

Fig. 7.47 Output characteristics for the bipolar power transistor at low collector bias voltages

collector current densities leading to conductivity modulation of the N-drift region. This is responsible for the low on-state voltage drop when the bipolar power transistor is operated in the saturation region. However, as the collector bias voltage increases, conductivity modulation does not extend over the entire N-drift region, which produces an increase in the on-state voltage drop as shown in the quasi-saturation region. These regions of operation are discussed in more detail below.

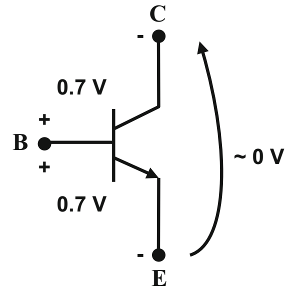

Fig. 7.48 Voltages across the bipolar power transistor in the saturation mode of operation

7.7.1 Saturation Region

The voltages across the terminals of the bipolar power transistor are illustrated in Fig. 7.48 when it is biased in the saturation mode. Due to the forward bias across both the base-emitter and base-collector junctions, the voltage drop between the base and emitter terminals, as well as between the base and collector terminals, becomes approximately 0.7 V. Consequently, the voltage drop between the collector and emitter terminals becomes equal to nearly zero. In practical devices, the two junctions are not symmetrical because of differing doping profiles, and there is a finite voltage drop across the N-drift region in spite of its conductivity modulation. These factors result in a finite on-state voltage drop between the collector and emitter terminals which increases with increasing collector current flow as shown in Fig. 7.47. However, the resistance exhibited by the device is much smaller than the drift region resistance as given by:

$$R_{\mathrm{D,sp}} = \rho_{\mathrm{D}}.W_{\mathrm{D}} = \frac{W_{\mathrm{D}}}{q\mu_{\mathrm{n}}N_{\mathrm{D}}} \tag{7.130}$$

The carrier distribution profile in the P-base region of the bipolar power transistor in the saturation mode can be obtained by superposition of the profiles for the forward active and reverse active modes of operation. The carrier profiles for these two modes are illustrated in the upper part of Fig. 7.49. In the forward active mode, the base-emitter junction is forward biased leading to an injected carrier density of $n_{\mathrm{B}}(0)$, while the base-collector junction is reverse biased leading to zero carrier density at W_{B}. Similarly, in the reverse active mode, the base-collector junction is forward biased leading to an injected carrier density of $n_{\mathrm{B}}(W_{\mathrm{B}})$, while the base-emitter junction is reverse biased leading to zero carrier density at 0. The injected carrier profile for the saturation mode is obtained by the addition of these two profiles as illustrated in the lower part of the figure. The collector current density is then given by:

$$J_{\mathrm{C,sat}} = \frac{[n_{\mathrm{B}}(0) - n_{\mathrm{B}}(W_{\mathrm{B}})]}{W_{\mathrm{B}}} \tag{7.131}$$

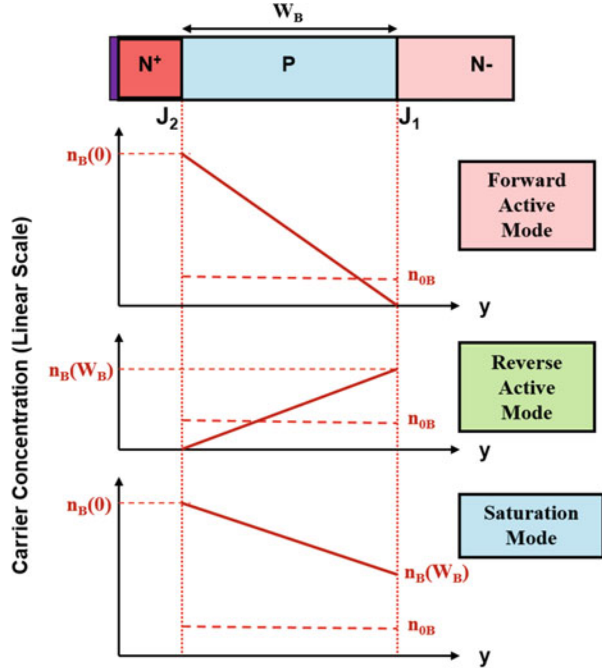

Fig. 7.49 Carrier distribution in the base region of the bipolar power transistor in the saturation mode of operation

This collector current density is smaller than that obtained in the forward active mode of operation, namely:

$$J_{\mathrm{C,fam}} = \frac{n_{\mathrm{B}}(0)}{W_{\mathrm{B}}} \tag{7.132}$$

Consequently, the bipolar power transistor is operating with a smaller current gain in the saturation mode than in the active region as is apparent from the characteristics shown in Fig. 7.47.

The voltage drop across the power bipolar transistor in the saturation mode can be analyzed by computing voltage developed in the N-drift region under conductivity modulation by the high-level injection of minority carriers [19, 20]. The bipolar power transistor is illustrated in Fig. 7.50 with a high concentration of minority carriers, which exceeds the doping level (N_{D}) in the drift region, through the entire drift region. Since charge neutrality must be satisfied in the drift region:

$$n(y) = p(y) + N_{\mathrm{D}} \tag{7.133}$$

Due to high-level injection conditions in the N-drift region:

$$\frac{dn}{dy} = \frac{dp}{dy} \tag{7.134}$$

$10#The conduction equation for holes in the N-drift region is:

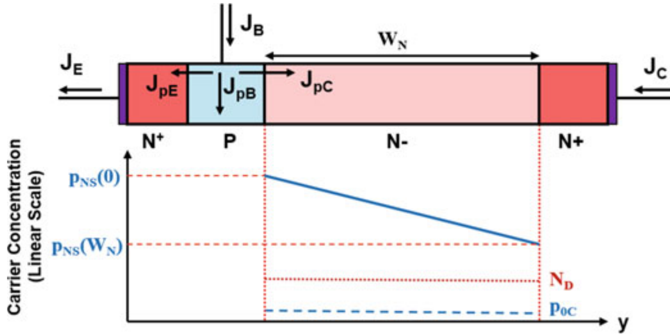

Fig. 7.50 Carrier distribution in the N-drift region of the bipolar power transistor in the saturation mode of operation

$$J_{\mathrm{pC}} = q\mu_{\mathrm{p}}pE - qD_{\mathrm{p}}\frac{dp}{dy} \tag{7.135}$$

while that for electrons in the N-drift region is:

$$J_{\mathrm{nC}} = q\mu_{\mathrm{n}}nE + qD_{\mathrm{n}}\frac{dn}{dy} \tag{7.136}$$

As indicated in Fig. 7.50, the base current supplies recombination in the emitter, base, and collector regions. The hole current in the collector drift region (J_{pC}) represents this recombination current. If the current gain is assumed to be large, this current density can be neglected for computation of the electric field profile from Eq. (7.135) resulting in:

$$E = \frac{kT}{q}\frac{1}{p}\frac{dp}{dy} \tag{7.137}$$

after utilizing the Einstein relationship between the mobility and the diffusion constant. Combining Eqs. (7.134 and 7.136) with Eq. (7.137):

$$J_{\mathrm{nC}} = q\mu_{\mathrm{n}}(p + N_{\mathrm{D}})\left(\frac{kT}{qp}\frac{dp}{dy}\right) + qD_{\mathrm{n}}\frac{dp}{dy} \tag{7.138}$$

Applying the Einstein relationship between the mobility and the diffusion constant and assuming that the total collector current density (J_{C}) is approximately equal to the electron current density (J_{nC}) due to the high current gain:

$$J_{\mathrm{C}} = 2qD_{\mathrm{n}}\left(1 + \frac{N_{\mathrm{D}}}{2p}\right)\frac{dp}{dy} \tag{7.139}$$

The minority carrier distribution in the N-drift region obtained from solving this differential equation is:

$$p(y) = p_{\mathrm{NS}}(0) - \frac{J_{\mathrm{C}}y}{2qD_{\mathrm{n}}} + \frac{N_{\mathrm{D}}}{2} \ln \left[\frac{p_{\mathrm{NS}}(0)}{p(y)}\right] \tag{7.140}$$

Since the N-drift region of high-voltage bipolar power transistors is very lightly doped, the last term in the above equation can be neglected giving:

$$p(y) = p_{\mathrm{NS}}(0) - \frac{J_{\mathrm{C}}y}{2qD_{\mathrm{n}}} \tag{7.141}$$

This expression indicates a linear carrier distribution as illustrated in Fig. 7.50.

The carrier concentration at the base-collector junction can be obtained by using Boltzmann's relationship:

$$p_{\mathrm{NS}}(0) = p_{0\mathrm{C}} e^{qV_{\mathrm{BCJ}}/kT} \tag{7.142}$$

where V_{BCJ} is the voltage across the base-collector junction. The voltage across the base-collector junction is not equal to the base-collector bias because of the internal voltage drop across the drift region (V_{D}) within the bipolar power transistor:

$$V_{\mathrm{BCJ}} = V_{\mathrm{BC}} - V_{\mathrm{D}} \tag{7.143}$$

The voltage drop in the drift region can be computed from the electric field given by Eq. (7.137):

$$V_{\mathrm{D}} = -\int_{0}^{W_{\mathrm{N}}} E dy = -\frac{kT}{q} \int_{p_{\mathrm{NS}}(0)}^{p_{\mathrm{NS}}(W_{\mathrm{N}})} \frac{dp(y)}{p(y)} = \frac{kT}{q} \ln \left[\frac{p_{\mathrm{NS}}(0)}{p_{\mathrm{NS}}(W_{\mathrm{N}})}\right] \tag{7.144}$$

Combining these equations yields a quadratic expression for the carrier concentration [$p_{\mathrm{NS}}(0)$] in terms of the base-collector voltage and the collector current density:

$$p_{\mathrm{NS}}^2(0) - p_{\mathrm{NS}}(0) p_{0\mathrm{C}} e^{qV_{\mathrm{BC}}/kT} + \frac{J_{\mathrm{C}} W_{\mathrm{N}}}{2qD_{\mathrm{n}}} p_{0\mathrm{C}} e^{qV_{\mathrm{BC}}/kT} = 0 \tag{7.145}$$

from which the carrier distribution can be obtained.

The voltage drop across the N-drift region in the saturation mode can then be obtained by using Eq. (7.144). Using Eq. (7.141) to obtain the carrier concentration at the interface between the collector drift region and the N^+ substrate:

$$V_{\mathrm{D}} = \frac{kT}{q} \ln \left[\frac{p_{\mathrm{NS}}(0)}{p_{\mathrm{NS}}(0) - (J_{\mathrm{C}} W_{\mathrm{N}}/2qD_{\mathrm{n}})}\right] \tag{7.146}$$

The on-state voltage drop in the saturation mode is approximately equal to this voltage. Typical values for the on-state voltage drop in the saturation mode are in the range of 100–300 mV.

It is worth pointing out that there is a substantial amount of charge stored within the N-drift region when the bipolar power transistor is operating in the saturation mode. This stored charge is given by:

$$Q_{\mathrm{Sat}} = \frac{q[p_{\mathrm{NS}}(0) + p_{\mathrm{NS}}(W_{\mathrm{N}})]W_{\mathrm{N}}}{2} \tag{7.147}$$

The charge in the drift region must be sustained by supplying a base current. The component of the base current flowing into the collector drift region responsible for supporting the recombination of these carriers is given by:

$$J_{\mathrm{pC}} = \frac{Q_{\mathrm{Sat}}}{\tau_{\mathrm{HL}}} = \frac{q[p_{\mathrm{NS}}(0) + p_{\mathrm{NS}}(W_{\mathrm{N}})]W_{\mathrm{N}}}{2\tau_{\mathrm{HL}}} \tag{7.148}$$

7.7.2 *Quasi-Saturation Region*

The carrier distribution in the base region for the bipolar power transistor, when operating in the quasi-saturation region, is similar to that shown in Fig. 7.49. Consequently, the bipolar power transistor operates with a smaller current gain in the quasi-saturation mode than in the active region as is apparent from the characteristics shown in Fig. 7.47. However, its current gain is larger than when operating in the saturation region.

The voltage drop across the power bipolar transistor in the quasi-saturation mode can be analyzed by computing the voltage developed in the N-drift region using the same approach as for the saturation region. However, high-level injection does not extend throughout the N-drift region in the quasi-saturation mode as illustrated in Fig. 7.51. The Eq. (7.141) derived in the previous section for the carrier distribution

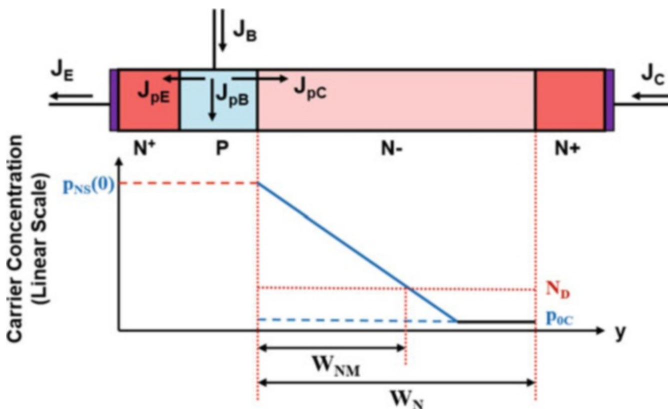

Fig. 7.51 Carrier distribution in the N-drift region of the bipolar power transistor in the quasi-saturation mode of operation

is also applicable for the quasi-saturation mode within the portion of the N-drift region with width W_{NM} that operates under high-level injection conditions. At this location, the minority carrier concentration becomes equal to the majority carrier concentration in equilibrium (N_D). The width of the conductivity-modulated region is obtained by using this information in Eq. (7.141):

$$W_{NM} = \frac{2qD_n}{J_C}[p_{NS}(0) - N_D] \quad (7.149)$$

Since the injected carrier concentration is far greater than the majority carrier concentration in the drift region:

$$W_{NM} = \frac{2qD_n}{J_C} p_{NS}(0) \quad (7.150)$$

The voltage drop across the drift region in the quasi-saturation mode becomes dominated by the resistive voltage drop produced by the collector current flow through the unmodulated portion of the drift region:

$$V_D = \frac{J_C(W_N - W_{NM})}{q\mu_n N_D} \quad (7.151)$$

Consequently, a substantial voltage drop can occur across the drift region in the quasi-saturation mode. As the collector bias is increased, the unmodulated portion of the drift region becomes larger. Eventually, the entire drift region becomes unmodulated at the boundary between the quasi-saturation region and the active region. This boundary is then defined by the specific resistance of the drift region (see Eq. (7.130)) as illustrated in Fig. 7.47. The characteristics illustrated in this figure are based upon assuming a uniformly doped P-base region with much larger doping concentration than the N-drift region. In practical devices fabricated using a diffused P-base region with a highly graded doping profile, the collector current continues to increase beyond the boundary defined by the drift region resistance because of an increase in the current gain due to the reduction of the effective base width by the extension of the depletion layer in the P-base region with increasing collector bias voltage. In addition, the current crowding at the edge of the emitter closest to the base contact makes the local collector current density much larger than the average collector current density. This increases the voltage drop across the unmodulated drift region making the quasi-saturation boundary move to larger collector bias voltages.

As in the case of the saturation mode, there is a substantial amount of charge stored within the N-drift region when the bipolar power transistor is operating in the quasi-saturation mode. This stored charge is given by:

$$Q_{Q-\mathrm{Sat}} = \frac{qp_{NS}(0)W_{NM}}{2} \quad (7.152)$$

The component of the base current flowing into the collector drift region that is responsible for supporting the recombination of these carriers is given by:

$$J_{\text{pC}} = \frac{Q_{Q-\text{Sat}}}{\tau_{\text{HL}}} = \frac{qp_{\text{NS}}(0)W_{\text{NM}}}{2\tau_{\text{HL}}} \quad (7.153)$$

The stored charge in the quasi-saturation mode is smaller than that in the saturation mode. When the bipolar power transistor is switched from the on-state to the blocking state, the stored charge in the drift region must be removed by a reverse base drive current before the transistor can support voltage across the base-collector junction. It is therefore preferable to operate the bipolar power transistor in the quasi-saturation mode during the on-state to achieve a faster switching speed. However, this produces larger on-state power dissipation due to the larger on-state voltage drop in the quasi-saturation region.

Simulation Example

The results of two-dimensional numerical simulations are described here for the baseline device structure (bjt8) to validate the model for the quasi-saturation characteristics of the bipolar power transistor. For this structure, a doping concentration of 5×10^{13} cm^{-3} was used for the N-drift region with a thickness of 80 μm. The specific resistance for the drift region obtained by using these parameters is 0.735 Ω-cm^2.

The output characteristics for the baseline bipolar power transistor structure (bjt8) are shown in Fig. 7.52 at lower collector bias voltages to display the saturation and quasi-saturation regions. The saturation region occurs at collector bias voltages below 0.5 V. In order to operate in the saturation region to obtain a low on-state voltage drop with reasonable (20 A/cm^2) collector current density, it is necessary to increase the base drive current density to above 10 A/cm^2 resulting in a very low current gain. The quasi-saturation region extends to much larger collector bias voltages in the range of 15 V even for a relatively modest collector current density of 20 A/cm^2. This demonstrates that the on-state voltage drop for the power bipolar transistor is quite large.

The minority carrier distribution profiles in the N-drift region for the baseline bipolar power transistor structure (bjt8) are shown in Fig. 7.53. Note that the distance scale begins at the edge of the base-collector junction in this plot. When the device is operated in the saturation region (at point A in Fig. 7.52), the injected minority carrier density is far greater than the background doping concentration throughout the drift region (see profile A in Fig. 7.53) confirming the high-level injection assumption used for the analysis of the saturation region.

When the device is operated at the boundary between the saturation and quasi-saturation regions (at point B in Fig. 7.52), the injected minority carrier density becomes equal to the majority carrier concentration at the boundary between the N-drift region and the N$^+$ substrate (see profile B in Fig. 7.53). The on-state voltage drop is low at this operating point because the conductivity modulation still extends throughout the drift region. When the device is operated at a larger collector bias

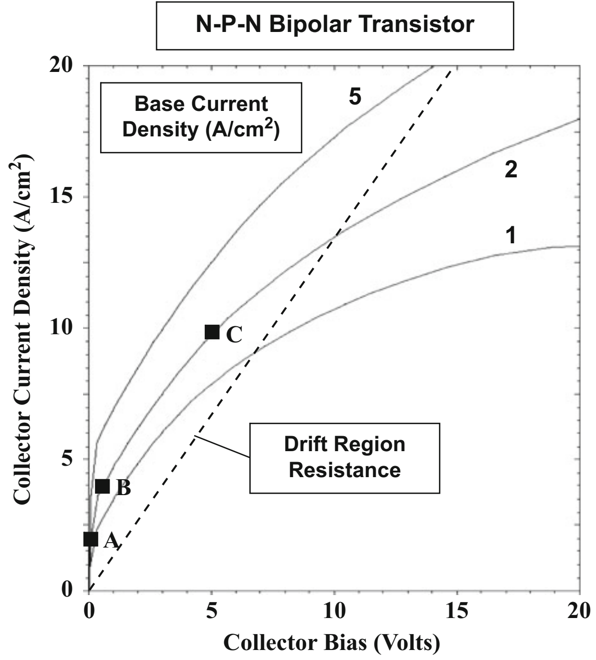

Fig. 7.52 Quasi-saturation characteristics for a bipolar power transistor

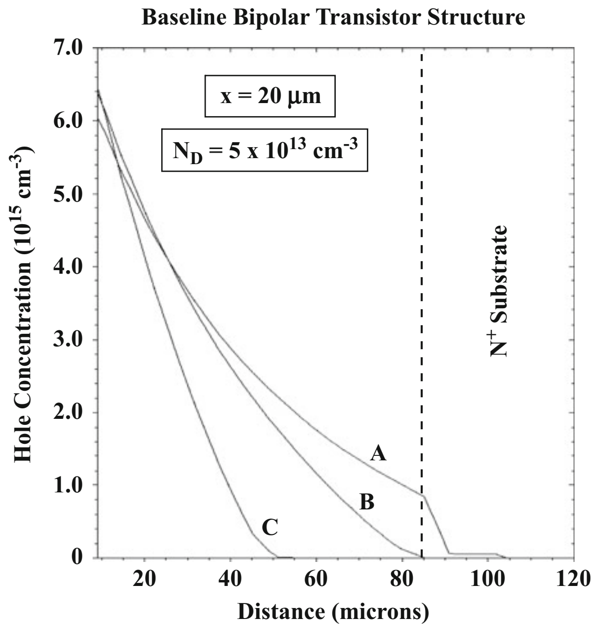

Fig. 7.53 Minority carrier profiles in the drift region for a bipolar power transistor operating in the saturation and quasi-saturation regions

voltage (at point C in Fig. 7.52), the high-level injection extends only through a portion of the drift region (see profile C in Fig. 7.53). The on-state voltage drop is large at this operating point because a portion of the drift region is not conductivity modulated. The carrier profile is approximately linear in shape for all the cases as predicted by the analytical model.

7.8 Switching Characteristics

Bipolar power transistors were developed as switches in power circuits used for applications such as motor control. In these circuits, the device is switched between the on-state and the off-state to regulate the current being delivered to the load. The bipolar power transistor is usually used in the common-emitter configuration as shown in Fig. 7.3. The loads can be either resistive or inductive in nature. For a resistive load, the locus for the collector current-voltage trajectory is determined by the load resistance as indicated in Fig. 7.54 by the blue line. For an inductive load, the locus for the collector current-voltage trajectory is determined by the red line indicated in Fig. 7.54. The device switches from the blocking state, while supporting the collector supply voltage (V_{CS}) at point A, to the on-state with a voltage drop V_{ON} at point B during the turn-on transient. The device switches from the on-state to the collector supply voltage during the turn-off transient. These transitions are discussed in this section because they determine the power losses incurred when the bipolar power transistor is operated at high frequencies.

7.8.1 Turn-On Transition

At the beginning of the turn-on transition process, the bipolar power transistor is biased with the base-emitter junction under reverse bias due to the external drive circuit shown in Fig. 7.3. Although it is sufficient to short circuit the base and emitter

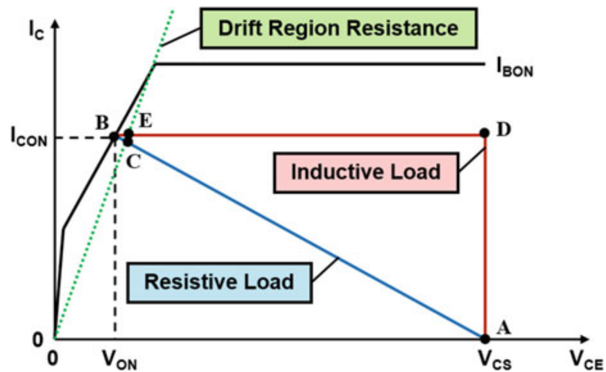

Fig. 7.54 Switching loci for the bipolar power transistor

terminals to maintain the power bipolar transistor in the blocking state, the reverse bias voltage (V_{BS2}) is necessary to produce a reverse base current to accelerate the turn-off process. The base current can be assumed to be equal to zero in the blocking state with the base-collector junction supporting the applied collector bias voltage with no collector current flow.

When the device is turned on by opening switch S_2 and closing switch S_1 in Fig. 7.3, a base current begins to flow limited by the base drive resistance R_{B1}. If the switching time for the switches S_1 and S_2 is small, the base current is initially given by:

$$I_{B0} = \frac{(V_{BS1} + V_{BS2})}{R_{B1}} \tag{7.154}$$

because the potential at the base electrode is initially equal to the reverse bias voltage (V_{BS2}). Once the base-emitter junction becomes forward biased, the base current is given by:

$$I_B = \frac{(V_{BS1} - V_{bi})}{R_{B1}} \tag{7.155}$$

where V_{bi} is the built-in potential (~ 0.8 V) for the base-emitter junction.

During the turn-on process, collector current flow does not begin to occur until the electrons injected from the base-emitter junction arrive at the base-collector junction. This time interval is given by the *base transit time* [8]:

$$t_T = \frac{W_B^2}{2D_n} \tag{7.156}$$

where W_B is the base width. For a base region with doping concentration of 1×10^{17} cm^{-3} and width of 10 μm, the transit time is found to be 24 ns. The collector current begins to increase after this time interval.

The stored electron charge in the P-base region of the N-P-N bipolar power transistor begins to develop after the onset of the injection of electrons from the emitter region. The charge has a linear profile in the P-base region as illustrated by the green line in Fig. 7.55 with a maximum value of $n_B(0,t)$ at the base-emitter junction and zero at the base-collector junction. The charge control equation that governs the buildup of the electron charge in the base region is:

$$\frac{dQ_{nB}}{dt} = \beta J_B - \frac{Q_{nB}}{\tau_n} \tag{7.157}$$

where $Q_{nB}(t)$ is the electron charge per unit area in the base region and τ_n is the recombination lifetime for electrons. If the recombination in the base region is assumed to be negligible:

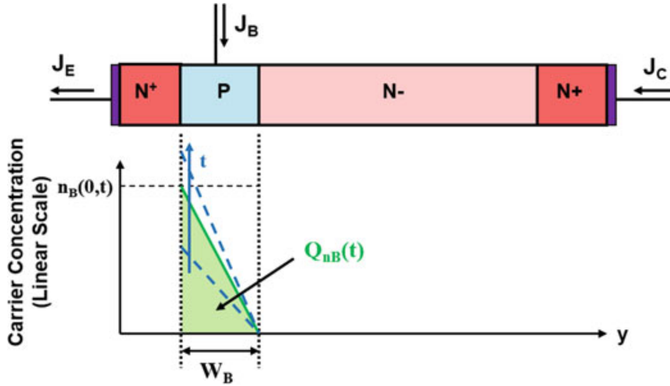

Fig. 7.55 Buildup of the stored charge in the base region of the bipolar power transistor during the turn-on transient

$$\frac{dQ_{\mathrm{nB}}}{dt} = \beta J_{\mathrm{B}} \tag{7.158}$$

Consequently:

$$Q_{\mathrm{nB}}(t) = \beta J_{\mathrm{B}} t \tag{7.159}$$

The electron stored charge in the P-base region is given by the triangular green area in Fig. 7.55:

$$Q_{\mathrm{nB}}(t) = \frac{1}{2} q n_{\mathrm{B}}(0, t) W_{\mathrm{B}} \tag{7.160}$$

Using this relationship with Eq. (7.159) yields:

$$n_{\mathrm{B}}(0, t) = \frac{2\beta J_{\mathrm{B}}}{q W_{\mathrm{B}}} t \tag{7.161}$$

which describes the growth of the injected carrier concentration at the base-emitter junction. The dashed blue lines in Fig. 7.55 indicate the evolution of the injected carrier concentration with time. The collector current corresponding to this carrier concentration is:

$$J_{\mathrm{C}}(t) = q D_{\mathrm{n}} \frac{dn}{dx} = q D_{\mathrm{n}} \frac{n_{\mathrm{B}}(0, t)}{W_{\mathrm{B}}} = \frac{2 D_{\mathrm{n}} \beta J_{\mathrm{B}}}{W_{\mathrm{B}}^2} t \tag{7.162}$$

Based upon this expression, it can be concluded that the collector current will increase linearly with time during the turn-on process.

The rise-time for the collector current to increase from zero to the on-state current density ($J_{\mathrm{C,ON}}$) is then given by:

$$t_{I,\mathrm{ON}} = \frac{W_{\mathrm{B}}^2 J_{\mathrm{C,ON}}}{2D_{\mathrm{n}}\beta J_{\mathrm{B}}} = \frac{W_{\mathrm{B}}^2}{2D_{\mathrm{n}}} \tag{7.163}$$

because $J_{\mathrm{C,ON}} = \beta J_{\mathrm{B}}$. It is advantageous to reduce the rise-time for the collector current in order to decrease the switching losses. This can be achieved by decreasing the width of the P-base region, which also increases the current gain (β). However, this can lead to a reduction of the breakdown voltage due to the reach-through phenomenon.

Resistive Load

The above expressions were derived under the assumption that the base-collector junction is reverse biased during the transient. This is applicable for the resistive load from operating point A in the blocking state (see Fig. 7.54) until point C where the load line intersects the boundary of the quasi-saturation region as defined by the resistance of the N-drift region. Once the bipolar power transistor enters its quasi-saturation region, this assumption is no longer valid because the base-collector junction becomes forward biased with the injection of holes into the N-drift region. The rate of reduction of the collector voltage (and therefore the increase of the collector current) now becomes limited by the development of the stored charge in the N-drift region. As the stored charge in the N-drift region increases, the unmodulated portion of the drift region becomes smaller resulting in a smaller voltage drop.

The waveforms for the terminal currents and voltages are illustrated in Fig. 7.56 during turn-on with a resistive load with points labeled corresponding to points in Fig. 7.54. Initially there is a surge in the base current because the potential across the base resistor is (V_{BS1} + V_{BS2}). During the time interval 0 to t_1, the base-emitter voltage changes from the reverse bias potential V_{BS2} to the forward biased junction potential V_{bi}. At this time, the injection of electrons from the base-emitter junction begins to occur. The collector current does not begin to increase until after the transit time for electrons, i.e., the time interval $(t_2 - t_1) = t_{\mathrm{T}}$. The collector current then increases at a linear rate until time $t_3 = (t_2 + t_{\mathrm{I,ON}})$. The collector voltage simultaneously decreases at a linear rate due to the resistive load. At time t_3, the bipolar power transistor enters the quasi-saturation region of operation at point C on the characteristics. The collector voltage gradually decreases to the steady-state on-voltage drop at time t_4. This slow reduction of the collector voltage produces significant power dissipation during the turn-on event.

Analytical modeling of the voltage drop in the quasi-saturation region during the turn-on process can be performed using the assumption that the minority (and hence the majority) carrier concentration at the base-collector junction increases exponentially with time. The carrier distribution within the N-drift region is linear, as shown by the green line in Fig. 7.57, which is determined by the physics described earlier for the quasi-saturation region:

$$p_{\mathrm{NS}}(y,t) = p_{\mathrm{NS}}(0,t) - \frac{J_{\mathrm{C}}(t)}{2qD_{\mathrm{n}}}y \approx p_{\mathrm{NS}}(0,t) - \frac{J_{\mathrm{C,ON}}}{2qD_{\mathrm{n}}}y \tag{7.164}$$

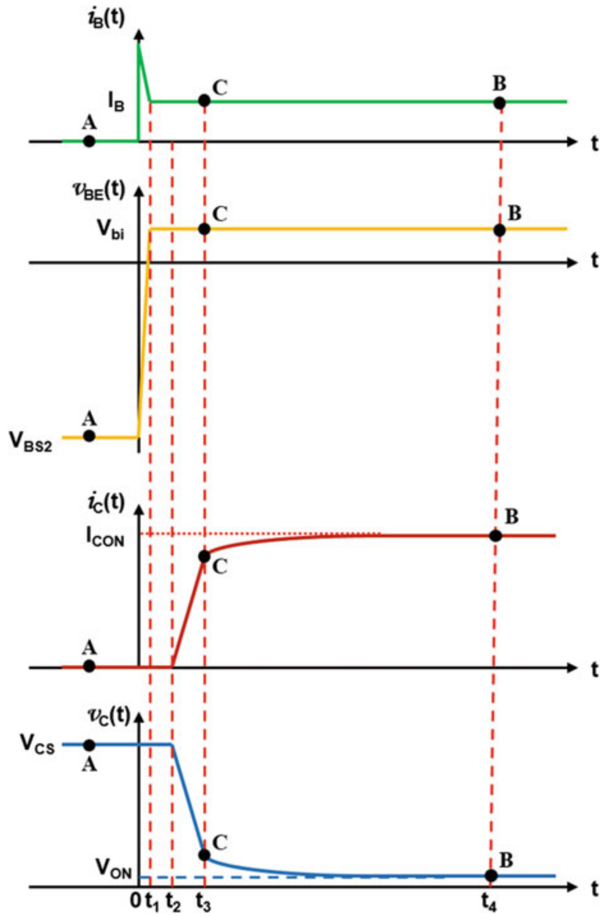

Fig. 7.56 Switching waveforms for the bipolar power transistor during the turn-on transient with a resistive load

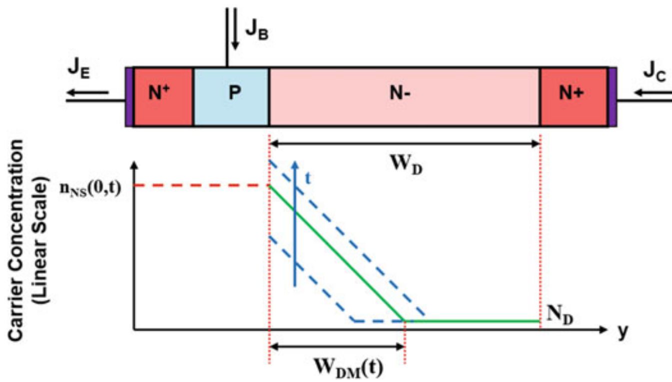

Fig. 7.57 Buildup of the stored charge in the drift region of the bipolar power transistor during the turn-on transient

because the collector current density remains close to the on-state current density during this portion of the turn-on transient. The buildup of the stored charge in the N-drift region is illustrated in Fig. 7.57 with the dashed blue lines indicating the evolution of the charge. Note that the slope of the carrier distribution profile remains constant according to the above equation.

The width of the modulated portion of the drift region during turn-on can be determined by using Eq. (7.150):

$$W_{\mathrm{DM}}(t) = \frac{2qD_{\mathrm{n}}}{J_{\mathrm{C}}(t)} p_{\mathrm{NS}}(0, t) = \frac{2qD_{\mathrm{n}}}{J_{\mathrm{C,ON}}} p_{\mathrm{NS}}(0, F)\left(1 - e^{-t/\tau}\right) \tag{7.165}$$

where $p_{\mathrm{NS}}(0,\mathrm{F})$ is the final steady-state hole concentration at the base-collector junction at the end of the turn-on process and τ is the minority carrier lifetime. Although the collector current density increases slightly during the transition through the quasi-saturation region, its value can be assumed to be approximately equal to the final steady-state collector current density ($J_{\mathrm{C,ON}}$). The collector voltage of the bipolar power transistor is then given by:

$$V_{\mathrm{QS}}(t) = \rho_{\mathrm{D}}[W_{\mathrm{D}} - W_{\mathrm{DM}}(t)] J_{\mathrm{C,ON}} K_{\mathrm{CC}} \tag{7.166}$$

where K_{CC} is the current crowding parameter to account for the larger local current density near the edge of the emitter closest to the base contact.

As an example, consider a bipolar power transistor with a drift region with doping concentration of 5×10^{13} cm^{-3} and thickness of 80 μm. The slow reduction of the collector voltage is shown in Fig. 7.58 after the transistor enters the quasi-saturation

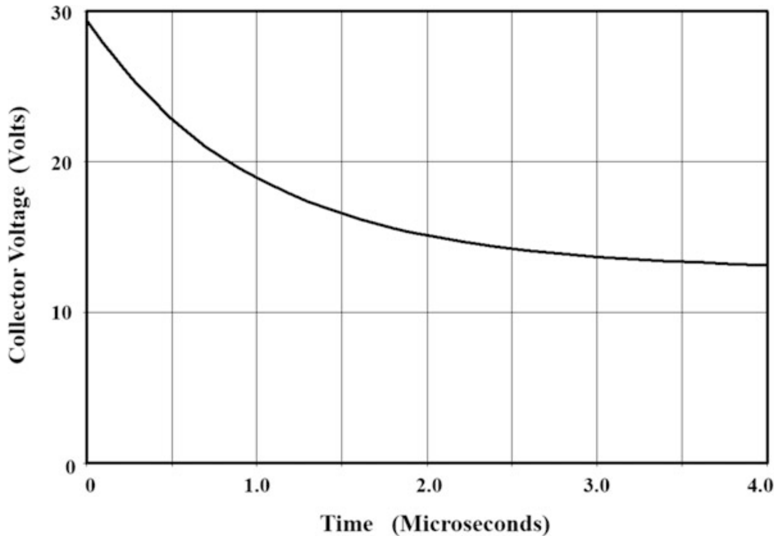

Fig. 7.58 Reduction of the on-state voltage drop for the bipolar power transistor during the turn-on transient

region during the turn-on process. The current crowding parameter was assumed to have a value of 2. It can be observed that the on-state voltage drop decreases from about 29 V to about 12 V in 4 μs. The power dissipation within the bipolar transistor is significantly enhanced due to the large collector current density during this time interval.

Simulation Example
The results of two-dimensional numerical simulations are described here for the baseline device structure (bjt8) to validate the model for the turn-on process for the bipolar power transistor with a resistive load,. For this structure, a doping concentration of 5×10^{13} cm^{-3} was used for the N-drift region with a thickness of 80 μm. The device was initially biased with a negative base drive voltage of 5 V with a base resistance to limit the current to obtain a steady-state blocking condition with 800 V applied to the collector terminal. The base drive voltage was rapidly switched to positive 5 V to initiate the turn-on process. A load resistance was attached between the collector terminal and its bias supply to emulate the resistive load conditions.

The terminal current-voltage waveforms obtained from the numerical simulations are shown in Fig. 7.59. There is an initial surge in the base drive current after which it settles down to the steady-state base drive current. The base electrode voltage crosses zero at the time t_1 indicated in the figure, while the collector current begins to rise at the time t_2 indicated in the figure. The transition time for the collector current is about 50 ns. This delay is consistent with the transit time for electrons in the P-base region. The collector current increases linearly with time as described by the analytical model until the device enters the quasi-saturation region at time t_3. The collector voltage then reduces slowly with time from an initial value of about 25 V. The reduction of the collector voltage occurs over a time frame of about 3 μs. This behavior is consistent with the behavior predicted by the analytical model.

The slow reduction of the collector voltage during the transition through the quasi-saturation region is shown in Fig. 7.60. It can be observed that the collector voltage is about 22 V at the beginning of this time interval and then reduces to the steady-state value of about 10 V in 3 μs. The time taken for this slow decay of the collector voltage is consistent with a lifetime of 1 μs in the N-drift region and in agreement with the assumptions of the analytical model.

The current crowding at the edge of the emitter near the base contact in the bipolar power transistor is shown in Fig. 7.61 during the turn-on process. During the initial stages of the turn-on process, the current density increases as shown by the solid lines up to a time of 75 ns. A very high current density (ten times the steady-state average current density) develops at the edge of the emitter finger closest to the base contact. The current then spreads over the emitter finger as shown by the dashed lines until the distribution reaches the steady-state condition with a current density at the edge of the emitter of twice the average current density. The larger current density at the edge of the emitter during the time interval from 190 to 461 ns enhances the voltage drop in the collector drift region making the power dissipation larger.

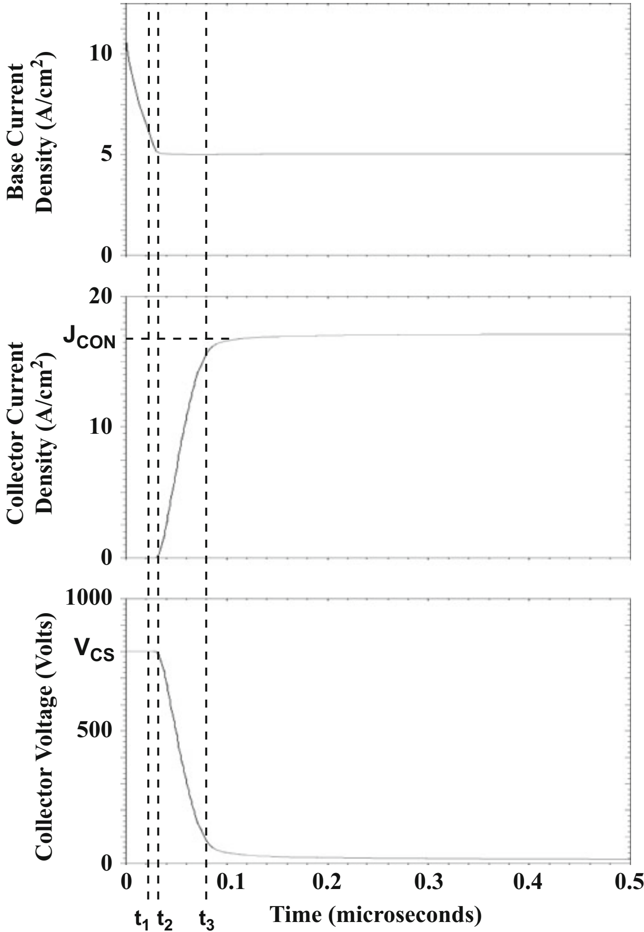

Fig. 7.59 Typical turn-on waveforms for a bipolar power transistor with a resistive load

The modulation of the conductivity of the N-drift region during the turn-on transient can be observed in Fig. 7.62 where the electron concentration is plotted at various time instances. The stored charge in the N-drift region begins to build up after 190 ns at which time the collector voltage is at 22 V. The profile for the electrons is linear in the N-drift region as described by the analytical model. The slope for the carrier distribution remains the same for all the time instances as predicted by the analytical model (see Eq. (7.164)).

Inductive Load

In the case of an inductive load, the locus for the current-voltage trajectory during the turn-on process is as shown by the red lines in Fig. 7.54. The collector current increases until it reaches the on-state value at point D, while the collector voltage remains constant at V_{CS}. All the current flowing through the flyback diode

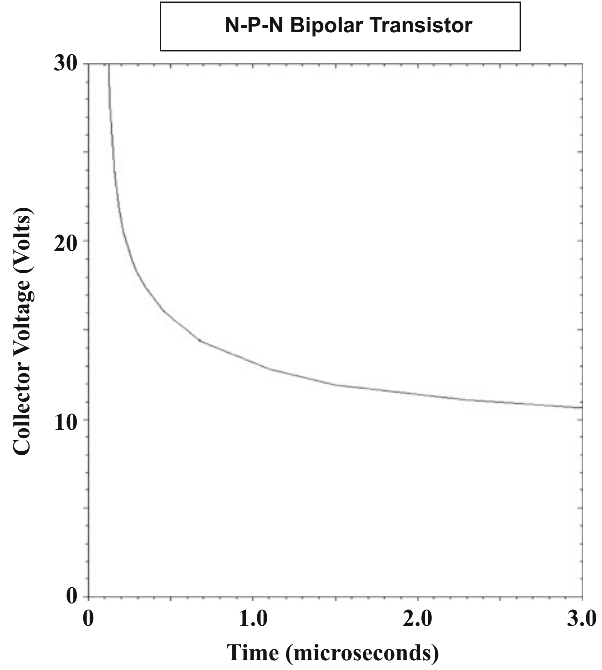

Fig. 7.60 Reduction of the on-state voltage drop for the bipolar power transistor during the turn-on transient

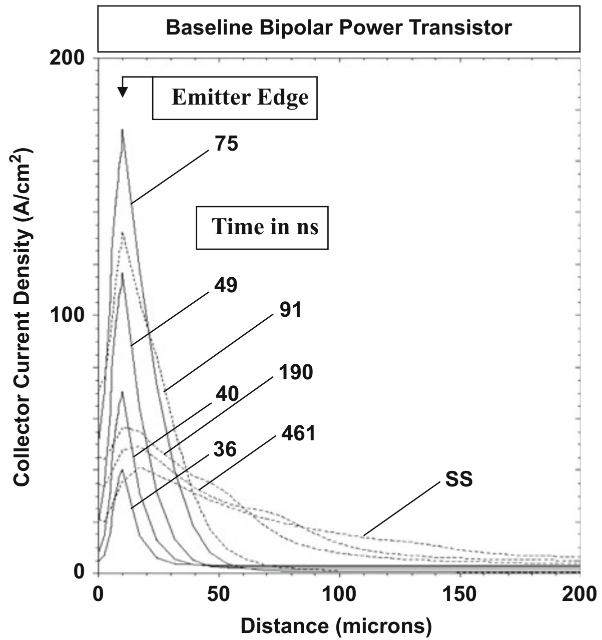

Fig. 7.61 Current distribution along emitter finger during turn-on of the bipolar power transistor

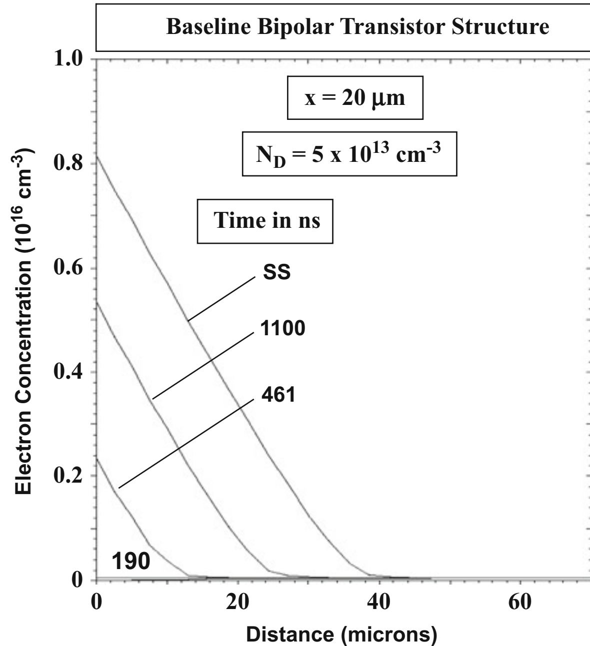

Fig. 7.62 Carrier distribution in the drift region during turn-on of the bipolar power transistor

(see Fig. 7.3) has been transferred to the transistor at this point in time. The collector voltage then reduces, while the collector current remains constant. The previously derived expressions for the delay time (Eq. 7.156) and the transition time (Eq. 7.163) are valid for the inductive load situation as well. These expressions were derived under the assumption that the base-collector junction is reverse biased during the transient. This is applicable for the inductive load from operating point A in the blocking state until point E in Fig. 7.54. Once the bipolar power transistor enters its quasi-saturation region, the base-collector junction becomes forward biased with the injection of holes into the N-drift region. The rate of reduction of the collector voltage (and therefore the increase of the collector current) now becomes limited by the development of the stored charge in the N-drift region. As the stored charge in the N-drift region increases, the unmodulated portion of the drift region becomes smaller resulting in a smaller voltage drop.

The waveforms for the terminal currents and voltages are illustrated in Fig. 7.63 during turn-on with an inductive load. Initially there is a surge in the base current because the potential across the base resistor is (V_{BS1} + V_{BS2}). During the time interval 0 to t_1, the base-emitter voltage changes from the reverse bias potential V_{BS2} to the forward biased junction potential V_{bi}. At this time, the injection of electrons from the base-emitter junction begins to occur. The collector current does not begin to increase until after the transit time for electrons, i.e., the time interval $(t_2 - t_1) = t_T$. The collector current then increases at a linear rate until time $t_3 = (t_2 + t_{I,ON})$ when it becomes equal to the steady-state on-current. The collector voltage remains constant during this time.

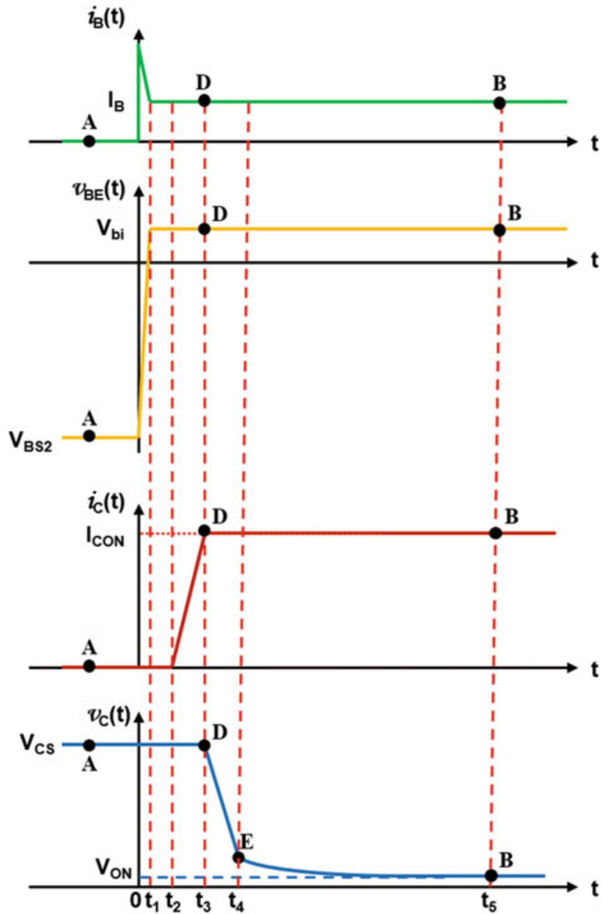

Fig. 7.63 Switching waveforms for the bipolar power transistor during the turn-on transient with an inductive load

After time t_3, the collector voltage reduces with time, while the collector current remains constant. The time taken for the collector voltage to decrease to the voltage at point E in Fig. 7.54 can be estimated by assuming that the space-charge region at the base-collector junction is removed by the collector current flow. Thus:

$$t_{V,\mathrm{ON}} = t_4 - t_3 = \frac{Q_{\mathrm{SC}}}{J_{\mathrm{C,ON}}} = \frac{(qN_{\mathrm{D}}W_{\mathrm{D}} + qN_{\mathrm{AB}}W_{\mathrm{B}})}{J_{\mathrm{C,ON}}} \tag{7.167}$$

which accounts for the space charge on both sides of the base-collector junction. A typical value for this voltage transition time is between 10 and 50 ns.

At time t_4, the bipolar power transistor enters the quasi-saturation region of operation at point E on the characteristics. The collector voltage gradually decreases to the steady-state on-voltage drop at time t_5. This slow reduction of the collector voltage produces significant power dissipation during the turn-on event. The same

analytical model for the slow reduction of the collector voltage in the quasi-saturation region developed for the resistive load case can be used for the inductive load case as well.

Simulation Example

The results of two-dimensional numerical simulations are described here for the baseline device structure (bjt8) to validate the model for the turn-on process for the bipolar power transistor with an inductive load. For this structure, a doping concentration of 5×10^{13} cm^{-3} was used for the N-drift region with a thickness of 80 μm. The device was initially biased with a negative base drive voltage of 5 V with a base resistance to limit the current to obtain a steady-state blocking condition with 800 V applied to the collector terminal. The base drive voltage was rapidly switched to positive 5 V to initiate the turn-on process. The base electrode voltage crosses zero at the time t_1 indicated in the figure, while the collector current begins to rise at the time t_2 indicated in the figure. This delay is consistent with the transit time for electrons in the P-base region (Fig. 7.64).

There is an initial surge in the base drive current after which it settles down to the steady-state base drive current. The transition time for the collector current is about 30 ns. Then, the collector current increases linearly with time as described by the analytical model until the device enters the quasi-saturation region at time t_3. After this, the collector voltage decreases rapidly over a time interval of about 40 ns and then reduces slowly with time from an initial value of about 25 V. The reduction of the collector voltage occurs over a time frame of about 3 μs. This behavior is consistent with the behavior predicted by the analytical model.

The current distribution within the bipolar power transistor is shown in Fig. 7.65 during the first part of the turn-on process for the inductive load case when the collector current is increasing, while the collector voltage is maintained at the initial blocking voltage. During the initial stages of the turn-on process, the current density increases up to a time of 52 ns. A very high current density (ten times the steady-state average current density) develops at the edge of the emitter finger closest to the base contact.

During the second phase of the turn-on process with an inductive load, the collector current remains constant, while the collector voltages decreases rapidly. The current distribution along the emitter during the second phase is shown in Fig. 7.66 with the distribution at the beginning of this phase indicated by the dashed line. The current density first increases at the edge of the emitter closest to the base contact. The current then spreads along the emitter finger until the distribution reaches the steady-state condition with a current density at the edge of the emitter of twice the average current density. The larger current density at the edge of the emitter during the time interval from 63 to 405 ns enhances the voltage drop in the collector drift region making the power dissipation larger.

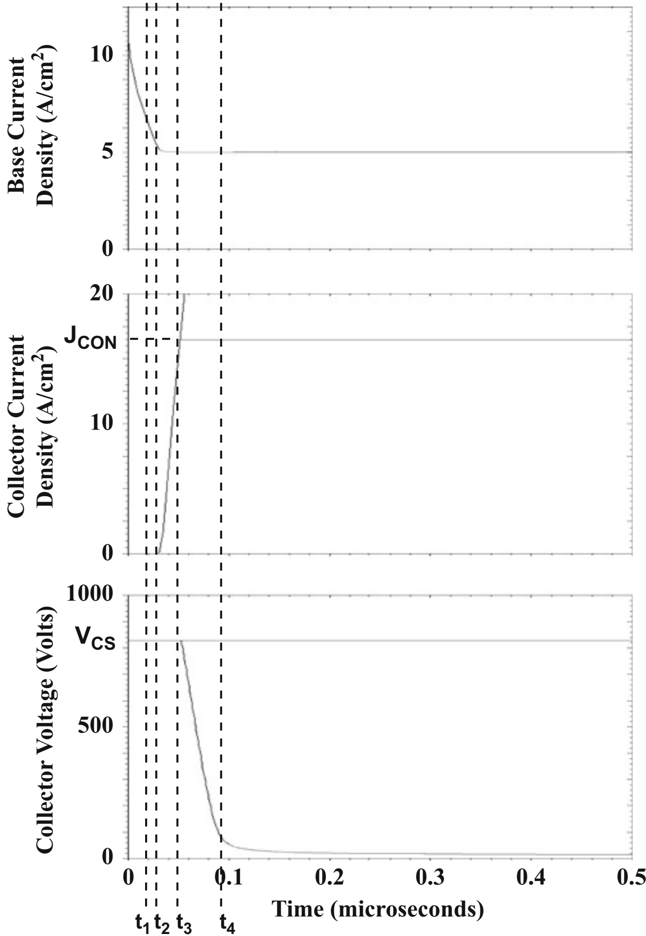

Fig. 7.64 Typical turn-on waveforms for a bipolar power transistor with an inductive load

7.8.2 Turn-Off Transition

The bipolar power transistor is operated with the base-emitter junction under forward bias by the external drive circuit shown in Fig. 7.3 at beginning of the turn-off transition process with switch S_1 closed and switch S_2 open. The turn-off transition is initiated by opening switch S_1 and closing switch S_2. Only the inductive load case will be discussed in this section.

Initially, a reverse base current begins to flow limited by the base drive resistance R_{B2}. If the switching time for the switches S_1 and S_2 is small, the reverse base current is:

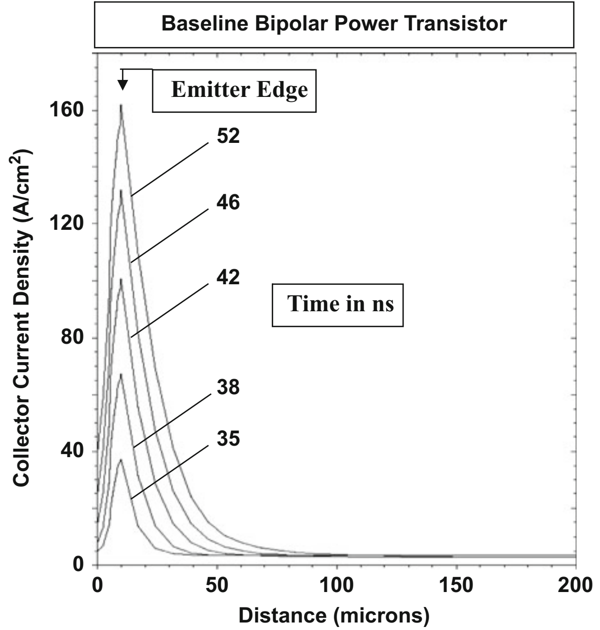

Fig. 7.65 Current distribution during the first phase of the turn-on of the bipolar power transistor

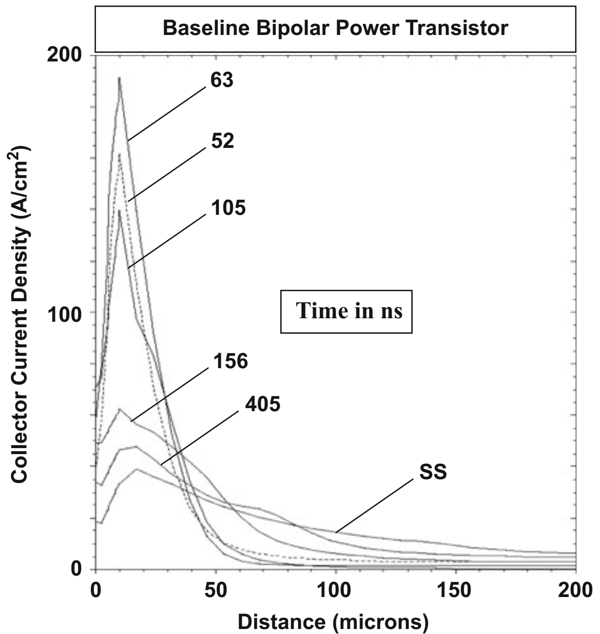

Fig. 7.66 Current distribution during the second phase of the turn-on of the bipolar power transistor

$$I_{\mathrm{BR}} = \frac{(V_{\mathrm{BS2}} + V_{\mathrm{bi}})}{R_{\mathrm{B2}}} \tag{7.168}$$

because the potential at the base electrode is initially equal to the forward bias junction potential (V_{bi}). As the base-emitter junction becomes reverse biased, the base current reduces to:

$$I_{\mathrm{BR}} = \frac{V_{\mathrm{BS2}}}{R_{\mathrm{B2}}} \tag{7.169}$$

During the turn-off process, collector current is squeezed toward the center of the emitter finger because the reverse base drive current first extracts the stored charge located closest to the base contact terminal. Consequently, the current density at the center of the emitter increases with time under inductive load conditions resulting in high local power dissipation within the transistor. The turn-off process occurs by the removal of the stored charge in the P-base region as well as a portion of the stored charge located in the collector drift region. The base-collector junction is unable to support a high voltage until the charge at the base-collector junction is removed allowing a depletion layer to be established. The delay between the rise of the bipolar transistor collector voltage and the application of the reverse base drive current is referred to as the *storage time*. Bipolar power transistors exhibit large values for the storage time which inhibits their ability to operate at higher frequencies.

Inductive Load

The locus for the current-voltage trajectory during the turn-off process is shown by the red lines in Fig. 7.54 for the case of an inductive load. The corresponding switching waveforms during the turn-off process are illustrated in Fig. 7.67. During the initial turn-off process, the reverse base drive current remains constant and removes the stored charge in the base and drift regions. The collector current remains constant at the on-state value until the stored charge in the N-drift and P-base regions have been removed by the reverse base drive current. The voltage drop across the bipolar power transistor increases from point B to point E in Fig. 7.54 during this time due to an increase in the collector drift region resistance. Once the base-collector junction becomes reverse biased, the collector voltage increases rapidly, while the collector current remains constant from point E to point D in Fig. 7.54. The collector current begins to transfer to the flyback diode after the collector voltage rises to one diode drop above the supply voltage. The collector and base drive current then decrease rapidly as shown in Fig. 7.67. This corresponds to the transition from point D to point A in Fig. 7.54.

Storage Time Model

Emitter current crowding in the on-state confines most of the stored charge near the edge of the emitter closest to the base contact at the beginning of the turn-off transient. Consequently, a simple one-dimensional analysis for the storage time can be performed by using charge control analysis. In the initial on-state condition, excess electron charge is present in the P-base region due to the injection of electrons

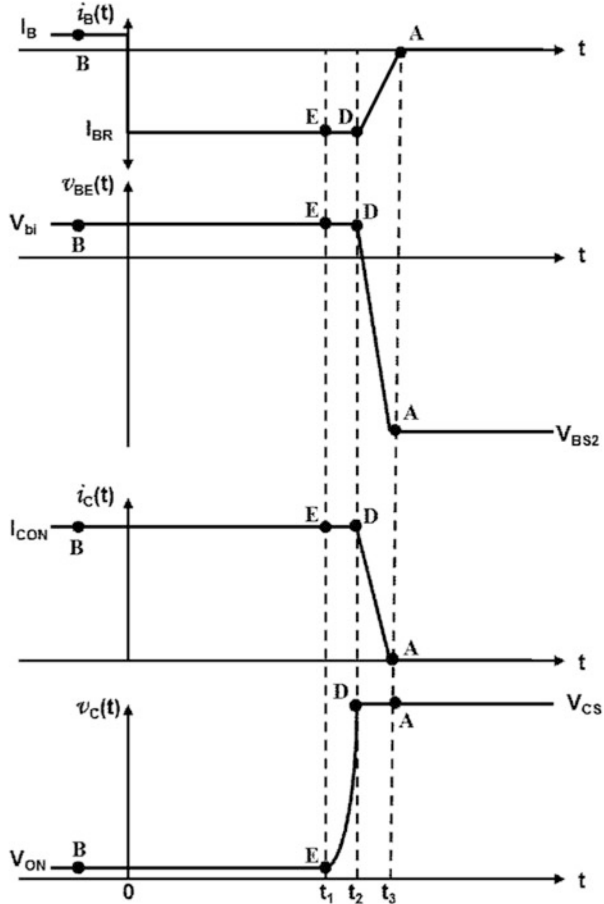

Fig. 7.67 Switching waveforms for the bipolar power transistor during the turn-off transient with an inductive load

from the emitter. In addition, excess electron and hole charge is present in the N-drift region due to the injection of holes into the drift region across the forward biased base-collector junction. The electron concentration profile in the P-base region is shown in Fig. 7.68 as a straight line because the recombination in the base has been neglected. The hole concentration profile in the N-drift region is also shown in the figure. As discussed previously, under quasi-saturation conditions, the hole concentration profile is linear and extends partially through the drift region to a depth W_{NM}. Due to high-level injection conditions in the N-drift region, the electron concentration profile matches that for the holes in the conductivity-modulated portion.

Due to the high doping concentration in the P-base region when compared to the N-drift region for bipolar power transistors, the injected electron concentration in the P-base region at the base-collector junction in the on-state is much smaller than that at the base-emitter junction as illustrated in Fig. 7.68. The stored electron charge in

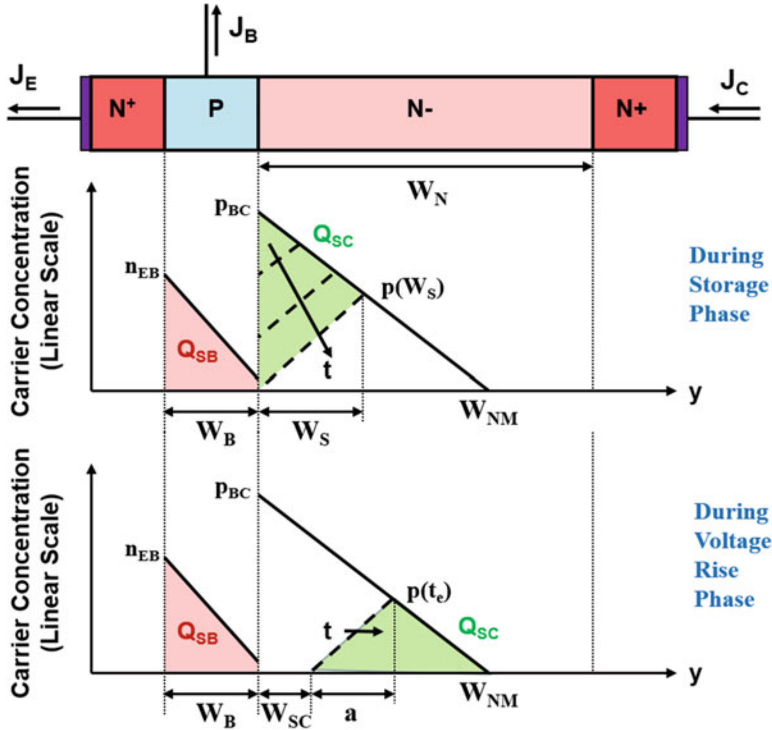

Fig. 7.68 Stored charge in the base and collector regions of the bipolar power transistor during the turn-off transient

the P-base region (shaded pink area in the P-base region in the figure) is then given by:

$$Q_{SB} = \frac{1}{2} q n_{EB} W_B \tag{7.170}$$

where n_{EB} is the injected electron concentration at the emitter-base junction. If the P-base region is operating under low-level injection conditions, the initial on-state collector current density is given by:

$$J_{C,ON} = qD_{nB} \frac{dn}{dy} = qD_{nB} \frac{n_{EB}}{W_B} \tag{7.171}$$

Consequently:

$$n_{EB} = \frac{J_{C,ON} W_B}{qD_{nB}} \tag{7.172}$$

Using this in Eq. (7.170) yields:

$$Q_{SB} = \frac{J_{C,ON} W_B^2}{2D_{nB}} \tag{7.173}$$

The stored charge in the collector drift region is partially removed by the reverse base current. The progressive removal of the holes from the N-drift region by the reverse base drive current is indicated by the dashed lines in Fig. 7.68. The slope of the carrier profiles indicated by the dashed lines remains constant during this process because of the constant reverse base drive current. The slope of the carrier concentration indicated by the solid line also remains constant because the collector current is constant for an inductive load operating condition. Eventually, the hole concentration at the base-collector junction is reduced to zero enabling the junction to begin supporting a high collector voltage. The stored charge in the collector drift region (green-shaded area in the N-drift region in the figure) removed by the reverse base drive current is therefore given by:

$$Q_{SC} = \frac{1}{2} q p_{BC} W_S \tag{7.174}$$

where p_{BC} is the injected hole concentration at the base-collector junction.

The reverse base drive current is related to the concentration profiles for the holes defined by the dashed lines in the figure:

$$J_{BR} = 2qD_{pD}\frac{dp}{dy} = 2qD_{pD}\frac{p(W_S)}{W_S} \tag{7.175}$$

where $p(W_S)$ is the hole concentration at the distance W_S from the base-collector junction. Note that this equation takes into account high-level injection conditions within the N-drift region. This concentration is also determined by the initial hole concentration profile:

$$p(W_S) = p_{BC}\frac{(W_{NM} - W_S)}{W_{NM}} \tag{7.176}$$

Combining Eqs. (7.175 and 7.176):

$$W_S = \frac{2qD_{pD} W_{NM} p_{BC}}{J_{BR} W_{NM} + 2qD_{pD} p_{BC}} \tag{7.177}$$

The initial on-state collector current density is also related to the initial hole concentration profile in the N-drift region:

$$J_{C,ON} = 2qD_{nD}\frac{dn}{dy} = 2qD_{nD}\frac{dp}{dy} = 2qD_{nD}\frac{p_{BC}}{W_{NM}} \tag{7.178}$$

$10#Consequently:

$$p_{\mathrm{BC}} = \frac{J_{\mathrm{C,ON}} W_{\mathrm{NM}}}{2qD_{\mathrm{nD}}} \tag{7.179}$$

Using this expression in Eq. (7.177):

$$W_{\mathrm{S}} = \frac{D_{\mathrm{pD}} W_{\mathrm{NM}} J_{\mathrm{C,ON}}}{D_{\mathrm{nD}} J_{\mathrm{BR}} + D_{\mathrm{pD}} J_{\mathrm{C,ON}}} \tag{7.180}$$

Substituting Eqs. (7.179 and 7.180) in Eq. (7.174) yields:

$$Q_{\mathrm{SC}} = \frac{D_{\mathrm{pD}} W_{\mathrm{NM}}^2 J_{\mathrm{C,ON}}^2}{4D_{\mathrm{nD}} \left(D_{\mathrm{nD}} J_{\mathrm{BR}} + D_{\mathrm{pD}} J_{\mathrm{C,ON}}\right)} \tag{7.181}$$

The stored charge, given by the sum of Q_{SB} and Q_{SC}, is removed by the reverse base current flow (J_{BR}) during the storage time interval (t_{S}):

$$J_{\mathrm{BR}} t_{\mathrm{S}} = Q_{\mathrm{SB}} + Q_{\mathrm{SC}} \tag{7.182}$$

Using Eqs. (7.173 and 7.181) provides a solution for the storage time:

$$t_{\mathrm{S}} = \left(\frac{J_{\mathrm{C,ON}}}{J_{\mathrm{BR}}}\right) \left[\frac{W_{\mathrm{B}}^2}{2D_{\mathrm{nB}}} + \frac{W_{\mathrm{NM}}^2}{4D_{\mathrm{nD}}} \frac{D_{\mathrm{pD}} J_{\mathrm{C,ON}}}{\left(D_{\mathrm{nD}} J_{\mathrm{BR}} + D_{\mathrm{pD}} J_{\mathrm{C,ON}}\right)}\right] \tag{7.183}$$

From this expression, it can be concluded that the storage time can be reduced by increasing the reverse base drive current at the disadvantage of a larger, more expensive, drive circuit.

For the case of a bipolar power transistor with a base width of 10 μm and a modulated drift region with width of 40 μm in the initial on-state, the storage time obtained by using this equation is 270 ns if the on-state current density is 17.5 A/cm^2 and the reverse base drive current is 5 A/cm^2. These operating conditions correspond to an injected electron concentration n_{EB} of 3×10^{15} cm^{-3} at the emitter-base junction, an injected hole concentration p_{BC} of 6×10^{15} cm^{-3} at the base-collector junction, a stored charge Q_{SB} of 2.5×10^{-7} C/cm^2 in the P-base region, and a stored charge Q_{SC} of 1.12×10^{-6} C/cm^2 in the N-drift region. These values are consistent with the assumption of low-level injection conditions in the P-base region and high-level injection conditions in the N-drift region used for the analysis.

Voltage Rise-Time Model

Once the carrier concentration becomes zero at the base-collector junction, it is able to support a large collector voltage by the formation of a depletion region. For a one-dimensional structure, the extension of the depletion region is constrained by the remaining stored charge in the N-drift region. However, in a two-dimensional structure, the depletion layer expands at the edge of the emitter closest to the base contact by pushing the stored charge into the remaining segment of the emitter finger. A simple model for the growth of the depletion layer can be derived by using charge control analysis for a one-dimensional structure representing the edge of the

emitter finger near the base contact. At an elapsed time t_e after the storage phase, the charge removed to form the depletion region is given by:

$$Q_{SD}(t_e) = qN_D W_D(t_e) \tag{7.184}$$

where $W_D(t_e)$ is the width of the depletion region at this time. This charge is also equal to the product of the reverse base drive current and the elapsed time:

$$J_{BR} t_e = Q_{SD}(t_e) = qN_D W_D(t_e) \tag{7.185}$$

The depletion region width at time t_e is then obtained:

$$W_D(t_e) = \frac{J_{BR} t_e}{qN_D} \tag{7.186}$$

The voltage supported across this depletion region is given by:

$$V_C(t_e) = \frac{qN_D}{2\varepsilon_S} W_D^2(t_e) \tag{7.187}$$

Using Eq. (7.186) in Eq. (7.187) yields:

$$V_C(t_e) = \frac{J_{BR}^2 t_e^2}{2q\varepsilon_S N_D} \tag{7.188}$$

indicating that the collector voltage will increase as the square of the time interval after the storage time.

The time taken for the collector voltage to increase to the collector supply voltage, called the *voltage rise-time* (t_V), can be derived from Eq. (7.188):

$$t_V = \frac{\sqrt{2q\varepsilon_S N_D V_{CS}}}{J_{BR}} \tag{7.189}$$

The voltage rise-time can be reduced by increasing the reverse base drive current at the disadvantage of a larger, more expensive, drive circuit. In the case of a bipolar power transistor with a drift region doping concentration of 5×10^{13} cm^{-3} switching to a collector supply voltage of 800 V using a reverse base drive current of 5 A/cm^2, the voltage rise-time predicted by this equation is 23 ns.

A more accurate model for the voltage rise duration can be derived by taking into account the charge being removed from the drift region by the reverse base drive current. A space-charge region forms during the voltage rise interval to support the collector voltage in the drift region. The charge distribution in the drift region during this time interval is illustrated at the bottom in Fig. 7.68 if recombination is neglected. The green area shows the stored charge remaining in the drift region at an elapsed time t_e during the voltage rise.

The slope of the carrier distribution indicated by the dashed line is related to the reverse base drive current density:

$$J_{BR} = 2qD_{pD}\frac{p(t_e)}{a(t_e)} \quad (7.190)$$

The peak hole concentration is given by:

$$p(t_e) = p_{BC}\frac{[W_{NM} - W_{SC}(t_e) - a(t_e)]}{W_{NM}} \quad (7.191)$$

Combining these expressions:

$$p(t_e) = p_{BC}\frac{[W_{NM} - W_{SC}(t_e)]}{\left[\frac{W_{NM}}{p_{BC}} + \frac{2qD_{pD}}{J_{BR}}\right]} \quad (7.192)$$

The charge removed during a small time interval dte by the reverse base drive current can be related to stored charge:

$$dQ_{SC}(t_e) = qp(t_e)dW_{SC} = J_{BR}dt_e \quad (7.193)$$

because the reverse base drive current is constant during the voltage rise-time. This provides a differential equation for the growth of the space-charge layer:

$$\frac{dW_{SC}}{dt_e} = \frac{J_{BR}}{qp(t_e)} \quad (7.194)$$

Using Eq. (7.192) yields:

$$[W_{NM} - W_{SC}(t_e)]dW_{SC} = \frac{J_{BR}}{q}\left(\frac{W_{NM}}{p_{BC}} + \frac{2qD_{pD}}{J_{BR}}\right)dt_e \quad (7.195)$$

Integrating this equation on both sides:

$$W_{SC}^2 - 2W_{NM}W_{SC} + 2\left(\frac{J_{BR}W_{NM}}{qp_{PC}} + 2D_{pD}\right)t_e = 0 \quad (7.196)$$

The applicable solution for this quadratic equation is:

$$W_{SC}(t_e) = W_{NM}\left\{1 - \sqrt{1 - 2\left(\frac{J_{BR}}{qp_{BC}W_{NM}} - \frac{2D_{pD}}{W_{NM}^2}\right)t_e}\right\} \quad (7.197)$$

This analysis predicts that the space-charge layer will expand as the square root of time.

The voltage supported by the space-charge layer is given by:

$$V_C(t_e) = \frac{qN_D}{2\varepsilon_S} W_{SC}^2$$
$$= \frac{qN_D}{2\varepsilon_S} W_{NM}^2 \left\{ 1 - \sqrt{1 - 2\left(\frac{J_{BR}}{qp_{BC}W_{NM}} - \frac{2D_{pD}}{W_{NM}^2}\right)t_e} \right\}^2 \tag{7.198}$$

According to this analytical model, the collector voltage increases approximately linearly with time.

Once the collector voltage reaches the supply voltage, the load current is transferred to the flyback diode shown in Fig. 7.3. This process results in a reduction of the collector current of the bipolar power transistor, while the collector voltage remains at the collector supply potential. At the beginning of this transient, a portion of the emitter finger of width X_V has been turned off as illustrated in Fig. 7.69. Within the N-drift region of this portion, the collector current flows by the transport of electrons at the saturated drift velocity. Within the P-base region of this segment, the collector current is sustained by the injected electron concentration whose profile is shown on the right-hand side. The width of this segment can be obtained by charge control analysis.

The total stored charge in the base region removed during the voltage rise-time is given by:

$$Q_{SB}(t_V) = \frac{1}{2} qn_{EB} W_B X_V L_E \tag{7.199}$$

where L_E is the length of the emitter finger orthogonal to the cross section. Using Eq. (7.172) to relate the electron concentration at the emitter-base junction to the on-state collector current density:

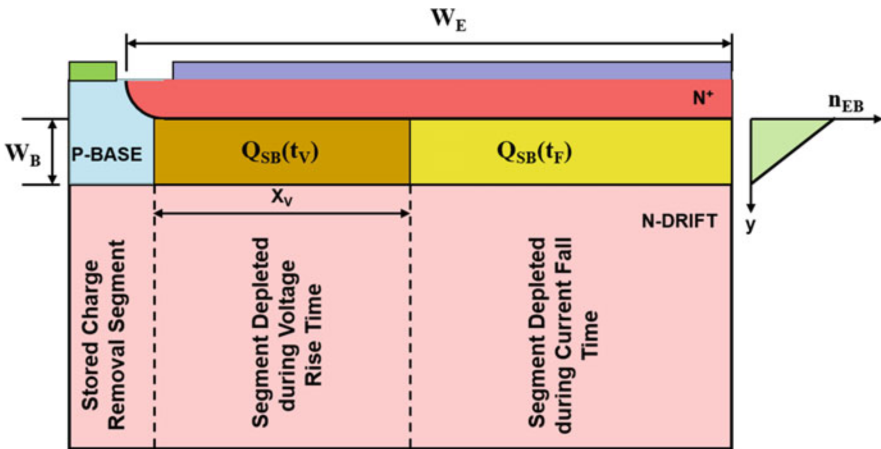

Fig. 7.69 Current constriction in the bipolar power transistor during the turn-off transient

$$Q_{SB}(t_V) = \frac{J_{C,ON} W_B^2 X_V L_E}{2D_{nB}} \tag{7.200}$$

The above charge is also equal to the charge removed by the reverse base drive current during the voltage rise-time:

$$\frac{J_{C,ON} W_B^2 X_V L_E}{2D_{nB}} = J_{BR} W_E L_E t_V \tag{7.201}$$

From this expression, the width of the finger that has been turned off during the voltage rise-time is obtained:

$$\frac{X_V = 2D_{nB} W^{nB} \mathrm{E} J_{BR} t_V}{J_{C,ON} W_B^2} \tag{7.202}$$

For a typical power bipolar transistor with an emitter width of 200 μm and P-base width of 10 μm, the width (X_V) that has turned off at the end of the voltage rise-time is found to be 110 μm when the on-state collector current density is 15 A/cm^2 and reverse base current density is 5 A/cm^2. Thus, approximately half of the emitter finger is turned off at this time, while the collector current remains constant leading to an increase in the current density in the remaining portion of the emitter finger.

Current Fall-Time Model

The collector current decreases after the collector voltage reaches the collector supply voltage because the current transfers to the flyback diode. The time taken for the collector current to reduce to zero is determined by the removal of the stored charge remaining in the P-base region after the voltage transient. This stored charge [$Q_{SB}(t_F)$] is indicated by the yellow-shaded region on the right-hand side of the P-base region in Fig. 7.69.

The fall time for the collector current can be derived by analysis of the extraction of the stored charge in the P-base region by the reverse base drive current. The stored charge (electrons) has a linearly decreasing concentration in the *y*-direction as illustrated on the right-hand side of Fig. 7.70 within the on-portion of the emitter finger. Its concentration along the *x*-direction is uniform within the on-portion of the emitter finger and decays exponentially, with a characteristic diffusion length for electrons, away from the on-portion within the off-portion of the emitter finger as illustrated at the top of Fig. 7.70 at the emitter-base junction. These concentration profiles are based upon the assumption that the collector current density is uniform within the on-portion of the emitter finger and remains constant during the collector fall time. Under these conditions, the electron distribution is given by:

$$n(x,y) = n_{EB}\left(1 - \frac{y}{W_B}\right) e^{-(x - X_{ON})/L_n} \tag{7.203}$$

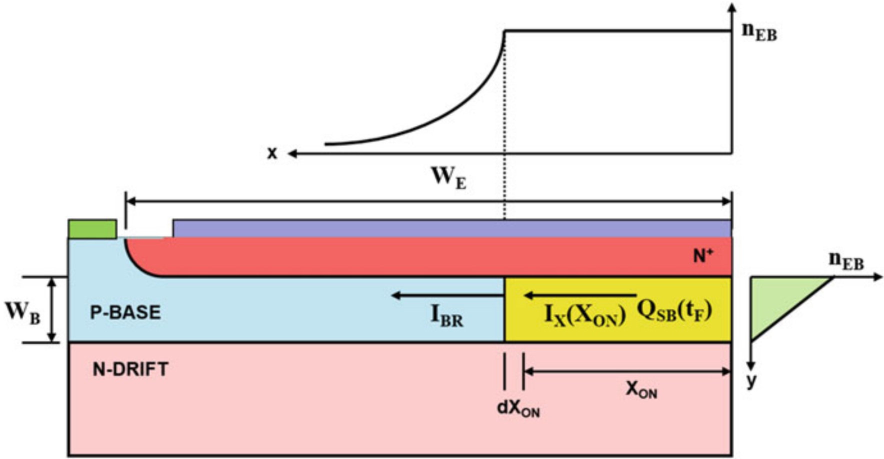

Fig. 7.70 Charge distributions for the current fall-time analysis in the bipolar power transistor during the turn-off transient

where L_n is the diffusion length for electrons in the P-base region. The stored charge within the segment dX_{ON} is given by:

$$dQ_{SB} = \frac{1}{2} q n_{EB} . W_B . L_E . dX_{ON} \tag{7.204}$$

Using Eq. (7.172) for the electron concentration at the emitter-base junction:

$$dQ_{SB} = \frac{J_{CON} W_B^2 L_E}{2 D_{nB}} dX_{ON} \tag{7.205}$$

Consequently:

$$\frac{dQ_{SB}}{dt} = \frac{J_{CON} W_B^2 L_E}{2 D_{nB}} \frac{dX_{ON}}{dt} \tag{7.206}$$

The stored charge within the segment dX_{ON} is also determined by the difference between the current entering the segment from the on-portion in the x-direction [$I_x(X_{ON})$] and the current leaving the segment (I_{BR}):

$$\frac{dQ_{SB}}{dt} = I_X(X_{ON}) - I_{BR} \tag{7.207}$$

The current entering the segment in the x-direction from the on-portion can be obtained by using:

$$I_x(X_{ON}) = \int_0^{W_B} J_x L_E dy \tag{7.208}$$

with the current density in the x-direction given by:

$$J_x = qD_{nB}\frac{\delta n}{\delta x}|_{x=X_{ON}} \tag{7.209}$$

Using Eq. (7.203) for the electron distribution yields:

$$J_x = q\frac{D_{nB}}{L_n}n_{EB}\left(1 - \frac{y}{W_B}\right) \tag{7.210}$$

Substituting this expression in Eq. (7.208):

$$I_x(X_{ON}) = \frac{qD_{nB}n_{EB}W_B L_E}{2L_n} \tag{7.211}$$

Using Eq. (7.172) for the electron concentration at the emitter-base junction:

$$I_x(X_{ON}) = \frac{J_{CON}W_B^2 L_E}{2L_{nB}} \tag{7.212}$$

Substituting Eqs. (7.206 and 7.212) into Eq. (7.207) yields:

$$\frac{W_B^2 J_{C,ON} L_E}{2D_{nB}}\frac{dX_{ON}}{dt} = \frac{J_{C,ON}W_B^2 L_E}{2L_{nB}} - I_{BR} \tag{7.213}$$

Expressing the reverse base current in terms of a reverse base drive current density:

$$I_{BR} = J_{BR}W_E L_E \tag{7.214}$$

provides the expression:

$$\frac{dX_{ON}}{dt} = \frac{D_n}{L_{nB}} - \frac{2D_{nB}W_E J_{BR}}{W_B^2 J_{C,ON}} \tag{7.215}$$

The first term on the right-hand side of this expression is smaller in magnitude than the second term indicating the width of the on-portion (X_{ON}) is shrinking with time. Defining a velocity for the movement of the on-portion as:

$$v_{ON} = \frac{2D_{nB}W_E J_{BR}}{W_B^2 J_{C,ON}} - \frac{D_{nB}}{L_{nB}} \tag{7.216}$$

and substituting into Eq. (7.215):

$$\frac{dX_{ON}}{dt} = -v_{ON} \tag{7.217}$$

The evolution of the width of the on-portion with time can be obtained by integration of this expression from an initial on-portion width of ($W_E - X_V$):

$$X_{ON}(t) = (W_E - X_V) - v_{ON}t_e \tag{7.218}$$

where t_e is the elapsed time after the end of the voltage rise transient.

Since the current density in the on-portion has been assumed to remain constant during this transient, the collector current is given by:

$$I_C = J_{C,ON}X_{ON}(t)L_E = J_{C,ON}[(W_E - X_V) - v_{ON}t_e]L_E \tag{7.219}$$

The average collector current density, defined as the ratio of the collector current to the device area ($W_E.L_E$), is then given by:

$$J_C(t) = \frac{J_{C,ON}}{W_E}[(W_E - X_V) - v_{ON}t_e] \tag{7.220}$$

The collector current decreases linearly with time according to this analysis. The time taken for the collector current to decrease to zero, defined as the *current fall time*, can be obtained from the above expression:

$$t_F = \frac{W_E - X_V}{v_{ON}} \tag{7.221}$$

For a typical power bipolar transistor with an emitter width of 200 μm and P-base width of 10 μm, the velocity for the movement of the on-portion is found to be 4.5×10^5 cm/s (or 4.5 μm/ns) when the on-state collector current density is 15 A/cm^2 and reverse base current density is 5 A/cm^2. Using a width of 110 μm for the portion turned off during the voltage transient, the collector current fall time is then found to be 20 ns.

Turn-Off Waveforms for an Inductive Load

The waveforms for the current and voltage for the bipolar power transistor can be constructed based upon the above analysis for the storage time, the voltage rise-time, and the current fall time. For the typical device structure with an emitter width of 200 μm and a base width of 10 μm, the waveforms obtained using the analytical models are shown in Fig. 7.71 for the case of a collector on-state current density of 15 A/cm^2 and reverse base drive current density of 5 A/cm^2.

The power dissipated during the turn-off transient can be obtained from the above analysis by using the time intervals for the voltage and current transients (and linearizing the waveforms). The energy loss per turn-off event is given by:

$$E_{OFF} = \int_0^{t_e} J_C(t).V_C(t)dt = \frac{J_{CON}V_{CS}}{3}t_v + \frac{J_{CON}V_{CS}}{2}t_F \tag{7.222}$$

The power dissipation (per unit area) can then be obtained by taking the product of the switching energy and the operating frequency. Due to the short transition times

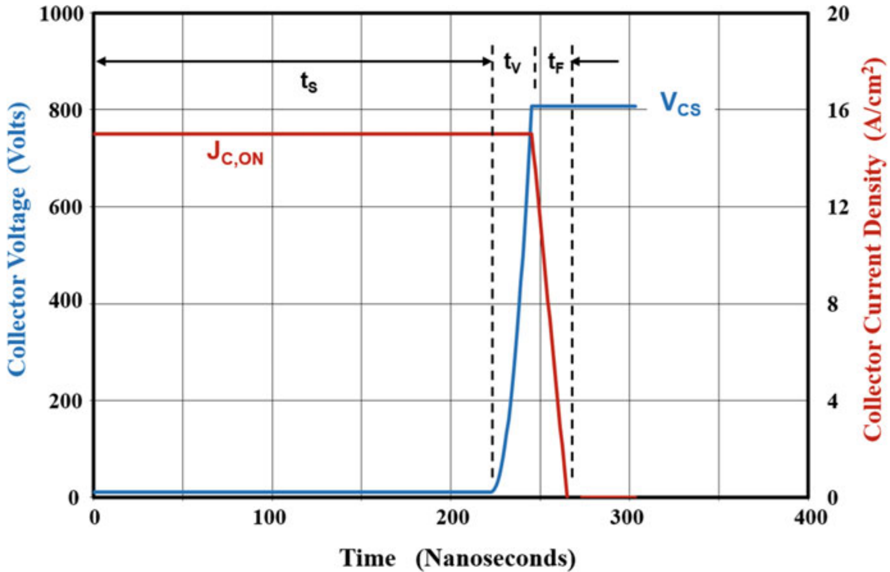

Fig. 7.71 Analytically calculated waveforms for the bipolar power transistor during the turn-off transient

for the voltage and current for the bipolar power transistor, the switching power loss is low making it an attractive power switch in high-frequency applications such as lamp ballasts. However, the on-state voltage drop for the structure is relatively large producing high power dissipation in the on-state. In addition, its maximum operating frequency is limited by the long storage time interval.

Simulation Example

The results of two-dimensional numerical simulations are described here for the baseline device structure (bjt8) to validate the model for the turn-off process for the bipolar power transistor with an inductive load. For this structure, a doping concentration of 5×10^{13} cm^{-3} was used for the N-drift region with a thickness of 80 μm. The device was initially biased with a positive base drive voltage of 5 V with a base resistance to limit the base current to 5 A/cm^2. The base drive voltage was rapidly switched to negative 5 V to initiate the turn-off process while maintaining a constant collector current to emulate the inductive load conditions. The switching waveforms obtained from the numerical simulations are shown in Fig. 7.72.

The base drive current immediately switches to about -5 A/cm^2 upon initiation of the turn-off process. The collector current and voltage remain constant during a storage time interval of 235 ns. The analytical model provides an accurate prediction of this storage time. The collector voltage then begins to increase as the square of the elapsed time as predicted by the analytical model. The collector voltage reaches 800 V after 22 ns (voltage rise-time). The analytical model is able to accurately predict this voltage transition time. After this, the collector current decreases linearly

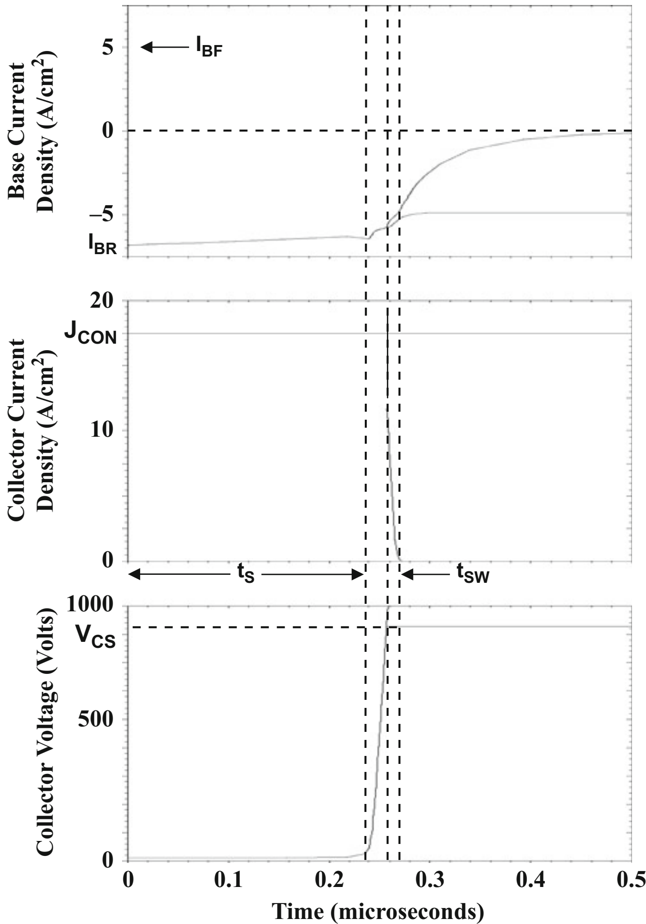

Fig. 7.72 Typical turn-off waveforms for a bipolar power transistor with an inductive load

with time as predicted by the analytical model. The transition time for the collector current (fall time) is 15 ns. This is also consistent with the behavior predicted by the analytical model.

It is instructive to examine the electron distribution within the bipolar power transistor structure at various stages of the turn-off process to gain further insight into the turn-off physics. The electron concentration profile near the edge of the emitter closest to the base contact is shown in Fig. 7.73. It can be observed that the profile at $t = 39$ and 107 ns has the shape illustrated in Fig. 7.68 allowing analysis of the storage time with a one-dimensional model.

The physics determining the turn-off process for the bipolar power transistor can be understood by examination of the electron distribution within the two-dimensional structure. Three-dimensional views of the electron concentration are provided in Figs. 7.74, 7.75, 7.76, 7.77, 7.78, 7.79, 7.80, and 7.81 at various

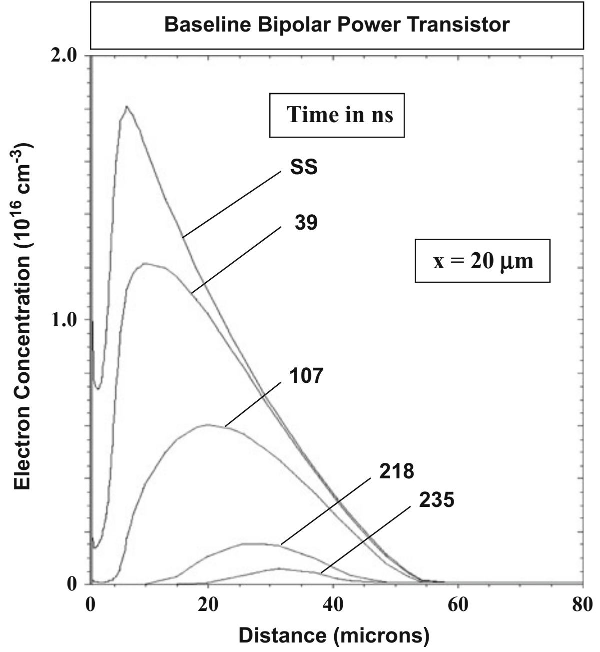

Fig. 7.73 Electron concentration profile in the vertical direction within the bipolar power transistor

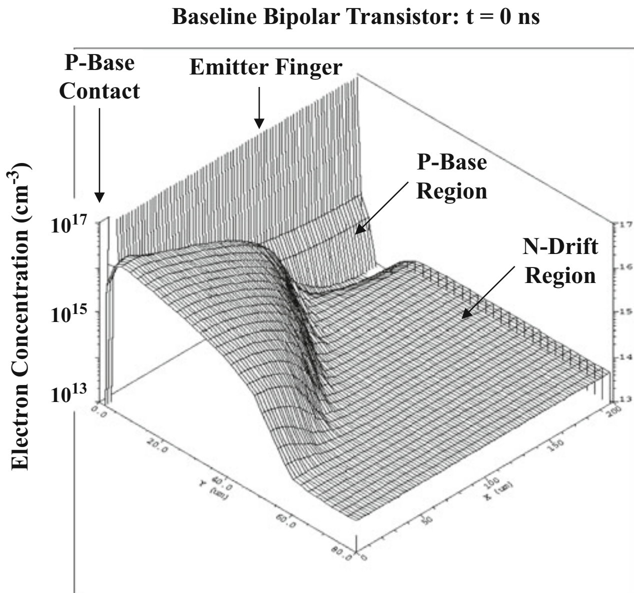

Fig. 7.74 Three-dimensional view of the initial electron charge distribution within the bipolar power transistor

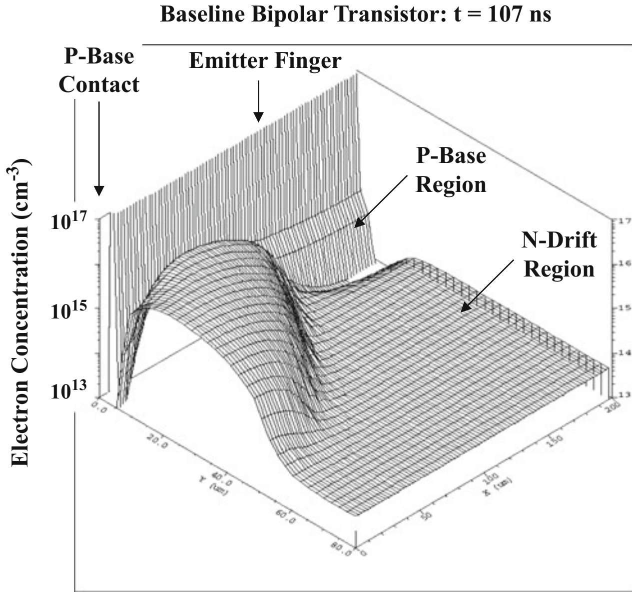

Fig. 7.75 Three-dimensional view of the electron charge distribution within the bipolar power transistor during the turn-off transient

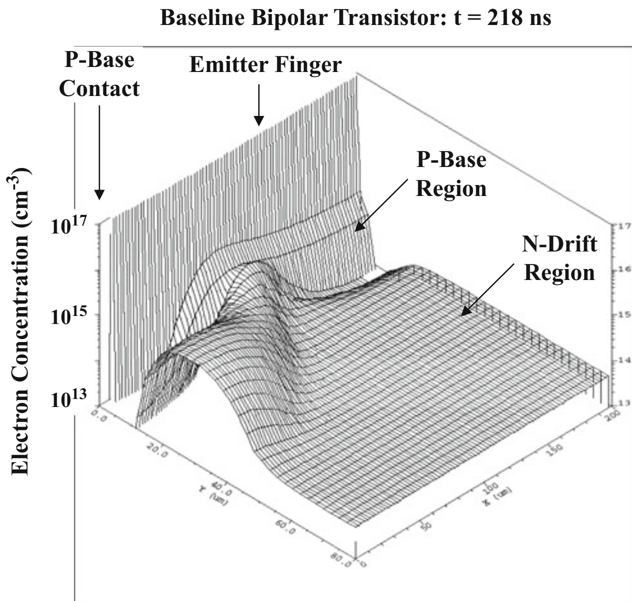

Fig. 7.76 Three-dimensional view of the electron charge distribution within the bipolar power transistor during the turn-off transient

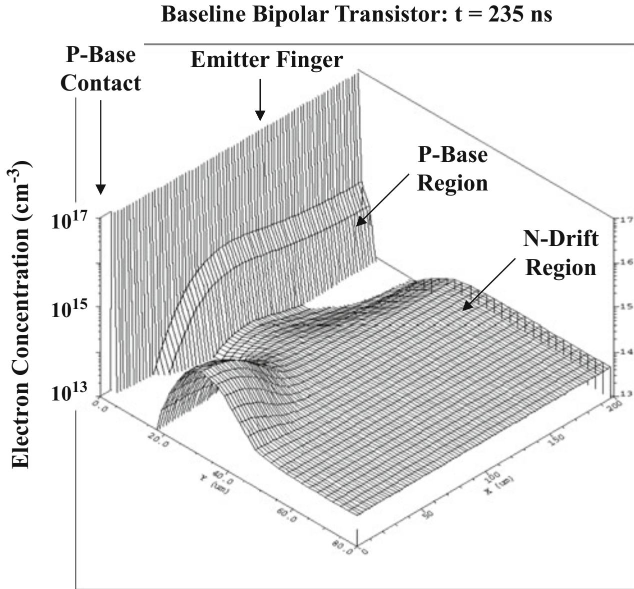

Fig. 7.77 Three-dimensional view of the electron charge distribution within the bipolar power transistor during the turn-off transient

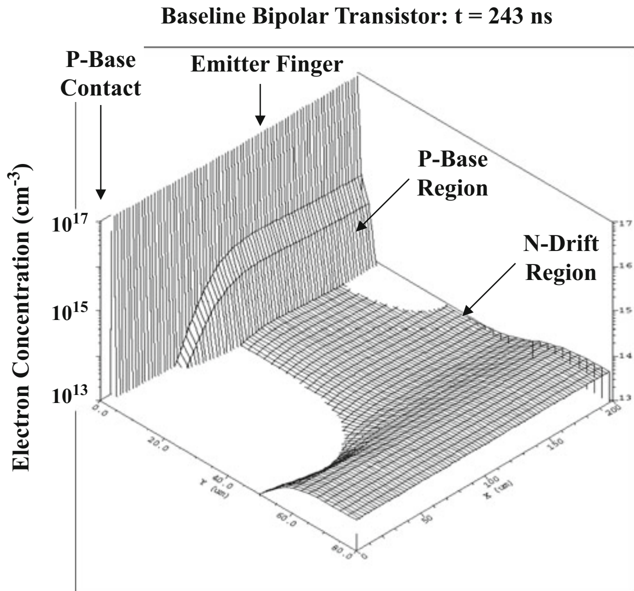

Fig. 7.78 Three-dimensional view of the electron charge distribution within the bipolar power transistor during the turn-off transient

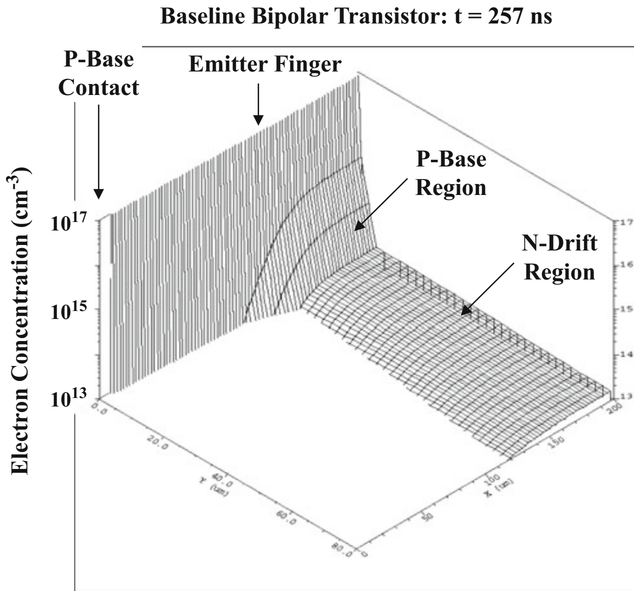

Fig. 7.79 Three-dimensional view of the electron charge distribution within the bipolar power transistor during the turn-off transient

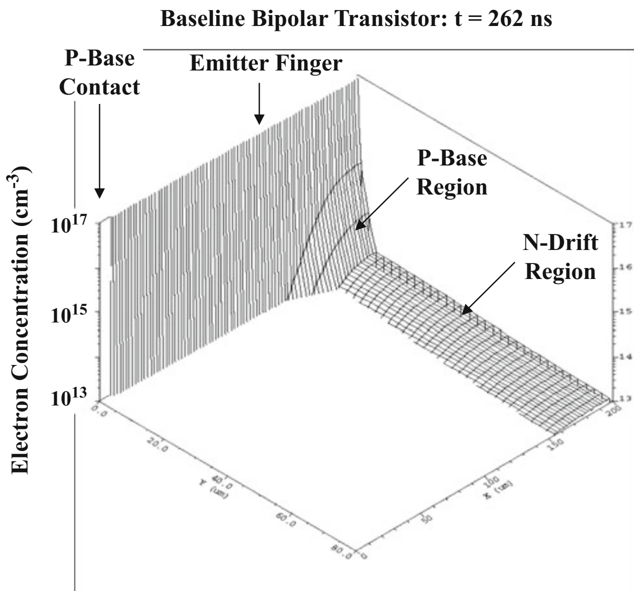

Fig. 7.80 Three-dimensional view of the electron charge distribution within the bipolar power transistor during the turn-off transient

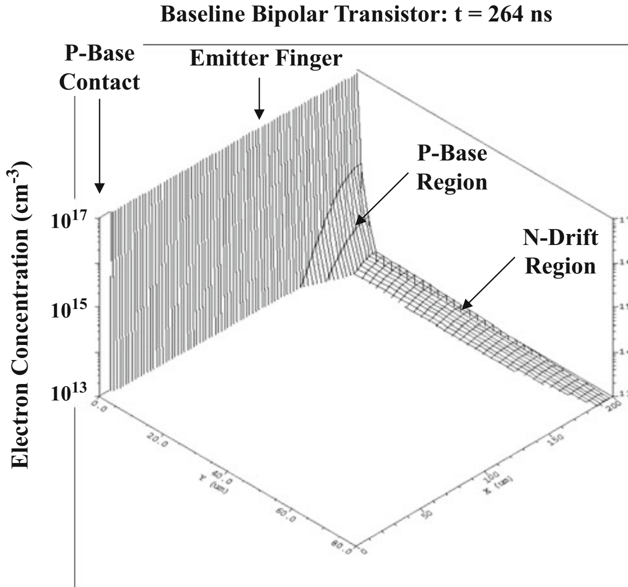

Fig. 7.81 Three-dimensional view of the electron charge distribution within the bipolar power transistor during the turn-off transient

stages during the turn-off process. The initial ($t = 0$ ns) on-state electron distribution during operation in the quasi-saturation region is shown in Fig. 7.74. It can be observed that the highest concentration of electrons is resident at the edge of emitter closest to the base contact because of the emitter current crowding phenomenon. The concentration of electrons in the N-drift region is observed to be much greater than that within the P-base region.

The electron distribution during the storage time is provided in Figs. 7.75, 7.76, and 7.77 as the time progresses to 107, 218, and 235 ns, respectively. It can be observed from these figures that the stored charge is being extracted mostly from the edge of the structure in proximity with the base contact. This allows a one-dimensional analysis for the storage time. At $t = 235$ ns, the electron concentration in this region becomes equal to zero at the base-collector junction located at a depth of about 10 μm enabling the bipolar power transistor to begin supporting higher collector voltages.

The electron distribution during the voltage rise-time is provided in Figs. 7.78 and 7.79 as the time progresses to 243 and 257 ns, respectively. It can be observed from these figures that a depletion region is forming at the edge of the structure in proximity with the base contact. This allows analysis of the voltage rise-time with a one-dimensional analysis. The depletion layer width increases with time in the y-direction due to the larger voltage being supported across the bipolar power transistor [V_{CE}(243 ns) = 105 V; V_{CE}(257 ns) = 828 V]. In addition, the depletion region expands in the x-direction as described in the analytical model (see Fig. 7.69). At the

end of the voltage rise-time, a portion of the emitter finger with a width (X_{ON}) of 80 μm is still carrying the initial on-state collector current, while a segment with a width (X_V) of 110 μm has been turned off. The analytical model provides an accurate assessment of these widths.

It can be observed from these figures that the collector current is sustained in the on-segment by the injection of electrons in the P-base region and the transport of electrons through the collector region at the saturated drift velocity. The concentration of electrons in the N-drift region is therefore given by:

$$n_D = \frac{J_C}{q v_{sat,n}} \tag{7.223}$$

For an initial on-state collector current density of 17.5 A/cm^2, the electron concentration obtained by using the above expression with a saturated drift velocity of 1×10^7 cm/s is between 1 and 2×10^{13} cm^{-3} after taking into account the reduced conduction area within the structure at this stage of the turn-off process. This is in agreement with the observed electron concentration in the N-drift region within the on-segment.

The electron distribution during the current fall time is provided in Fig. 7.80 and Fig. 7.81 as the time progresses to 262 and 264 ns, respectively. It can be observed that the on-segment shrinks in size as described by the two-dimensional analytical model for this part of the turn-off process. In order to provide further insight into the turn-off process, the electron concentration profile along the x-direction is provided in Fig. 7.82 during various points of the collector fall-time interval. It can be observed that the electrons are diffusing from the on-segment into the off-segment as assumed in the two-dimensional analytical model (see Fig. 7.70). The electron concentration remains approximately constant during a portion of the transient as assumed in the analytical model and then decreases toward the end of the current fall interval. This results a slightly smaller collector current fall time than predicted by the model.

The evolution of the collector current density within the emitter finger is provided in Fig. 7.83 to complete the description of the turn-off process. The collector current density profiles during the storage phase are shown by the dotted lines at time $t = 39$, 218, and 235 ns. In these cases, a high current density is observed at the edge of the emitter finger near the base contact. The collector current density profiles during the voltage rise phase are shown by the solid lines at time $t = 243$, 249, and 257 ns. In these cases, the current density increases at the center of the emitter finger because the area for the on-segment is decreasing, while the total collector current remains constant. The collector current density profiles during the current fall phase are shown by the dashed lines at time $t = 262$, 264, and 266 ns. In these cases, the current density is observed to initially remain approximately constant and then decrease rapidly as the collector current decreases.

The high current densities observed within the emitter finger of the bipolar power transistor produce local hot spots due to the enhanced power dissipation. These hot spots also promote current filamentation which can limit the safe operating area for the structure as discussed in the next section.

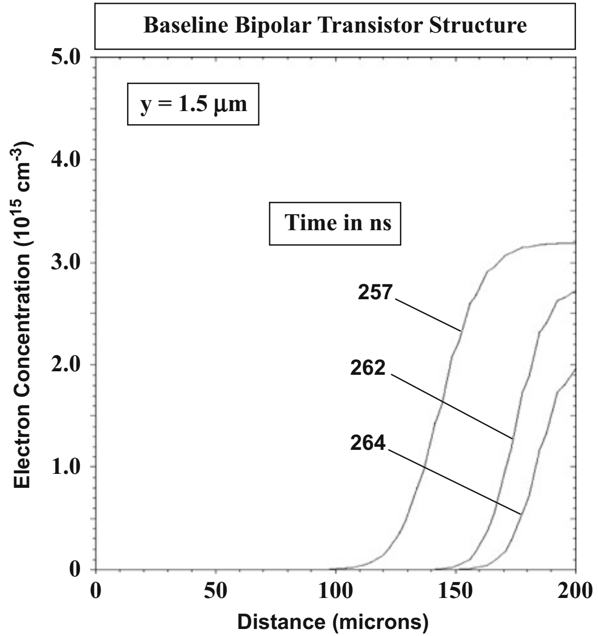

Fig. 7.82 Electron concentration profile within the P-base region of the bipolar power transistor during the turn-off transient

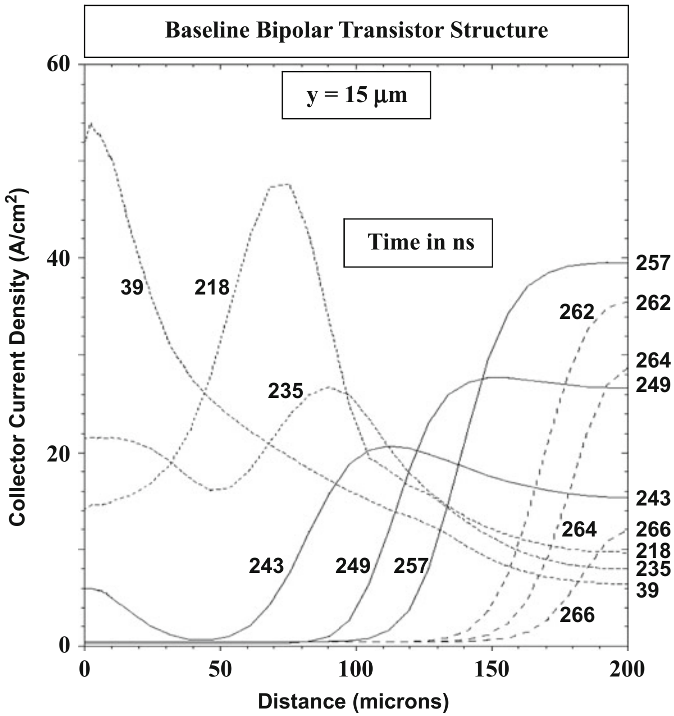

Fig. 7.83 Collector current density within the P-base region of the bipolar power transistor during the turn-off transient

7.9 Safe Operating Area

The trajectory for the collector current and voltage during the turn-off and turn-on events is illustrated in Fig. 7.84 for a bipolar power transistor. These switching loci are applicable for the circuit shown in Fig. 7.3 with an inductive load and a P-i-N rectifier used as the flyback diode. During the turn-off process shown in Fig. 7.84(a), the voltage increases with a constant current flowing through the transistor until the voltage reaches the collector supply voltage (V_{CS}). The current then transfers from the transistor to the flyback rectifier. An overshoot in the collector voltage is observed due to the presence of finite stray inductances in the collector circuit.

During the turn-on process shown in Fig. 7.84(b), the collector current in the bipolar power transistor increases until it becomes equal to the load current. During this time, the load current is being transferred from the flyback diode to the transistor. The collector current then continues to increase because of the reverse recovery current of the P-i-N rectifier until it settles down to the on-state collector current ($I_{C,ON}$). The bipolar power transistor must be capable of handling the large overshoot in current because the reverse recovery current for the P-i-N rectifier is typically as large as the load current.

The bipolar power transistor must be capable of handling operation in all portions of the turn-off and turn-on loci without destructive failure. Considerable power dissipation occurs within the bipolar power transistor due to the simultaneous large collector current and voltage during the transients. The steady-state thermally defined limit to the current-voltage locus is determined by the maximum permissible junction temperature [$T_{J(max)}$] and the thermal resistance (R_{TH}):

$$P_{D(max)} = (I_C . V_{CE}) = \frac{T_{J(max)} - T_A}{R_{TH}} \qquad (7.224)$$

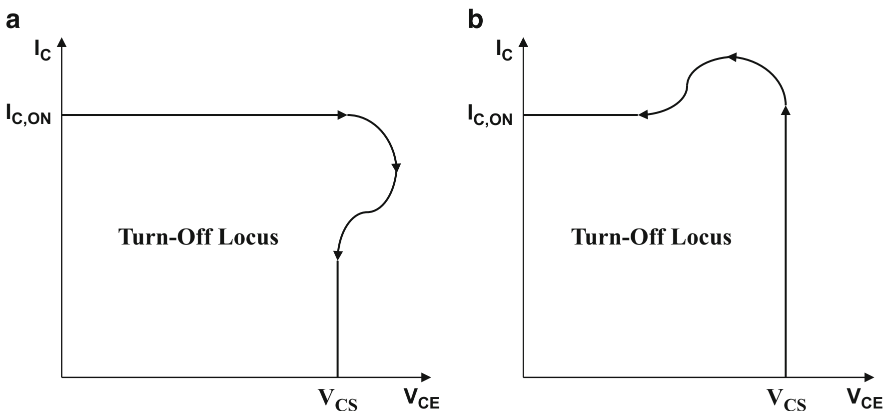

Fig. 7.84 Typical switching loci for the bipolar power transistor

where T_A is the ambient temperature [21]. For a constant thermal resistance, this expression indicates that the maximum collector current will reduce inversely with increasing collector voltage.

A larger instantaneous power can be tolerated during the short switching intervals. However, the safe operating area for the bipolar power transistor can become limited by the formation of hot spots accompanied by current filaments. The localization of the collector current can occur during operation with the emitter-base junction under forward bias as in the case of turn-on or with the emitter-base junction under reverse bias as in the case of turn-off. These limitations, commonly referred to as *second breakdown*, are discussed below.

7.9.1 Forward Biased Second Breakdown

The bipolar power transistor can undergo destructive failure due to thermal runaway when biased in the forward active region of operation. The emitter current becomes localized due to a positive thermal feedback phenomenon leading to the formation of a current filament with very high current density. The high power dissipation within the current filament raises the local temperature which favors even greater current flow in this area. This in turn produces a further rise in the local temperature. Eventually, the local temperature exceeds the eutectic temperature between silicon and the aluminum metallization leading to the melting of the emitter metal at the hot spot. The metal then penetrates through the junctions producing a short circuit, which destroys the device. The failure mechanism responsible for limiting the performance of the bipolar power transistor when the emitter-base junction is forward biased is referred to as the *forward biased second breakdown* phenomenon. The current-voltage locus within which the bipolar power transistor can be operated without destructive failure while the emitter-base junction is forward biased is referred to as the *forward biased safe operating area (FBSOA).*

Consider a bipolar power transistor driven by a voltage source (V_{BE}). The collector current density is then given by:

$$J_C = \frac{qD_{nB}n_{0B}}{W_B} e^{(qV_{BE}/kT)} \tag{7.225}$$

The minority carrier concentration in the base under equilibrium is given by:

$$n_{0B} = \frac{n_{iB}^2}{N_{AB}} \tag{7.226}$$

where n_{iB} is the intrinsic carrier concentration and N_{AB} is the doping concentration in the P-base region. Using this expression in Eq. (7.225):

$$J_{\mathrm{C}} = \frac{qD_{\mathrm{nB}}n_i^2}{W_{\mathrm{B}}N_{\mathrm{AB}}}e^{(qV_{\mathrm{BE}}/kT)} \tag{7.227}$$

For a collector bias voltage V_{CE}, the steady-state power dissipation is:

$$P_{\mathrm{D}} = J_{\mathrm{C}}V_{\mathrm{CE}} \tag{7.228}$$

If the collector current density increases in a local region, the power dissipation in this region also becomes larger than in the rest of the transistor. The local temperature then increases in accordance with:

$$T_{\mathrm{J}} = P_{\mathrm{D}}R_{\mathrm{TH}} + T_{\mathrm{A}} = J_{\mathrm{C}}V_{\mathrm{CE}}R_{\mathrm{TH}} + T_{\mathrm{A}} \tag{7.229}$$

An increase in the local temperature produces an increase in the collector current density in this region because the intrinsic carrier concentration increases and is a strong function of temperature (see Chap. 2). This provides a positive feedback mechanism for the local collector current density and temperature to increase until destructive failure occurs at the hot spot because of the melting of the aluminum metallization at about 600 °C.

The localization of the collector current can be prevented by driving the bipolar power transistor with a current source instead of a voltage source. This can be achieved by using a base-emitter voltage source (V_{BS1}) with a series resistance as illustrated in Fig. 7.3. The base drive current during on-state operation is then given by:

$$I_{\mathrm{B}} = \frac{(V_{\mathrm{BS1}} - V_{\mathrm{bi}})}{R_{\mathrm{B1}}} \approx \frac{V_{\mathrm{BS1}}}{R_{\mathrm{B1}}} \tag{7.230}$$

if the base drive supply voltage is much greater than the built-in potential (0.8 V) for the P-N junction. The base current is then controlled by the external drive circuit, with the base-emitter voltage of the bipolar power transistor related to the base current density by (see Eq. (7.28)):

$$e^{(qV_{\mathrm{BE}}/kT)} = \frac{L_{\mathrm{pE}}J_{\mathrm{B}}}{qD_{\mathrm{pE}}p_{0\mathrm{E}}} = \frac{L_{\mathrm{pE}}N_{\mathrm{DE}}J_{\mathrm{B}}}{qD_{\mathrm{pE}}n_{\mathrm{iE}}^2} \tag{7.231}$$

Using this expression in Eq. (7.227):

$$J_{\mathrm{C}} = \frac{D_{\mathrm{nB}}L_{\mathrm{pE}}N_{\mathrm{DE}}n_{\mathrm{iB}}^2}{D_{\mathrm{pE}}W_{\mathrm{B}}N_{\mathrm{AB}}n_{\mathrm{iE}}^2}J_{\mathrm{B}} \tag{7.232}$$

Based upon this expression, it can be concluded that the collector current density is relatively insensitive to local temperature fluctuations because the strong temperature dependence of the intrinsic concentrations in the base and emitter regions is canceled out. This prevents the formation of current filaments and hot spots within the emitter fingers of bipolar power transistors. However, the base drive circuit

requires a relatively large supply voltage which increases the power dissipated in the control electronics.

A commonly used approach to increasing the uniformity of the collector current distribution within a bipolar power transistor is by the addition of an *emitter ballasting resistance* as illustrated in Fig. 7.85. When the emitter current increases at a local region within the emitter finger, the voltage drop across the emitter ballast resistance also increases. This reduces the forward bias for the base-emitter junction in this location suppressing the injection of electrons into the P-base region. This in turn reduces the collector current density at this location providing a stabilizing influence of the current distribution. It is worth pointing out that this approach cannot be implemented with an emitter ballasting resistance external to the bipolar transistor structure. The emitter ballasting resistance must be distributed within all portions of the emitter fingers to provide the stabilizing influence. In addition, since the entire emitter current flows through the emitter ballasting resistance, its magnitude must be small to avoid increasing the on-state voltage drop and power dissipation.

An elegant implementation of the emitter ballasting resistance in the bipolar power transistor can be achieved as illustrated in Fig. 7.86 by restricting the emitter

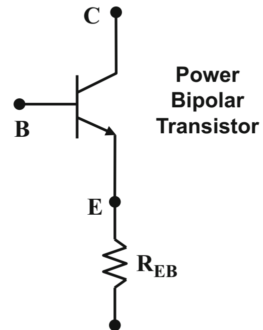

Fig. 7.85 Emitter ballasting resistance for the bipolar power transistor

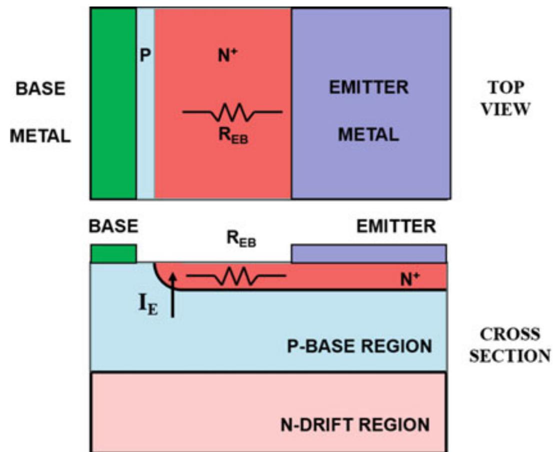

Fig. 7.86 Distributed emitter ballasting resistance within the bipolar power transistor structure

metallization to the center of the emitter finger. The emitter ballast resistance is derived from the sheet resistance of the N^+ emitter diffusion. Due to the high doping concentration of the N^+ emitter region required for obtaining a good injection efficiency, its sheet resistance is low (~ 10 ohms/square). This enables the formation of the emitter resistance with low values that are compatible with obtaining only a small increase in the on-state voltage drop.

It was previously shown that the emitter current crowds at the edge of the emitter closest to the base contact during operation in the on-state as indicated by the arrow in Fig. 7.86. Most of the emitter current is consequently forced to flow through the emitter ballast resistance. This produces the additional voltage drop required to promote uniform emitter current distribution. A significant advantage of this approach, to introducing an emitter ballast resistance that is uniformly distributed within the bipolar power transistor, is the absence of any additional process steps during device fabrication. The emitter ballast resistance is created during the layout of the emitter metallization relative to the edges of the emitter fingers.

7.9.2 Reverse Biased Second Breakdown

The safe operating area for the bipolar power transistor is limited by different physics when switching from the on-state to the blocking state. During the turn-off transient, the base drive current is reversed to remove the stored charge within the P-base and the N-drift regions. The failure mechanism encountered during the turn-off process is consequently referred to as the *reverse biased second breakdown* phenomenon. The current-voltage locus within which the bipolar power transistor can be operated without destructive failure, while the emitter-base junction is reverse biased, is referred to as the *reverse biased safe operating area (RBSOA)*.

As previously demonstrated in the section on turn-off physics for the bipolar power transistor, the collector current constricts to the middle of the emitter finger due to removal of charge from the proximity of the base contact by the reverse base drive current. In the case of an inductive load, the collector current remains constant during this stage of the turn-off process producing an increase in the collector current density in the middle of the emitter finger. As the collector voltage increases, the electric field in the N-drift region becomes large resulting in the transport of electrons at the saturated drift velocity. The electron concentration in the drift region at the middle of the emitter finger is then given by:

$$n_{\mathrm{D}} = \frac{J_{\mathrm{C}}}{q v_{\mathrm{sat},n}} \tag{7.233}$$

where J_{C} is the local collector current density.

The electron concentration exceeds the background doping level when the local current density becomes large. As an example, this would occur at a current density of 80 A/cm^2 for a drift region with doping concentration of 5×10^{13} cm^{-3}.

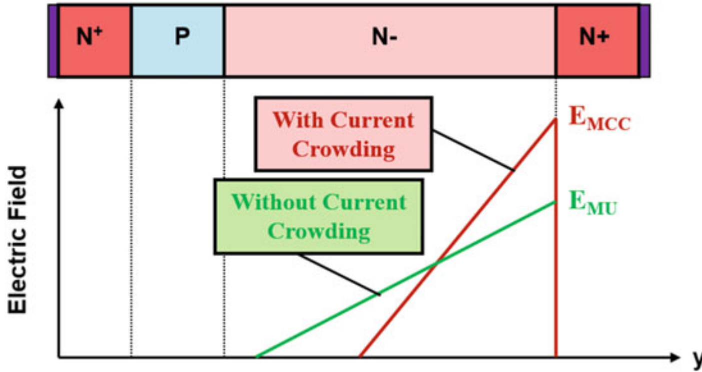

Fig. 7.87 Electric field profiles within the bipolar power transistor structure with and without current crowding during turn-off

The electric field then reverses in slope as shown previously in Fig. 7.19. When the collector current density is further increased and exceeds the Kirk current density (J_K), a current-induced base region forms at the base-collector junction with a peak electric field located at the interface between the N-drift region and the N$^+$ substrate. The electric field profiles under these conditions are illustrated in Fig. 7.87 with and without taking into account the current crowding at the middle of the emitter finger. It can be observed that a much larger maximum electric field occurs at the interface between the N-drift region and the N$^+$ substrate in the presence of current crowding. This precipitates avalanche breakdown at a lower voltage than expected for either the background doping concentration of the N-drift region or with a uniform current distribution within the structure.

When the electron concentration becomes far greater than the background doping concentration in the N-drift region, Poisson's equation in the drift region is given by:

$$\frac{d^2V(y)}{dy^2} = -\frac{dE}{dy} = -\frac{Q}{\varepsilon_S} = \frac{qn_D}{\varepsilon_S} = \frac{J_C}{\varepsilon_S v_{sat,n}} \tag{7.234}$$

by using Eq. (7.233) for the electron concentration in the N-drift region. The avalanche breakdown voltage in the presence of a high collector current density can be solved by using this equation with the Baliga's formula for the impact ionization coefficient:

$$\mathrm{BV}(J_C) = 4.45 \times 10^{13} \left(\frac{J_C}{qv_{sat,n}}\right)^{-3/4} \tag{7.235}$$

If the bipolar power transistor is turned off with a reverse base drive current that is substantially smaller than the local collector current density at the middle of the collector finger, the current gain of the transistor must be accounted for leading to:

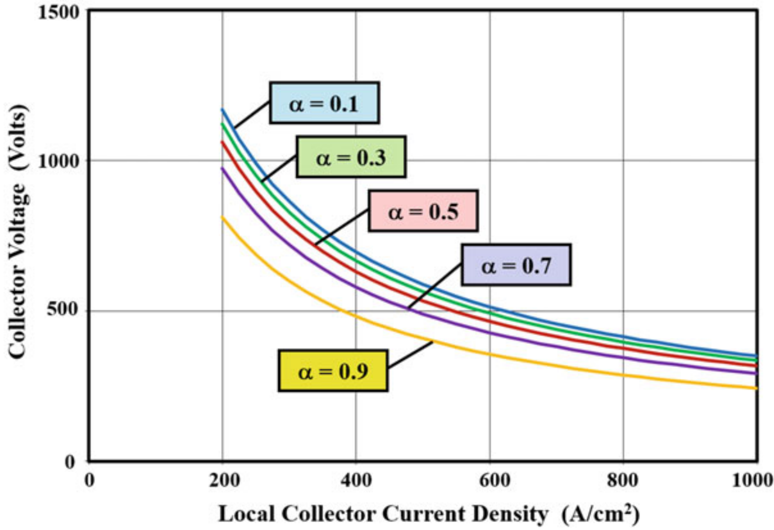

Fig. 7.88 Safe operating area for the bipolar power transistor structure during turn-off

$$\mathrm{BV_{RBSOA}} = \mathrm{BV}(J_\mathrm{C})\,(1-\alpha)^{1/n} \tag{7.236}$$

The reverse biased safe operating area computed by using the above equation is shown in Fig. 7.88 for various values for the common-base current gain. It can be observed from this figure that the maximum collector voltage that can be sustained by the bipolar power transistor is substantially reduced when the local collector current density becomes large. The RBSOA also degrades when the current gain of the transistor is increased. It is therefore necessary to ensure that the local current density at the middle of the emitter finger does not become extremely large during turn-off not just from a thermal standpoint but also to prevent local avalanche breakdown that can destroy the device.

One approach to improving the RBSOA of the bipolar power transistor without degrading the current gain during on-state operation is illustrated in Fig. 7.89. In this structure, the depth of the N^+ emitter region is made shallower in the middle of the emitter finger when compared with its depth at the edges of the emitter finger adjacent to the P-base contact. The deeper N^+ diffusion at the emitter edges produces a higher gain in this portion because of the narrower P-base width when compared with the middle of the emitter finger. Since most of the emitter current flows at the emitter edges during on-state operation due to the emitter current crowding phenomenon, this ensures a high gain in the conduction mode. At the same time, the current gain becomes smaller during turn-off due to the larger width of the P-base region at the middle of the emitter finger.

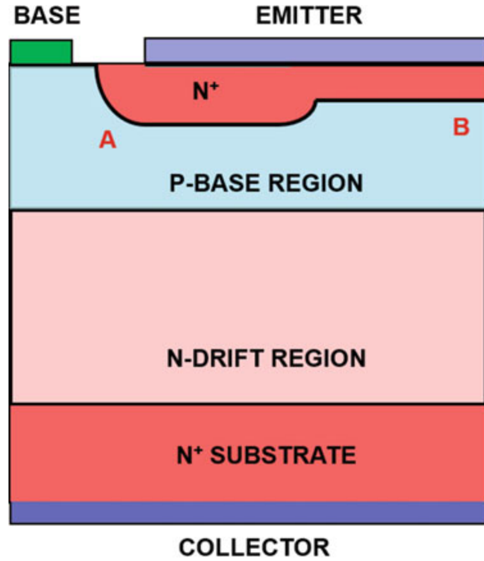

Fig. 7.89 Bipolar power transistor structure with reduced current gain at the middle of the emitter finger

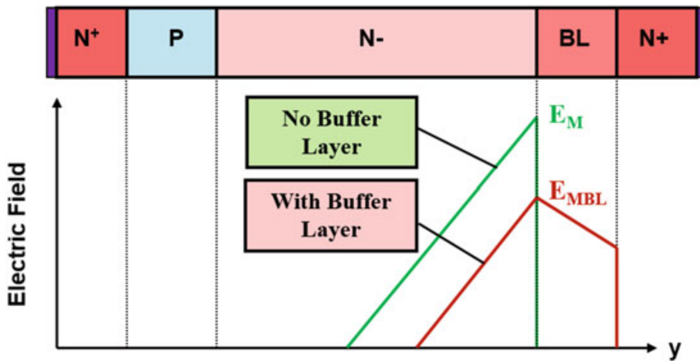

Fig. 7.90 Bipolar power transistor structure with buffer layer in the collector drift region

Another approach to improving the RBSOA of the bipolar power transistor is by the incorporation of a buffer layer in the N-drift region. The buffer layer is placed at the interface between the N-drift region and the N^+ substrate as illustrated in Fig. 7.90. The presence of the buffer layer reduces the peak electric field at the interface, as shown by the red line, suppressing premature avalanche breakdown. In order to be effective in reducing the electric field, the doping concentration of the buffer layer must be comparable to the electron concentration flowing through the drift region under the enhanced collector current density at the middle of the emitter finger. Typical doping concentration for the buffer layer is 5×10^{14} cm^{-3}, corresponding to a collector current density of 800 A/cm^2.

7.9.3 Boundary for Safe Operating Area

The safe operating area (SOA) for the bipolar power transistor defines the collector current-voltage space within which the device can be operated without destructive failure. One of the limits to the SOA is set by the maximum allowable collector current at low collector bias voltages. This limit is determined by the current handling capability of the emitter bond wires as shown by the horizontal line in Fig. 7.91. A second limit to the SOA is set by the maximum collector bias voltage at lower collector current levels. This boundary is determined by the breakdown voltage of the structure, including the impact of the edge termination, as shown by the vertical line in Fig. 7.91.

The third limit to the SOA is set by thermal considerations. The thermal limit is determined by the power dissipation within the device producing an increase in the junction temperature. The maximum allowable power dissipation is given by Eq. (7.215). When $T_{J,max}$ (the maximum junction temperature for reliable operation), T_A (the ambient temperature), and R_{TH} (the thermal resistance of the package) are fixed, this expression indicates that the maximum allowable collector current will decrease inversely with increasing collector voltage. This boundary is shown in Fig. 7.91 as the line with a slope of -1 on the log-log plot.

The fourth limit to the SOA is determined by the onset of the second breakdown phenomenon during the turn-off process. According to Eq. (7.227) in conjunction with Eq. (7.226), the maximum allowable collector voltage should decrease inversely as the ¾ power of the collector current. However, this does not account for the impact of current crowding in the emitter during the turn-off process. In practice, the RBSOA limit is found to follow a slope of -2 on the log-log plot as shown in the figure [21].

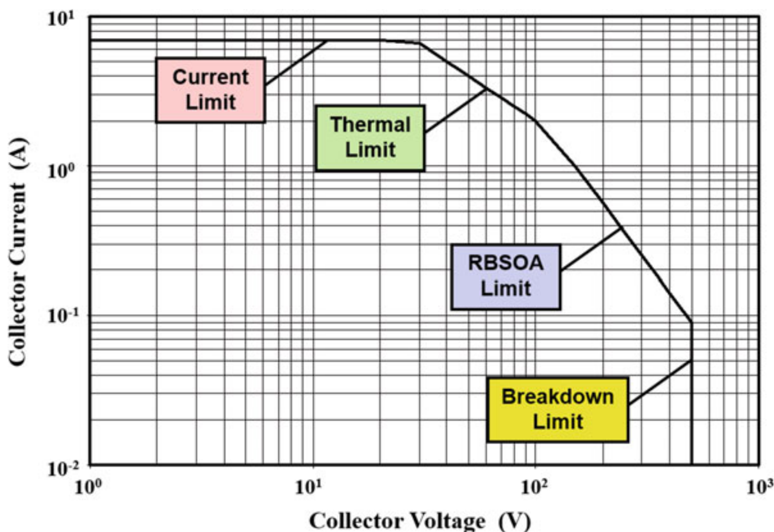

Fig. 7.91 Safe operating area boundaries for a typical bipolar power transistor

7.10 Darlington Configuration

In the previous sections, it has been demonstrated that the current gain of the bipolar power transistor is quite low (~5) due to various other design constraints. Consequently, a very large external base drive current is required to maintain the transistor in its on-state as well as during turn-off. This makes the base drive circuit bulky and expensive from an applications standpoint. The Darlington configuration [22] provides an approach to obtaining a high current gain within a monolithic bipolar transistor device structure. In the Darlington configuration, another bipolar power transistor is integrated together with the output bipolar power transistor, as illustrated in Fig. 7.92, to produce a larger current gain.

The base drive current for the composite structure is supplied to the input bipolar transistor T_1. The emitter current of this bipolar transistor is then fed to the base terminal of the second (output) bipolar transistor T_2. Note that the collectors for both the bipolar transistors are connected together creating the collector terminal for the composite device structure.

Since the base drive current I_{B2} for the output bipolar transistor is equal to the emitter current I_{E1} for the input bipolar transistor:

$$I_{B2} = I_{E1} = (1 + \beta_1)I_{B1} = (1 + \beta_1)I_{BD} \tag{7.237}$$

where β_1 is the common-emitter current gain of the input transistor. The collector current for the output transistor T_2 is then given by:

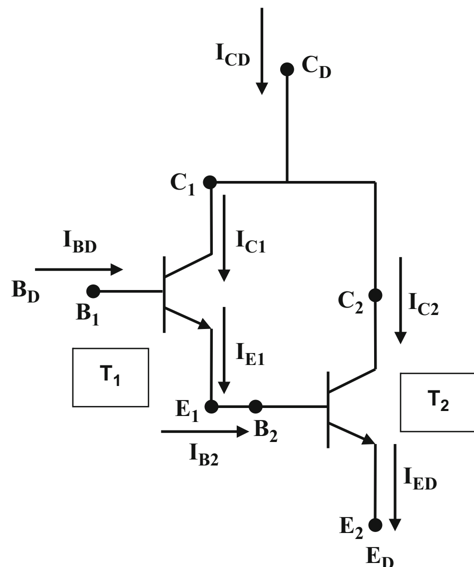

Fig. 7.92 Darlington configuration for the bipolar power transistor

$$I_{C2} = \beta_2 I_{B2} = \beta_2(1 + \beta_1)I_{BD} \tag{7.238}$$

where β_2 is the common-emitter current gain of the output transistor. The collector current for the input transistor T_1 is given by:

$$I_{C1} = \beta_1 I_{B1} = \beta_1 I_{BD} \tag{7.239}$$

Consequently, the collector current for the composite Darlington transistor structure is given by:

$$I_{CD} = I_{C1} + I_{C2} = \beta_1 I_{BD} + \beta_2(1 + \beta_1)I_{BD} \tag{7.240}$$

From this expression, the common-emitter current gain for the Darlington configuration is obtained:

$$\beta_{BD} = \frac{I_{CD}}{I_{BD}} = \beta_1 + \beta_2(1 + \beta_1) = \beta_1 + \beta_2 + (\beta_1\beta_2) \tag{7.241}$$

Thus, a significant increase in the current gain can be derived by utilizing the Darlington configuration.

The improved current gain obtained using the Darlington configuration is accompanied by a substantial increase in the on-state voltage drop. Since the base drive current for the output transistor is derived via the emitter current from the input transistor, the collector potential for the Darlington configuration consists of the voltage drop across the input transistor plus the base-emitter voltage drop for the output transistor:

$$V_{CE,D} = V_{CE1} + V_{BE2} \tag{7.242}$$

Even if the input transistor is driven into saturation to reduce its on-state voltage drop, the voltage drop for the Darlington configuration becomes in excess of the voltage drop across a forward biased diode.

Several other considerations influence the design of the Darlington bipolar transistor configuration. Firstly, a high leakage current can arise from the amplification of the leakage current of the input transistor by the current gain of the output transistor. Secondly, a path for removal of the stored charge in the output transistor by the reverse base drive current must be provided to avoid a very long storage phase. This is accomplished by the addition of shunting resistances across the emitter-base junctions of both the internal transistors as illustrated in Fig. 7.93. The shunting resistances reduce the current gains for the internal transistors at low current levels preventing the amplification of the leakage current. The shunt resistance R_1 also provides a path for extraction of the stored charge within the output transistor with the reverse base drive current during turn-off. In addition, it is convenient to integrate an antiparallel diode with the transistors for use as a flyback diode in H-bridge circuits commonly used for motor control applications.

A three-dimensional view of the layout of the monolithic Darlington bipolar transistor configuration is illustrated in Fig. 7.94. The input bipolar transistor is

Fig. 7.93 Darlington configuration for the bipolar power transistor with internal shunting resistances and antiparallel diode

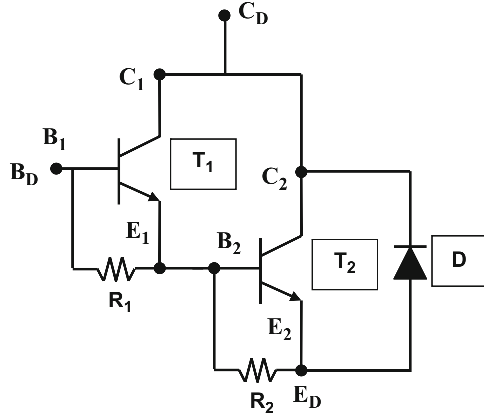

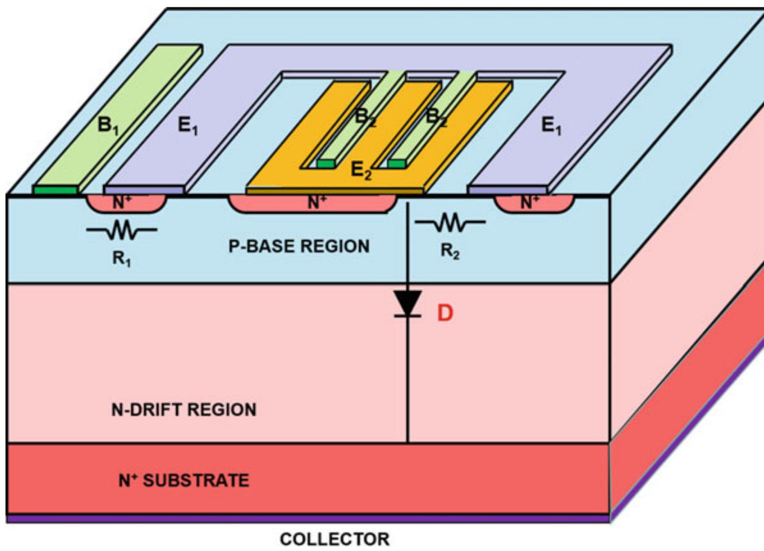

Fig. 7.94 Implementation of the monolithic Darlington bipolar power transistor configuration with internal shunting resistances and antiparallel diode

located on the left-hand side of the chip with its shunting resistance created by overlapping the emitter metal over the emitter-base junction of transistor T_1 on the edge away from its base contact. The emitter metal E_1 of the input transistor is not connected to the external terminals and is usually covered by a polyimide insulating layer. This metal layer also serves as the base terminal for the output transistor whose emitter is interdigitated with it in the central portion of the chip. The second resistance R_2 is created on the right-hand side of the chip. The antiparallel diode D is formed by overlapping the emitter terminal E_2 with the P-base region.

The relative size of the input and output transistors must be optimized to achieve the best gain and total area for the Darlington transistor configuration [23]. A good balance between the operating current density of the input transistor and the output transistor is required to match the roll-off in the current gain with total collector current density. It is also possible to extend the Darlington concept to multiple stages of bipolar transistors. Although this enables increasing the current gain, the on-state voltage drop also grows because of additional diode voltage drops for the stages.

7.11 Summary

The physics of operation of the bipolar power transistor has been described in this chapter. The bipolar transistor is a current controlled structure whose current gain depends upon the doping concentrations of the emitter and base regions as well as the width of the base region. A decrease in the current gain occurs in the bipolar power transistor due to high-level injection in the base region, which degrades its power gain. Severe current crowding occurs at the edge of the emitter in the power bipolar transistor which elevates the local current density. The common-emitter current gain of the power bipolar transistors optimized to support large voltages becomes smaller than 10 at typical operating current levels. The large stored charge within the P-base and N-drift regions of the bipolar power transistor in the on-state reduces the maximum operating frequency. The large resistance of the N-drift region produces a quasi-saturation region which increases the on-state voltage drop. These characteristics produce significant power losses within the device and the control circuit.

The bipolar power transistor is also prone to failure modes associated with emitter current crowding during the on-state and turn-off modes. Snubber circuits must be added across the device to avoid failure during operation in inductive load applications. All of these complexities have motivated the development of alternative power switches for applications. The most successful among these alternatives is the insulated gate bipolar transistor (IGBT) [24]. Its development in the early 1980s has resulted in the complete displacement of the bipolar power transistor leading to its extinction from the power semiconductor landscape. However, the physics of operation for the bipolar power transistor continues to have relevance because it is incorporated within the IGBT structure.

Problems

7.1 A bipolar transistor has a common-emitter current gain of 50. Determine its common-base current gain.

7.2 The open-emitter breakdown voltage of the above bipolar transistor is 1000 V. Determine its open-base breakdown voltage.

7.3 Consider an N^+PN-N^+ bipolar power transistor structure with uniformly doped emitter, base, and collector drift regions. The N^+ emitter region has a doping concentration of 2×10^{19} cm^{-3} and thickness of 10 μm. The P-base

region has a doping concentration of 2×10^{17} cm^{-3} and thickness of 10 μm. The N collector drift region has a doping concentration of 2×10^{14} cm^{-3} and thickness of 40 μm. The Shockley-Read-Hall (low-level, high-level, and space-charge generation) lifetimes are 10 ns in the emitter region, 1 μs in the base region, 10 μs in the collector drift region. Calculate the emitter injection efficiency at low injection levels in the P-base region ignoring bandgap narrowing and Auger recombination.

7.4 Determine the base transport factor for the power bipolar transistor described in Problem 7.3.

7.5 Determine the common-emitter and common-base current gains for the power bipolar transistor described in Problem 7.3 at low injection levels in the P-base region.

7.6 Determine the open-emitter breakdown voltage (BV_{CB0}) for the power bipolar transistor described in Problem 7.3 using the critical electric field for the doping concentration in the collector drift region. Make sure to take punch-through into account for the drift region. Confirm that the depletion region has not penetrated the entire base region.

7.7 Calculate the open-base breakdown voltage (BV_{CE0}) for the power bipolar transistor described in Problem 7.3 using $n = 6$ in the equation for the multiplication factor.

7.8 Determine the leakage current density at 300°K at a collector bias of 200 V due to space-charge generation in the collector drift region. What is the open-base leakage current density under these conditions?

7.9 Calculate the quasi-saturation-specific resistance for the power bipolar transistor described in Problem 7.3.

7.10 Determine the Webster current density for the power bipolar transistor described in Problem 7.3.

7.11 What is the common-emitter current gain for the power bipolar transistor described in Problem 7.3 at a current density of 1000 A/cm^2?

7.12 Determine the Kirk current density for the power bipolar transistor described in Problem 7.3 at a collector bias of 300 V.

7.13 What is the Early voltage for the power bipolar transistor described in Problem 7.3?

7.14 Determine the on-state voltage drop (V_{CEsat}) for the power bipolar transistor described in Problem 7.3 in the saturation region of operation. Assume that the injected hole concentration at the B-C junction [$p_{NS}(0)$] is 2×10^{16} cm^{-3} and the injected hole concentration is equal to the doping concentration at the N-drift/N$^+$ substrate interface. What is the collector current density under these operating conditions? Calculate the stored charge in the collector drift region under these conditions.

7.15 The power bipolar transistor described in Problem 7.3 is turned off from an initial on-state condition described in Problem 7.14 by using a reverse base drive current density of 5 A/cm^2. Determine the storage time during the turn-off process.

7.16 What is the voltage rise-time under the turn-off conditions described in Problem 7.15 if the collector bias voltage is 300 V? Determine the width of the emitter finger that has been turned off at this point in time if the emitter width (W_E) is 200 μm.
7.17 Determine the velocity for shrinking the on-portion of the emitter finger during the turn-off process. What is the collector current fall time for the conditions described in Problems 7.15 and 7.16?
7.18 Calculate the energy loss incurred during the turn-off process described in Problems 7.15, 7.16, and 7.17.
7.19 A Darlington power transistor is designed with a common-emitter current gain of 10 for the input transistor and 5 for the output transistor. What is the current gain for the Darlington transistor?
7.20 What is the typical on-state voltage drop for the Darlington transistor?

References

1. "The solid-state century", Scientific American special issue, January 1998
2. Shockley W (1984) The path to the conception of the junction transistor. IEEE Trans Electron Devices ED-31:1523–1546
3. Bardeen J, Brattain WH (1948) The transistor, a semiconductor triode. Phys Rev 74:230–231
4. Shockley W (1949) The theory of p-n junctions in semiconductors and p-n junction transistors. Bell Syst Tech J 28:435–489
5. Adler MS et al (1984) The evolution of power device technology. IEEE Trans Electron Devices ED-31:1570–1591
6. Baliga BJ (1979) Enhancement and depletion mode vertical channel MOS gated thyristors. Electron Lett 15:645–647
7. Baliga BJ et al (1982) The insulated gate rectifier (IGR): a new power switching device. IEEE Int Electron Devices Meet Abstr 10(6):264–267
8. Streetman BG, Banerjee SK (2006) Solid state electronic devices, 6th edn. Prentice Hall, New Jersey
9. Sze SM (1981) Physics of semiconductor devices, 2nd edn. Wiley, New Jersey, pp 265–270
10. Mertens R, Van Overstraeten RJ (1976) Measurement of the minority carrier parameters in heavily doped silicon. Solid State Electron 19:857–862
11. Possin GE, Adler MS, Baliga BJ (1984) Measurement of the pn product in heavily doped epitaxial emitters. IEEE Trans Electron Devices ED-31:3–17
12. Webster WM (1954) On the variation of junction-transistor current amplification factor with emitter current. Proc IRE 42:914–916
13. Kirk CT (1966) A theory of transistor cut-off frequency fall-off at high current densities. IEEE Trans Electron Devices ED-9:164–174
14. Blicher A (1981) Field-effect and bipolar power transistor physics. Academic Press, New Jersey, pp 140–143
15. Hauser RJ (1964) The effects of distributed base potential on emitter-current injection density and effective base resistance for stripe transistor geometries. IEEE Trans Electron Devices ED-11:238–242
16. Ghandhi SK (1977) Semiconductor power devices. Wiley, New Jersey, pp 157–161
17. Fletcher NH (1955) Some aspects of the design of power transistors. Proc IRE 43:551–559
18. Early JM (1952) Effects of space-charge layer widening in junction transistors. Proc IRE 40:1401

19. Ghandhi SK (1977) Semiconductor power devices. Wiley, New Jersey, pp 146–150
20. Chudobiak WJ (1970) The saturation characteristics of *npvn* power transistors. IEEE Trans Electron Devices ED-17:843–852
21. Oettinger FF, Blackburn DL, Rubin S (1976) Thermal characteristics of power transistors. IEEE Trans Electron Devices ED-23:831–838
22. S. Darlington, Semiconductor signal translating device, U.S. Patent 2,663,806, Issued 22 Dec 1953
23. Wheatley CF, Einthoven WG (1976) On the proportioning of chip area for multi-stage darlington power transistors. IEEE Trans Electron Devices ED-23:870–878
24. Baliga BJ et al (1984) The insulated gate transistor. IEEE Trans Electron Devices ED-31:821–828